HYDROGEN-BONDED LAYER-BY-LAYER FILMS OF POLY(D,L-LACTIC-*co*-GLYCOLIC ACID)-*b*-POLY(ETHYLENE GLYCOL) POLYMERSOMES AND TANNIC ACID

A THESIS SUBMITTED TO
THE GRADUATE SCHOOL OF NATURAL AND APPLIED SCIENCES
OF
MIDDLE EAST TECHNICAL UNIVERSITY

BY

GÖKÇE ÇALIŞ

IN PARTIAL FULFILLMENT OF THE REQIREMENTS
FOR
THE DEGREE OF MASTER OF SCIENCE
IN
POLYMER SCIENCE AND TECHNOLOGY

JUNE 2017

Approval of the thesis;

HYDROGEN-BONDED LAYER-BY-LAYER FILMS OF POLY(D,L-LACTIC-*co*-GLYCOLIC ACID)-*b*-POLY(ETHYLENE GLYCOL) POLYMERSOMES AND TANNIC ACID

submitted by **GÖKÇE ÇALIŞ** in partial fulfillment of the requirements for the degree of **Master of Science in Polymer Science and Technology Department, Middle East Technical University** by,

Prof. Dr. Gülbin Dural Ünver _____
Dean, Graduate School of **Natural and Applied Sciences**

Prof. Dr. Necati Özkan _____
Head of Department, **Polymer Science and Technology**

Assoc. Prof. Dr. İrem Erel Göktepe _____
Supervisor, **Chemistry Dept., METU**

Assoc. Prof. Dr. Sreeparna Banerjee _____
Coadvisor, **Biology Dept., METU**

Examining Committee Members:

Prof. Dr. Ayşen Yılmaz _____
Chemistry Dept., METU

Assoc. Prof. Dr. İrem Erel Göktepe _____
Chemistry Dept., METU

Assoc. Prof. Dr. Sreeparna Banerjee _____
Biology Dept., METU

Assoc. Prof. Dr. Ali Çırpan _____
Chemistry Dept., METU

Assoc. Prof. Dr. Yasemin Udum _____
Advanced Technologies Dept., Gazi University

Date: 01.06.2017

I hereby declare that all information in this document has been obtained and presented in accordance with academic rules and ethical conduct. I also declare that, as required by these rules and conduct, I have fully cited and referenced all material and results that are not original to this work.

Name, Last name: Gökçe ÇALIŞ

Signature:

ABSTRACT

HYDROGEN-BONDED LAYER-BY-LAYER FILMS OF POLY(D,L-LACTIC-*co*-GLYCOLIC ACID)-*b*-POLY(ETHYLENE GLYCOL) POLYMERSOMES AND TANNIC ACID

Çalış, Gökçe

M. Sc., Department of Polymer Science and Technology

Supervisor: Assoc. Prof. Dr. İrem Erel Göktepe

Coadvisor: Assoc. Prof. Dr. Sreeparna Banerjee

June 2017, 97 pages

Poly(lactic-*co*-glycolic acid)-*b*-poly(ethylene glycol) (PLGA-*b*-PEG) can self-assemble into core/shell nanostructures in aqueous environment due to its amphiphilic nature. These nanostructures have been widely used as drug carriers in the biomedical applications due to biocompatibility and biodegradability of PLGA-*b*-PEG. Biodegradable character of the nanostructures provides an advantage for controlled drug delivery systems. The drug release occurs through hydrolytic degradation of PLGA core. There are studies reporting on the aqueous solution behavior of PLGA-*b*-PEG nanocarriers. However, there are limited numbers of studies concerning use of PLGA-*b*-PEG polymersomes as building blocks in preparation of layer-by-layer (LbL) self-assembled films.

In this study, Doxorubicin and Paclitaxel loaded PLGA-*b*-PEG polymersomes were prepared and used as building blocks together with Tannic Acid (TA) in the preparation of LbL films. It was shown that multilayer deposition conditions affected the kinetics of drug release from the surface at acidic conditions. Moreover, it was demonstrated that release kinetics could also be controlled by constructing barrier layers within the LbL films.

Incorporation of PLGA-*b*-PEG polymersomes into multilayers is important to increase the loading capacity of the films and to enhance the stability of polymersomes in the bloodstream. Considering the biodegradability of PLGA-*b*-PEG, important biological properties of TA and controllable release kinetics via LbLfilm architecture, such multilayers may be promising for controlled delivery applications from surfaces.

Keywords: PLGA-*b*-PEG, polymersomes, biodegradability, drug release, layer-by-layer films.

ÖZ

HİDROJEN BAĞLI POLİ(LAKTİK-*ko*-GLİKOLİK ASİT)-*b*-POLİ(ETİLEN GLİKOL) POLİMERZOM VE TANNİK ASİT KATMAN-KATMAN FİLMLERİ

Çalış, Gökçe
Yüksek Lisans, Polimer Bilimi ve Teknolojisi Bölümü
Tez Yöneticisi: Doç. Dr. İrem Erel Göktepe
Ortak Tez Yöneticisi: Doç. Dr. Sreeparna Banerjee

Haziran 2017, 97 sayfa

Poli(laktik-*ko*-glikolik asit)-*b*-poli(etilen glikol) (PLGA-*b*-PEG) amfifilik karaktere sahiptir ve bu özellik sayesinde sulu ortamda çekirdek ve kabuk yapısını oluşturabilirler. Bu PLGA-*b*-PEG nanoyapıları, biyouyumlu ve biyobozunabilir olduklarından biomedikal uygulamalarda ilaç taşıyıcı sistem olarak yaygın şekilde kullanılırlar. Kontrollü ilaç salımı uygulamaları için biyobozunur PLGA-*b*-PEG nanoyapılarını avantajlı sistemlerdir. İlaç salımı bu sistemlerde PLGA çekirdeğinin hidrolizi ile olur. Literatürde PLGA-*b*-PEG nanoyapılarının sulu çözeltilerindeki ilaç salımı davranışını inceleyen makaleler mevcuttur. Ancak PLGA-*b*-PEG polimerzomlarının yapı taşı olarak kullanıldığı katman-katman filmler hakkında sınırlı sayıda çalışma vardır.

Bu çalışmada, Doksorubisin ve Paklitasel ilaçlarının yüklendiği PLGA-*b*-PEG polimerzomeları hazırlanmış ve Tannic acid (TA) molekülü ile katman-katman filmlerde yapı taşı olarak kullanılmışlardır. Katman-katman filmlerin hazırlanma koşullarının bu filmlerden ilaç salınma kinetiğini etkilediği gösterilmiştir. Buna ek

bu filmlerin yapısına bariyer katmanları koyarak, yüzeyden ilaç salımı kinetiği kontrol edilmiştir.

PLGA-*b*-PEG polimerzomlarının katman-katman filmlere yüklenmesi, filmlerin ilaç yükleme kapasitesini artırdığı ve polimerzomeların kan dolaşımında ki stabilitesini arttırdığı için önemlidir. PLGA-*b*-PEG polimerinin biyobozunabilmesi, TA'in önemli biyolojik özellikleri ve katman-katman sistemlerden ilaç salımı kinetiğinin kontrol edilebilmesi, bu sistemlerin yüzeyden ilaç salım uygulamalarında gelecek vaat eden çalışmalar olduğunu gösterir.

Anahtar Kelimeler: PLGA-*b*-PEG, nanoyapılar, polymerzom, biyobozunma, ilaç salımı, katman-katman filmler.

To My Precious Family…

ACKNOWLEDGEMENTS

First and foremost, I would like to express my deepest gratitude to my supervisor Assoc. Prof. Dr. İrem Erel Göktepe for the valuable guidance, advice and unwavering support throughout my graduate education. Thanks to her consistent and kind guidance and encouragement, I learned worthwhile knowledge about research, interpretation and problem solving. I would like to also thank to my coadvisor Assoc. Prof. Dr. Sreeparna Banerjee for allowing to perform experiments in her laboratory and for her kind support.

This work was financially supported by The Scientific and Technological Research Council of Turkey, TUBITAK (Grant Number: 113Z586). I also thank TUBITAK for the scholarship from this project between February 9th, 2015 and February 14th, 2017.

I would like to express my sincere appreciation to my dear friend Dilara Gündoğdu. During all time of my research, she helped and supported me with her kindness. I also would like to specially thank to Giray İsmetoğlu for his endless understanding and support. Besides, I would like to thank to Dilan Aslan for her lifelong friendship.

I would like to show my gratitude to my lab members Bora Onat, Cansu Üstoğlu, Eda Çağlı, Majid Akbar and Meltem Haktanıyan for their unconditional friendship and support.

Last but not least, I would like to thank my family; my mother Ayfer Çalış, my father Zeki Çalış and my little brother Göker Çalış. They have always been there for me with their endless love, understanding and support.

TABLE OF CONTENTS

LIST OF FIGURES

FIGURES

LIST OF TABLES

TABLES

LIST OF SCHEMES

SCHEMES

LIST OF ABBREVIATIONS

AFM	Atomic Force Microscopy
BCM	Block Copolymer Micelle
BPEI	Branched Poly(ethyleneimine)
CMC	Critical Micelle Concentration
CAC	Critical Aggregation Concentration
DOX	Doxorubicin
DIPEA	N,N-Diisopropylethylamine
DCM	Dichloromethane
DI	Deionize
DLS	Dynamic Light Scattering
EDC	N-(3-Dimethylaminopropyl)-N'-ethylcarbodiimide hydrochloride
FTIR	Fourier Transform Infrared Spectroscopy
FDA	Food and Drug Administration

^{1}H-NMR	Proton Nucler Magnetic Resonance
LbL	Layer-by-Layer
NHS	N-Hydroxysuccinimide
PLGA	Poly (D, L-lactic-*co*-glycolic acid)
PEG	Poly (ethylene glycol)
PLGA-*b*-PEG	Poly (D, L-lactic-*co*-glycolic acid)-*block*- polyethylene glycol
PBS	Phosphate Buffered Saline
PGA	Poly (glycolicolide)
PLA	Poly (D, L-lactide)
PCL	Polycaprolactone
PVA	Poly (vinylalcohol)
PVCL	Poly (N-vinylcaprolactam)
PTX	Paclitaxel
TA	Tannic acid

CHAPTER 1

INTRODUCTION

1.1 Biodegradable Polymers

Polymeric systems are widely used in the biomedical applications due to their favorable physical, chemical and mechanical properties [1,2]. Additionally, carbon based nature of polymers is very similar to the biological tissues so polymeric materials are convenient for medical applications [1].

Biodegradable polymers can be defined as polymers that can undergo chemical hydrolytic bond cleavage or enzyme-catalyzed hydrolysis bond cleavage in the physiological environment [3]. For biodegradation, polymers must possess hydrolytically degradable bonds including esters, anhydrides, amides, urethanes, acetals, ethers and phosphates [4]. Fig. 1 shows an example of hydrolytic degradation of an ester bond [5]. The rate of biodegradation reaction generally is affected by water uptake ability of polymer. For instance, if polymer is hydrophilic and porous, it is expected that biodegradation proceeds faster.

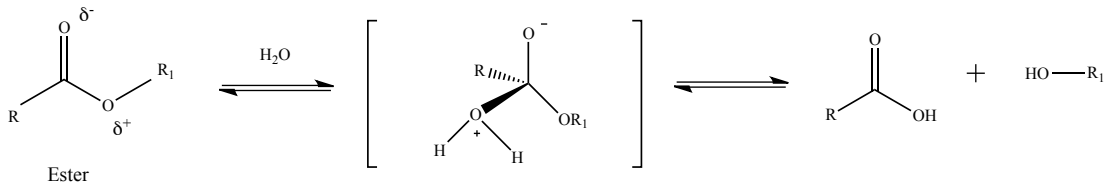

Figure 1.The hydrolytic degradation mechanism of ester bond.

The products of biodegradation reactions are generally biocompatible or nontoxic to the human body. Therefore, surgical opaaaaaerations are not required to remove the

biodegradable polymers from the body after they complete their functions. In other words, these polymeric systems can be safely excreted from the body by metabolism [6]. For this reason, biodegradable polymers are commonly used in implants and drug delivery devices [7].

The first synthetic biodegradable polymer that was used in medical applications in 1969 was poly (glycolic acid) (PGA) and it was used as a suture material. The trade name of this product is Dexon [8]. PGA sutures showed safe degradation profile in the clinical research, so PGA was considered as a suitable material for the controlled drug release applications. In 1989, the US Food and Drug Administration (FDA) approved the first biodegradable drug delivery system, which was microspheres of poly(lactic-*co*-glycolic acid) (PLGA). In this system, drug molecules were loaded into the microspheres, and slow hydrolysis of PLGA led to controlled release of drug molecules into the body, specifically to tissues suffering from prostate cancer [6].

1.1.1 Classification of Biodegradable Polymers

According to their origin, biodegradable polymers are classified as natural and synthetic.

Natural degradable polymers are biologically derived; in other words, they do not require a synthesis process. They are mostly water-soluble and biocompatible [6]. Owing to these properties, they can be used in the medical applications such as tissue engineering and drug delivery. However, natural polymers show variable degradation profiles because they have chains with different molecular weights. Moreover, they may include contaminants and functional groups in their natural origin. For this reason, there might be an undesirable immunogenic response to them in the body [9].

Gelatin and chitosan are common examples of natural biodegradable polymers which have been investigated extensively in the drug delivery studies. Gelatin is a

type of protein and derived from collagen by denaturation. It is a hydrophilic and an inexpensive polymer. Besides, it is nontoxic and biocompatible. Hence, it is commonly used as a packaging material in the food and medical products [10,11]. However, gelatin is not very advantageous for the drug delivery devices because its high water solubility causes very fast degradation of gelatin. Total dissolution of gelatin in the aqueous media is prevented by crosslinking. Crosslinked gelatin can be used in long-term drug release applications [12]. Crosslinking also leads to slower degradation of gelatin. Another example of natural polymers is chitosan, which is a positively charged linear polysaccharide. Like gelatin, it is also biocompatible, nontoxic, and biodegradable [3]. It has lots of applications in the medical area such as drug delivery, wound healing. It also shows anticoagulant properties [13]. Besides these, it was also suggested that chitosan has antitumor effect [14]. Therefore, it has a great potential in the treatment of cancer [13–15].

In contrast to natural degradable polymers, synthetic degradable polymers are produced by chemical reactions, so called "polymerization reactions". They can be designed with wide a range of composition, chain length and monomer arrangement. These features introduce controllable degradation behavior to synthetic polymers, i.e. reproducible and predictable degradation profile [9]. That's why they offer an advantage for biomedical applications. The major disadvantage of synthetic degradable polymers is lack of solubility in aqueous environment. Water insoluble molecules can be recognized as foreign materials in the body therefore they are problematic in biomedical applications. This problem is generally overcome by coupling them with hydrophilic co-monomers via copolymerization.

The common example of synthetic biodegradable polymers, especially for delivery systems, is polyesters, which are poly(lactic acid) (PLA), poly(glycolic acid) (PGA), poly(D, L-lactic-*co*-glycolic acid) (PLGA) and poly(caprolactone) (εPCL). εPCL is hydrophobic like most synthetic degradable polymers. The degradation rate of εPCL is very slow so it can be suitable for the production of implants or carriers for long-term drug delivery [10]. Similar to εPCL, PGA is hydrophobic but its

degradation rate is faster. Unfortunately, PGA has limited use as a drug carrier because it is not soluble in common organic solvents, and this prevents the formation of PGA nanocarries. To overcome this problem, more soluble copolymer forms of PGA are synthesized via copolymerization with PLA [16]. PLA is soluble in common organic solvents so nanoaggregates of copolymers of PLA and PGA can be formed for drug delivery applications. PLA is more hydrophobic than PGA due to one extra methyl group in its backbone. This leads to slower degradation rate than PGA. Total degradation of high molecular weight PLA takes 2-5 years [16]. PLGA is one of the mostly used biodegradable polymers in drug delivery applications. PLGA is a copolymer of glycolic acid and lactic acid. Copolymerization improves the solubility of PGA in water and shortens the degradation time of PLA. Physicochemical properties of PLGA can be arranged by changing ratios of lactic acid and glycolic acid units to design a better drug delivery device [3].

1.1.2 Factors Affecting Biodegradation Behavior

As discussed earlier, degradation of polymers occurs via hydrolysis of labile bonds in polymer backbone leading to decrease in molecular weight. The degradation is affected by several factors, mainly the chemical nature of the polymer backbone. The chemical structure and composition of the polymer are important parameters for degradation reactions [17]. Indeed, the nature of chemical bonds between monomer units affect the rate of degradation [18]. For example, ester bonds undergo faster hydrolysis than ether bonds due to more electrophile carbonyl group. Thus, polyesters shows higher rate of biodegradation [4].

Other factors influencing the biodegradation behavior of the polymers are water solubility, morphology and molecular weight of the polymer as well as additives and shape of the polymeric device. Among these factors, water solubility of polymer is very critical on the degradation rate because hydrophilicity of polymer permits water penetration into the polymer matrix so degradation of bonds by hydrolysis becomes faster. In contrast, hydrophobic polymers do not allow water

molecules to penetrate. This means hydrophobic polymers undergo slow hydrolysis [9]. Park and coworkers studied the effect of hydrophilic groups on biodegradation of a poly(ester amide)s. In this study, different number of amide groups were introduced into a hydrophobic aliphatic polyester, poly(1,4-buthylene adipate) and poly(1,4-buthylene succinate) so functionalized polyester gained more hydrophilic character. Owing to higher extent of moisture absorption, the hydrolytic degradation behavior of the polyester was improved. However, too much amide groups caused the phase separation between crystalline and amorphous regions. This amide resulted in decrease in degradability of polymer because water molecules could not penetrate into dense crystalline regions [19]. Molecular weight of polymers is also an important parameter for biodegradation behavior. The degradation time increases with increasing molecular weight of the polymer because there are more number of bonds to be broken. Another reason is that longer chains increase hydrophobicity of polymer, which reduces the ability of water uptake of polymer [9]. Additionally, size, porosity, and shape of polymeric device affect the total duration for biodegradation. The high surface to volume ratio of device results in greater accessibility of the functional groups to water molecules.

1.1.3 Mechanisms of Biodegradation

Generally, most of synthetic biodegradable polymers undergo the chemical hydrolytic bond cleavage whereas natural occurring biodegradable polymers are exposed to enzyme-catalyzed hydrolysis [20].

All biodegradable polymers have hydrolytically labile bonds in backbones such as ester, amide, and anhydride [21]. Owing to hydrolytic rupture of these bonds, water-soluble monomers and oligomers are formed. In the aqueous environment, these products leave the polymer structure. The sum of all these processes is called the polymer erosion via biodegradation [9,18]. According to the type of water diffusion mechanism into polymer matrix, erosion can take place by two different ways: i) the bulk erosion and ii) the surface erosion. Scheme 1 demonstrates biodegradation of polymers through different mechanisms. In the bulk erosion,

water molecules can penetrate into all over polymer; hence, polymer degrades homogenously in all parts. For example, polyesters such as PLGA, PGA, and PLA undergo bulk degradation. For the surface erosion, degradation occurs at the outer surface of the polymer matrix, not at inner parts of the polymer. Therefore, the surface erosion is a heterogeneous process. Polyanhydrides are examples of surface eroding polymers [20,22,23].

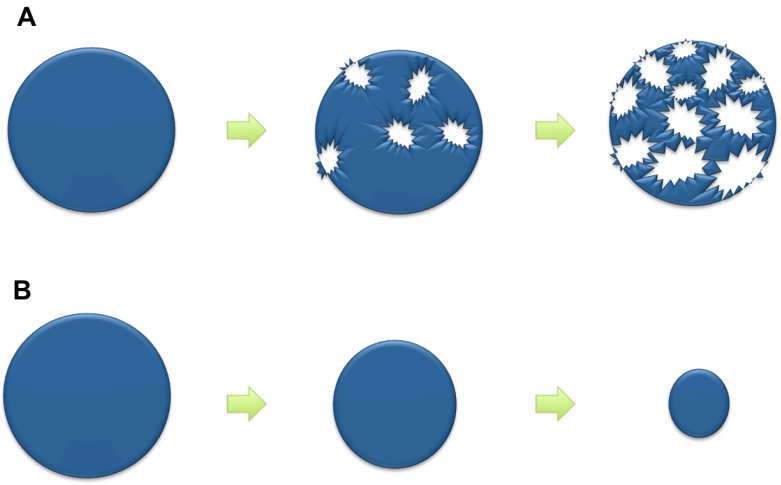

Scheme 1. Biodegradation of polymer through bulk erosion (A), surface erosion (B) mechanisms. Modified from Dinarvand et al., Int. J. Nanomedicine, 2011 [24].

1.2 Amphiphilic Block Copolymers

An amphiphilic block copolymer is composed of a hydrophilic and a hydrophobic block. The hydrophobic block tends to aggregate in water due to inter molecular hydrophobic-hydrophobic interactions among the polymer chains [25]. On the other hand, the block copolymer remains soluble in water due to the hydrophilic block. In aqueous environment, hydrophilic blocks expand into water whereas hydrophobic blocks tend to be together. This behaviour of the amphiphilic block copolymer in aqueous environment induces the self-assembly of the amphiphilic block copolymer resulting in formation of nanosized structures with different morphologies, such as

micelles and polymersomes in water [26]. Since amphiphilic block copolymers can form nanostructures in aqueous solution, they are attractive for the drug delivery applications. The drugs having poor solubility in water can create embolism, which happens via aggregation of drug molecules. Thus, free drugs cannot be given to the patients. Polymer micelles and polymersomes have the advantage of encapsulating hydrophobic drug molecules. In this way, the solubility of hydrophobic drugs in the body fluid is improved.

Encapsulating hydrophobic drug molecules in the polymer micelles or polymersomes provide longer life-time to the drug molecules because there is a decrease in possibility for recognization of them as foreign materials in body. In addition to these, some therapeutics especially cancer drugs are very toxic at high doses. Compared to free drugs, encapsulated ones lead to fewer side effects due to slower release rate [27]. As briefly discussed above, many of the challenges associated with therapeutics such as hydrophobicity, high toxicity, and short life-time in the body can be overcome by using polymer micelles or polymersomes [28].

1.2.1 Self-Assembled Structures of Amphiphilic Blok Copolymers

As discussed in Section 1.2, amphiphilic block copolymers can self-assemble into nanosized structures. According to their morphologies, such nanostructures can be mainly classified as micelles and polymersomes. Micelles have a core-shell structure, the hydrophilic block forming the corona and the hydrophobic block forming the micellar cores. Polymersomes are hollow cages with a hydrophilic core, a hydrophobic shell and hydrophilic corona.

1.2.1.1 Block Copolymer Micelles

In this structure, polymers self-assemble into nanoaggregates with hydrophobic core and hydrophilic shell structure. Schematic representation of a block copolymer micelle (BCM) in the aqueous environment is shown in Fig. 2.

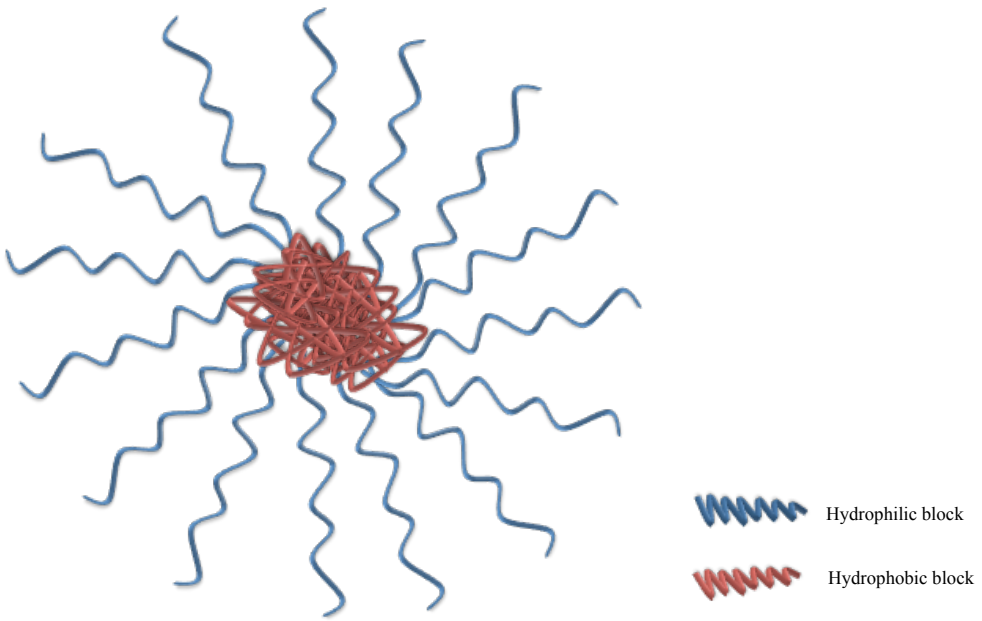

Figure 2. Schematic representation of a block copolymer micelle in aqueous environment**.**

At very low concentrations, the amphiphilic polymers exist only as individual chains. As the concentration increases, the free energy of the system increases due to unfavorable interactions between hydrophobic blocks and water molecules. To reduce this free energy, the hydrophobic blocks start to leave the aqueous media and interact with each other by the hydrophobic-hydrophobic interactions. This gives rise to the self-assembly of amphiphilic block copolymers to adopt low energy state configuration. The specific concentration at which the polymer starts to form micelle is called the critical micelle concentration (CMC). If the concentration is above the CMC, the micelle structures are thermodynamically stable [25-26,29].

There are two methods for the preparation of the BCMs depending on the water solubility of the polymer. These are: i) direct dissolution and ii) solvent exchange. Direct dissolution method is preferred for the polymers, which are relatively water soluble. In this method, BCMs are formed by direct dissolution of the polymer in water at a concentration above the CMC. Additionally, hydrophobic drug molecules can be loaded into the BCMs by adding the small amount of drug solution into prepared BCMs solution [25,30].

On the other hand, the BCMs of highly hydrophobic amphiphilic block copolymers are prepared by solvent exchange method. In this method, both the polymer and the hydrophobic drug are dissolved in an organic solvent, and then the solution is added into water. The formation of a BCM is triggered by removal of the organic solvent. Dialysis or oil-in-water (O/W) emulsion methods can be employed to induce micellization depending on miscibility of organic solvent with water. For water-miscible organic solvents, the BCMs are formed by dialysis against water. For water-immiscible organic solvents, the BCMs are prepared by emulsion method. In this method, polymers dissolved in water-immiscible organic solvent are homogenously dispersed by sonication, and BCMs are formed during removal of the solvent by evaporation [26]. For example, the BCMs were prepared from poly (ethylene oxide)-block-poly (β -benzyl-l-aspartate) (PEO-PBLA) by two different techniques, emulsion and dialysis. In emulsion method, the polymer was dissolved in chloroform and then added to the aqueous environment. The homogeneous emulsion was obtained by sonication, and then organic solvent was removed by evaporation. After evaporation of organic solvent, the BCMs were formed. In dialysis method, the polymer was dissolved in dimethylformamide (DMF). Owing to water miscible nature of DMF, the polymer solution was added into water and then the mixture was dialyzed against water to remove the organic solvent. These two preparation methods had different doxorubicin (DOX) encapsulation efficiencies, which is determined by UV absorption. For emulsification method, DOX content in the BCMs was determined as 12% whereas it was 8% for dialysis method [31,32].

In addition to the micellization methods discussed above, if the polymer exhibits stimuli responsive behaviour, i.e. they have ability to change their physical and chemical properties reversibly under external stimuli such as pH, temperature, and light, then micellization can also be induced by changing external stimuli.

For example, poly(2-vinlypyridine-*b*-ethylene oxide) (P2VP-*b*-PEO) is soluble in water at acidic pH. However, above pK_a of P2VP (pK_a 5), this block becomes deprotonated and it is not soluble in water anymore. PEO is a neutral polymer and its solubility is not affected by the pH changes. The enhanced hydrophobic-hydrophobic interactions among P2VP blocks induces the self-assembly in aqueous environment resulting in BCMs with PEO-coronaand P2VP-core structures [33].

1.2.1.2 Polymersomes

Polymersomes are hollow spheres with hydrophilic inner core, hydrophobic shell and hydrophilic corona which are also produced via self-assembly of an amphiphilic block copolymer in aqueous solution. They have a similar core-shell structure like BCMs, however their cores are hollow and hydrophilic. The core of these vesicles is surrounded by the hydrophobic block of the amphiphilic block copolymer like a membrane and the hydrophilic block heads towards the water molecules Fig. 3 shows schematic representation of a polymersome. Like BCMs, their formation depends on a critical concentration value, which is named critical aggregation concentration (CAC). Below CAC, the polymers exist as unimers and only above CAC, polymersomes are formed [34].

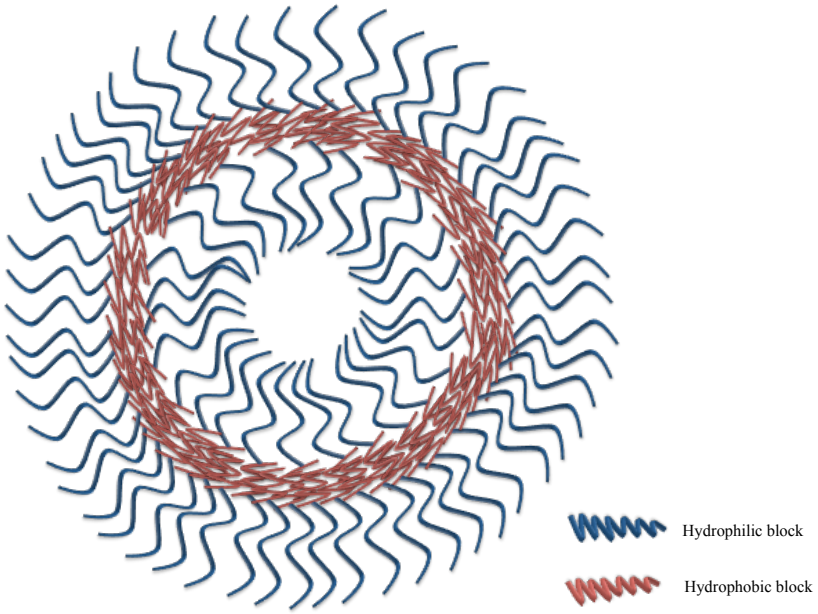

Figure 3. Schematic representation of a polymersome in aqueous environment.

The most commonly used method for preparation of polymersome is the solvent displacement. In this method, the amphiphilic block copolymer is dissolved in a good solvent for both blocks, and then water is gradually added to polymer solution. Finally, organic solvent is removed by either dialysis or evaporation. Similar to the formation of BCMs, in the aqueous environment, the hydrophobic parts tend to attract to each other for decreasing water interaction. At the same time, the hydrophilic blocks are dissolved in water. To stabilize the hydrophobic blocks, the hydropohilic blocks are arranged as a bilayer around the hydrophobic block. As a result of this self-assembly, hydrophobic blocks create a shell, and hydrophilic blocks are located at core and corona parts [26,35,36]. In the drug delivery applications, the hydrophilic cores of polymersomes act as a drug reservoir for hydrophilic drugs. They can also encapsulate hydrophobic drugs in their hydrophobic shell. Therefore, polymersomes are important nanocarriers for the dual drug delivery applications [37].

Generally, polymersomes are formed when hydrophobic block is longer than the hydrophilic block in the amphiphilic copolymer.

For example, Chen and coworkers studied drug release from degradable micelle or polymersomes of poly(ethyleneglycol-*block*-2,4,6-trimethoxybenzylidenepentaery thritolcarbonate) (PEG-*b*-PTMBPEC). They synthesized PEG-*b*-PTMBPEC with varying chain lengths and block ratios. Polymersomes were produced using PEG-*b*-PTMBPEC having a molar mass of 1.9 k and 6 k for the PEG and PTMBPEC blocks, respectively. BCMs were produced using PEG-*b*-PTMBPEC having a molar mass of 5 k and 5.8 k for the PEG and PTMBPEC blocks, respectively. In this study, polymersomes and micelles were prepared by the same method. Firstly, the polymer was dissolved in dioxane solution, and then water was added into this solution. To remove the organic solvent, the aqueous solution was dialyzed against water. The size of polymersomes and BCMs were about 120 nm and 35 nm, respectively. Both hydrophilic drug, Doxorubicin (DOX) and hydrophobic drug, Paclitaxel (PTX), could be loaded into the polymersomes. On the other hand, BCMs could only entrap PTX into their cores [38].

However, block ratio in an amphiphilic block copolymer is not the only criteria determining the morphology of nanostructures because by using different techniques, poylmersomes and BCMs structures can be prepared from the same polymer [39].

1.3 Biodegradable and Amphiphilic Block Copolymer; PLGA-*b*-PEG

Poly (lactic-*co*-glycolic acid)-*b*-poly (ethylene glycol) (PLGA-*b*-PEG) is composed of PEG and PLGA blocks (Fig. 4). It is an amphiphilic block polymer with hydrophilic PEG and hydrophobic PLGA segments. Owing to its amphiphilic nature, PLGA-*b*-PEG self-assembles into nanoaggregates in aqueous solution, which may act as carriers in drug delivery applications. PLGA-*b*-PEG has already been approved by FDA for therapeutic use in humans due to its biodegradable and biocompatible nature. Therefore, it is one of the mostly used polymers in the biomedical applications [40].

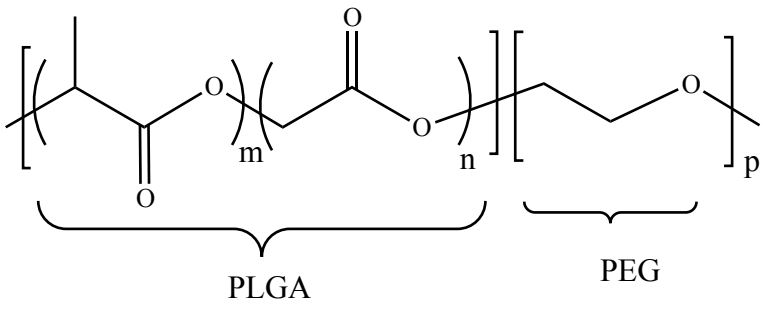

m = number of units of lactic acid
n = number of units of glycolic acid
p = number of units of ethylene glycol

Figure 4. Chemical structure of PLGA-*b*-PEG.

The first synthesis of PLGA-*b*-PEG was achieved by Gref and coworkers. The carboxylic acid end group of PLGA was covalently linked to the amine end group of PEG. The resulting block copolymer was used as the building block for the preparation of nanoaggregates. This study also discussed the effect of PEG outer-corona on the blood circulation time of nanoaggregates in vivo. They found that PEG outer-corona increased the circulation time via preventing recognition of hydrophobic PLGA units by the immune system [41].

PEG is a polyether. It is nonionic, hydrophilic, and biocompatible [42]. Owing to the hydrophilic nature, a PEG-corona stabilizes the nanoaggregates in aqueous environment. In other words, it improves the solubility of nanoaggregates and avoids aggregation of hydrophobic PLGA units by hydrophobic-hydrophobic interactions. Although it is not a biodegradable polymer, PEG having low molecular weights can be excreted from the human body [10,40]. The biodegradability of PLGA-*b*-PEG is due to its PLGA unit.

Ester bonds of PLGA go into hydrolytic degradation in water to produce lactic acid and glycolic acid monomers. These monomers are eliminated from the body as carbon dioxide and water by metabolism, Krebs cycle (Fig. 5) [40,43–45].

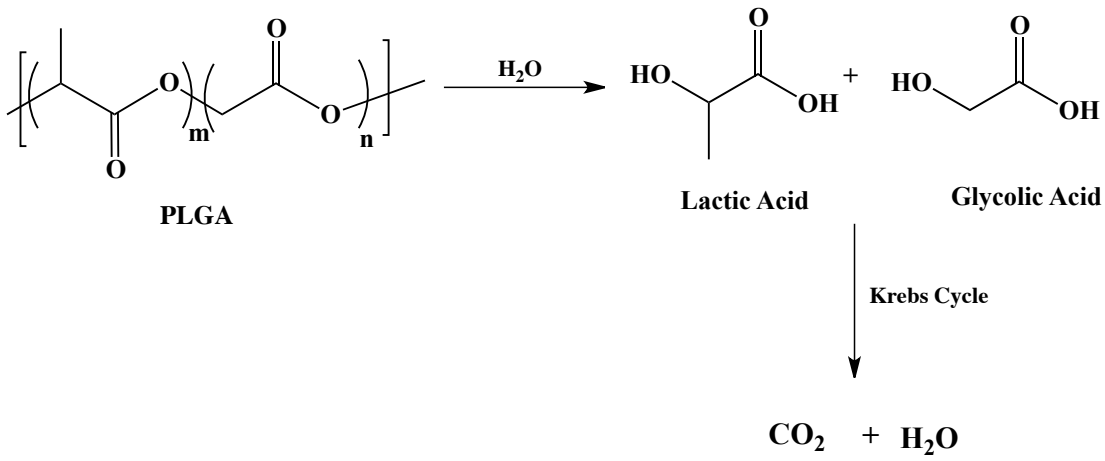

Figure 5. Hydrolytic degradation of PLGA in the body.

PLGA is a copolymer consisting of lactic and glycolic acid units. As discussed in Section 1.1.1 poly (lactic acid) (PLA) and poly (glycolic acid) (PGA) have different hydrophobicities and so show different degradation profiles. Because of the additional methyl group, PLA is more hydrophobic than PGA, thus PLA undergoes slower degradation. Thanks to this difference, the degradation kinetic of PLGA can be varied from days to months by changing the ratio of lactic acid to glycolic acid in the copolymer [43]. In 1995, Park published a study about the effect of copolymer composition on degradation of PLGA microspheres. In this study, PLGA polymers with 90:10, 80:20, 70:30, and 50:50 ratios of lactic acid to glycolic acid were analyzed. According to their results, the polymers with higher glycolic acid content, 70:30 and 50:50, demonstrated higher decrease in the molecular weight and PLGA with 50:50 ratio had the fastest the rate of degradation in long term according to the experiment results determining the lactic acid formation in the medium [46].

1.4 Layer-by-Layer Self-Assembly Technique and Polymer Multilayer Films

Layer-by-layer (LbL) technique is a method for fabricating thin films. It is based on alternating deposition of interacting polymers at the surface via self-diffusion

mechanism. LbL deposition was first introduced by Iler in 1966. In this work, negatively and positively charged colloidal particles were sequentially adsorbed onto the surface [47]. In 1992, Decher and Hong reported the first LbL self-assembled thin films of oppositely charged polyelectrolytes. Scheme 2 demonstrates the LbL process described by Decher and Hong. Firstly, the positively charged silicon surface, which was treated with aminopropylsilane and made positively charged, was immersed into polyanion solution for 20 minutes. Then, the surface was rinsed with pure water in order to remove loosely bound polyelectrolytes. The polyanion coated, negatively charged substrate was immersed into polycation solution for 20 minutes for the deposition of the second layer. Similarly, the coated substrate was rinsed with pure water to remove the loosely bound polymers. This cycle is repeated until the desired thickness or morphology is achieved. The driving force for the multilayer assembly is charge attraction of oppositely charged layers [48].

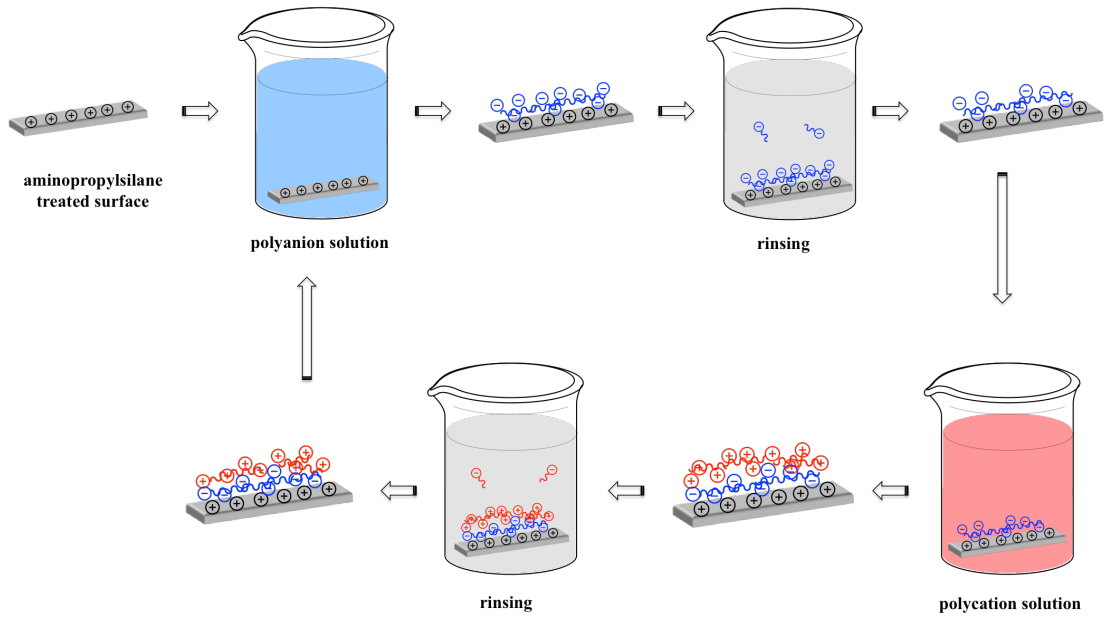

Scheme 2. Schematic representation of LbL thin film preparation technique for polyelectrolyte multilayers Modified from Desher et al., Thin Solid Films, 1992 [48].

The LbL coating has been intensively investigated for biomedical applications such as controlled release, biosensors, and tissue engineering due to possibility of film preparation in aqueous environment and versatility of interactions that could drive the LbL process, enabling the use of wide variety of polymers as building blocks in self-assembly [49,50]. LbL method offers simple and inexpensive preparation of multilayers. Additionally, the bioactive molecules like drugs, proteins and DNA can be safely incorporated in the LbL structure because the deposition process is performed in the aqueous medium at room temperature [51]. In addition, the LbL technique allows controlling the composition and morphology of the thin films at molecular level. Therefore, the medical surfaces can be designed as biocompatible and functional carrier systems for drugs, dyes, enzymes, and nucleic acids can be prepared [51,52].

The LbL self-assembly can be constructed in two-dimensional or three-dimensional substrates. Assembly on two-dimensional surfaces produces thin films, which can be used in controlled and sustained delivery of the bioactive molecules. Generally, depending on the characterization method of interest, 2D substrate is chosen among either of the following substrates in research studies: silicon wafer, glass, quartz or mica [53]. The first LbL deposition on 3D spherical template was achieved by Caruso in 1998. Polystyrene latex was used as a template, and multilayers of SiO_2/poly (diallyldimethylammonium chloride) (PDMAC) were electrostatically adsorbed onto the template. Dissolution of polystyrene template resulted in the formation of hollow capsule, in which drug molecules could be loaded [54]. LbL hollow capsules are promising for targeted drug delivery applications [55].

The LbL self-assembly is not limited to electrostatic interactions. Hydrogen bonding [56], hydrophobic interactions [57], van der Walls forces [58], coordination bonding [59,60], charge-transfer [61], metal-ligand [62,63] and bio-specific [64] interactions can also drive the LbL self-assembly. Among these, hydrogen-bonded multilayers attracted great attention for biomedical applications due to lower toxicity of neutral polymers than the polycations and the responsive properties of the films at mild pH conditions. Similar to electrostatic self-assembly,

hydrogen-bonded LbL films can be produced by alternating immersion of the substrate into solutions of hydrogen accepting and hydrogen donating polymers [65]. Hydrogen-bonded self-assembly at the surface was first demonstrated by Stockton and Rubner. They tried to self-assemble polyaniline with different nonionic polymers via hydrogen bonding onto glass, metal, silicon and plastic substrates. According to the FTIR results, they confirmed that both polyaniline/ poly(vinylpyrrolidone) and polyaniline/ poly(etyleneoxide) pairs were alternatingly bound to the surface via hydrogen bonding [66].

1.4.1 LbL Self-Assembly of Amphiphilic Block Copolymers

As discussed in Section 1.2.1, amphiphilic block copolymers can form nanoaggregates with core-shell structures in aqueous media, and these structures can be used as carriers for bioactive compounds. Incorporating such nanoaggregates into LbL films are of interest to increase the loading capacity of multilayers especially for hydrophobic drug molecules and improve the stability of the nanoaggregates in the bloodstream. Hydrophilic coronal blocks of polymer nanoaggregates expand to water in aqueous environment, and this morphology allows the hydrophilic block to interact with other compounds through electrostatic and physical interactions described for LbL process in Section 1.4, by the help of this feature, amphiphilic block copolymer structures can be incorporated into LbL films. For example, the electrostatic interaction between polyacrylic acid (PAA)-corona of polystyrene-*b*-poly(acrylic acid) (PAA-*b*-PS) micelles and poly(diallyl dimethylammonium chloride) (PDMAC) resulted in alternating deposition of PAA-*b*-PS micelles and PDMAC at the surface [67]. In another study, Kim et al. prepared hydrogen-bonded multilayers of poly (acrylic acid) and Triclosan loaded BCMs of poly(ethylene oxide)-*b*-poly(ε-caprolactone) (PEO-*b*-εPCL) with PEO-corona and PCL-core in acidic conditions. They demonstrated that the hydrogen bonds are disrupted at pH 7.5 due to deprotonation of PAA, PEO-*b*-εPCL micelles are released and Triclosan release was achieved via diffusion from the micellar cores [68].

1.4.2 Drug Release from The LbL Polymer Films

The LbL polymer films, loaded with functional molecules can be used as a matrix for controlled and sustained drug release applications. The LbL film acts as a diffusion barrier, lowers the rate of drug release and provides prolonged release [69]. Therefore, it is possible to control the rate of release from the LbL films by controlling the film properties during self-assembly [70].

Drug molecules can be incorporated into LbL films in two ways: i) incorporation of drugs or drug carriers in the film structure during the assembly process and ii) loading drug molecules into the multilayers at the post-assembly step. The drug release from LbL films can be achieved by diffusion, stimuli-induced disruption of interactions among the layers or rearrangements within the multilayers or degradation of the multilayers [49].

1.4.2.1 Drug Release from Polymers Multilayers via Diffusion

The basic mechanism of drug release from the multilayer is diffusion of small drug molecules through multilayers to body fluid. The multilayers can act as drug reservoirs and also diffusion barriers. Therefore, sustained release of drugs can be achieved by using multilayers.

For example, Nguyen and coworkers prepared Triclosan loaded poly(propylene oxide)-*b*-poly (amidoamine) micelles and used them as building blocks to construct LbL film with PAA through electrostatic interactions. Poly(propylene oxide)-*b*-poly(amidoamine) micelles/PAA multilayers were immersed into phosphate buffered saline (PBS) at pH 7.4 and 37 $^{\circ}$C and Triclosan released from the surface through diffusion [71].

1.4.2.2 Drug Release from Polymer Multilayers via Disruption of Interactions

Drug release from LbL films can be achieved by disruption of interactions between the building blocks. By controlling the interactions among the polymer layers or drug molecules, drug molecules will be free to escape from the LbL film surface.

It is not easy to break interactions between the polyelectrolytes. However, it is possible to manipulate net charge on the weak polyelectrolytes by changing pH. For instance, Chung and Rubner studied pH-controlled release of methylene blue from the multilayers of poly (acrylic acid) (PAA) and poly (allyamine hydrochloride) (PAH). The multilayers were constructed at pH 2.5 via electrostatic interactions. The pK_a of PAA and PAH is 5.5 and 8, respectively. Multilayers were produced at pH 2.5 when PAA was partially charged and the number of binding points among PAA and PAH was low, resulting in a loosely bound multilayer structure. This was preferred to allow efficient penetration of Methylene Blue (MB) molecules into the film matrix. Methylene blue was loaded by immersing the multilayers into MB solution at pH 7 at the post-assembly step. The loading was achieved via electrostatic interactions among positively charged MB and negatively charged PAA at pH 7. Note that ionization of PAA is enhanced with increasing pH. MB release studies were conducted in PBS solution at pH 3, pH 5 and pH 7. The greatest amount of release was recorded at pH 3 due to protonation of PAA and loss of electrostatic interactions between PAA and methylene blue [72].

As discussed in Section 1.4.1, hydrogen-bonded LbL films are more responsive to environmental changes than the electrostatic multilayers. Sukhishvili and coworkers produced erasable hydrogen-bonded LbL films composed of poly(ethylene oxide) and poly(methacrylic acid) (PMAA) at pH 2. The positively charged dye molecules, Rhodamine 6G, was incorporated into multilayers at pH 4 when PMAA was slightly more negative but multilayers were intact. Rhodamine 6G could be released by increasing the pH to 5.5 where PMAA was further ionized and hydrogen bonds among the layers were disrupted [73].

In another study, Erel et al. showed the disintegration of hydrogen-bonded multilayers via decreasing pH. Multilayers of poly [2-(N-morpholino) ethyl methacrylate-*block*-2- (diisopropylamino) ethyl methacrylate] (PMEMA-*b*-PDPA) micelles and Tannic Acid was constructed at pH 7.4 when TA was partially ionized and had protonated hydroxyl groups to drive the hydrogen-bonded self-assembly. Multilayers disintegrated at acidic conditions when PDPA micellar cores got protonated resulting in disintegration of the micelles as well as created a charge imbalance in the multilayers [74].

1.4.2.3 Drug Release from Polymer Multilayers via Rearrangement of Polymer Layers

In LbL structure, responsive polymer layers can alter their arrangements depending on the environmental changes such as temperature and pH. This rearrangement of polymers leads to formation of a porous structure within the multilayers, increasing the rate of drug release.

For example, Erel et al. showed the effect of pH-triggered dissolution of PMEMA-*b*-PDPA micelles on release of pyrene from the LbL films of PMEMA-*b*-PDPA micelles and TA. They found that pyrene released only via self-diffusion at pH 7.5 when both PMEMA-*b*-PDPA micelles and multilayers were intact. However, pyrene released from the surface was 2.5 times higher than that at pH 7.5 when the pH was lowered to 5 and PMEMA-*b*-PDPA micelles dissolved [74].

Polymers having temperature responsive behaviors are also used in the fabrication of LbL films and enables release of functional molecules from the film surface via temperature trigger. For temperature triggered release studies, poly (N-isopropylacrylamide) (PNIPAm) is the most commonly used polymer because its lower critical solution temperature (LCST) (32°C) [75] is close to the body temperature. Quinn and Caruso explained the release of Rhodamine B from LbL films of PNIPAm and PAA. Film deposition temperature was set as 30 °C for

PNIPAAm and 21 °C for PAA. When multilayers were exposed to 21 °C, 32 °C, 40 °C, or 50 °C at the post-assembly step, the fastest release was observed at 50 °C due to phase conformational changes in PNIPAm above its LCST resulting in formation of pores within the multilayers [76].

In another example, Sukhishvili and coworkers deposited poly(N-vinylpyrrolidone)-*b*-PNIPAm (PVPON-*b*-PNINAm) micelles and TA into LbL film at 40 °C. Poly(N-vinylpyrrolidone)-*b*-PNIPAm (PVPON-*b*-PNINAm) micelles have PVPON-corona and temperature-responsive PNINAm-core. The film deposition temperature, 40 °C, is above LCST of PNINAm. Doxorubicin (DOX) was loaded into these films at the post-assembly step by immersing the multilayers into DOX solution. They found that temperature-triggered release of DOX accelerated at 20 °C due to disintegration of PNIPAm micellar cores below its LCST [77].

1.4.2.4 Drug Release from Polymer Multilayers via Degradation of Polymer Layers

Degradable polymers are also used as building blocks in the LbL film assembly. By arranging the degradation profile of the polymers, the rate of drug release from multilayers can be controlled. In this way, sustained and controlled drug release may also be achieved via enzymatic or hydrolytic cleavage of the polymers when such degradable films are implanted into the body.

For example, electrostatic LbL films of negatively charged DNA and positively charged poly-L-lysine (PLL) enzymatically degraded when immersed into Trypsin solution. Trypsin which is a digestive enzyme for PLL resulted in degradation of PLL and disintegration of the multilayers. The release profile could also be controlled by crosslinking of the multilayers with glutaraldehyde. When multilayers were crosslinked, the rate of degradation decreased [78].

Hammond and coworkers reported on construction of LbL films of hydrolytically degradable poly (β-amino ester). As a complementary polyanion, poly(styrene sulfonate) was used in the fabrication of LbL films. When the film was immersed into PBS buffer at 37 °C, the thickness of LbL film gradually decreased. The hydrolytic cleavage of ester bonds in poly(β-amino ester) caused disintegration of the multilayers. It was expected that if drug molecules were introduced into the film structure, sustained release of drugs would be achieved [79]. In another study of the same group, Heparin release from the multilayers of Heparinand poly (β-amino ester) was achieved by hydrolytic degradation of poly (β-amino ester) and disruption of multilayers [80].

In another study by Park and coworkers poly(lactic-*co*-glycolic acid) grafted hyaluronic acid (HA-g-PLGA) micellar aggregates were incorporated into Heparin/PLL multilayers and sustained release of PTX was conducted from the surface via hydrolytic degradation of PLGA [81].

1.4.3 Dual Drug Release for Cancer Treatment

Different type of cancer therapeutics can be effective on cancer cells by individual anti-tumor mechanisms. For example, DOX interacts with DNA by intercalation and preventing the replication process whereas PTX inhibits microtubules disassembly and blocks the progression of mitosis. It was suggested when these two drugs are used for cancer treatment, the combination of two different mechanisms result in additive effect on cancer cells. The report about dual release of DOX and PTX from PEG-*b*-PLGA polymersomes showed that DOX and PTX loaded polymersomes were more effective than only PTX loaded polymersomes [82]

1.5 Aim of Thesis

This study aimed to incorporate PLGA-*b*-PEG polymersomes into LbL films to increase the loading capacity of multilayers films and provide dual drug release from the surface via hydrolytic degradation of the PLGA region of the PLGA-*b*-PEG polymersomes. This study also aimed to examine the effect of film deposition pH on the release of drug molecules at neutral and acidic conditions. Finally, this study aimed to examine the effect of barrier layers and film architecture on the release kinetics of drug molecules from the surface.

Polymer micellar aggregates are ideal drug carriers due to their hydrophobic cores which are capable of encapsulating drug molecules with low water solubility. Incorporating micellar aggregates into LbL films not only increases the loading capacity of the films for drug molecules with low water solubility but also provides stability to the micelles against dilution in the blood stream. Different from polymer micelles, polymersomes have the advantage of encapsulating both hydrophilic and hydrophobic drugs. Thus, incorporation of polymersomes into LbL films may provide dual drug release from the surface of a polymer matrix. In addition, layers in a film structure can act as diffusion barriers and enable control in the kinetics of drug release from the surface.

Although there are studies concerning drug-delivery from PLGA-b-PEG polymersomes, the number of studies concerning LbL films of PLGA-b-PEG polymersomes is limited. The major difficulty in the incorporation of polymersomes into LbL films is the relatively big size of polymersomes than that of micelles causing an instability in the multilayer structure due to discontinuous arrangements of polymersomes. Coustet studied layer-by-layer assembly of polymersomes and polyelectrolytes. It is reported that poly(benzylmethacrylate)-*block*-poly(dimethyl amino)ethylmethacrylate (PBzMA-*b*-PDMAEMA) polymersome did not formed fully covered monolayer with polystyrene sulphonate (PSS) because polymersomes disintegrated from the surface due to electrostatic attractions [83].

Different from these studies, this study reports on the LbL deposition of PLGA-*b*-PEG polymersomes and TA via hydrogen bonding interactions and examines the effect of film deposition pH and barrier layers on the release of functional molecules from the surface.

CHAPTER 2

EXPERIMENTAL

2.1 Materials

Poly(D, L-lactide-*co*-glycolide) (PLGA; acid terminated; M_w: 7,000-17,000); O-(2-Amoniethyl)-O'-(2-carboxyethyl) polyethylene glycol hydrochloride (NH_2-PEG-COOH·HCl; M_n: 3,000); poly (vinyl alcohol) (PVA; M_w: 9,000-10,000); branched poly(ethylenimine) (BPEI; M_w: 25,000); N-Hydroxysuccinimide (NHS; 98%); N-(3-Dimethylaminopropyl)-N'-ethylcarbodiimide hydrochloride (EDC); N,N-Diisopropylethylamine (DIPEA; >99%); phosphate buffered saline (PBS); disodium hydrogen phosphate dehydrate ($Na_2HPO_4.2H_2O$); sodium hydroxide; hydrochloric acid; dichloromethane (DCM; >99%); methanol (>99.9%); diethyl ether (>99.5%) were purchased from Sigma-Aldrich Chemical Co. Chloroform (>99.9%) was purchased from Acros Organics. Tannic acid (TA; M_w: 1701.2); sodium dihydrogen phosphate dehydrate ($NaH_2PO_4.2H_2O$); sulfuric acid (H_2SO_4; 98%) were purchased from Merck Chemicals. Poly (N-vinyl caprolactam) (PVCL; M_w: 1800, PDI: 1.3) was purchased from Polymer Source Inc. Doxorubicin hydrochloride (DOX·HCl) was purchased from European Pharmacopoeia Reference Standard. Paclitaxel (PXT; 99.5+%) was purchased from Alfa Aesar. The deionized (DI) water was purified by Milli-Q system (Millipore) at 18.2 MΩ. All chemicals and materials were used as received without any purification, and all solutions were prepared by DI water.

Table 1. The Structures of Polymers and Chemicals

PLGA	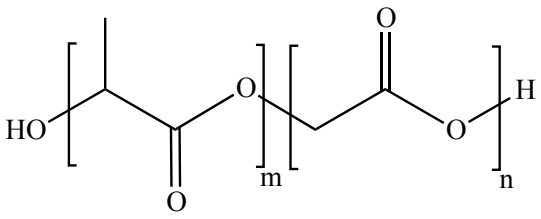
PEG	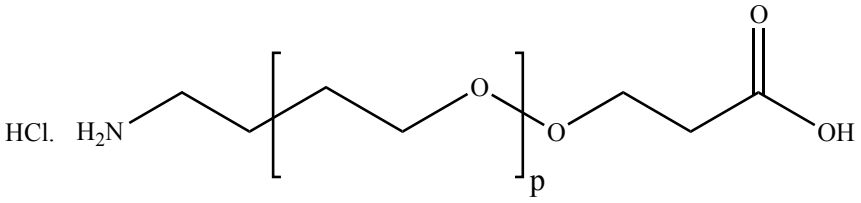
Tannic Acid	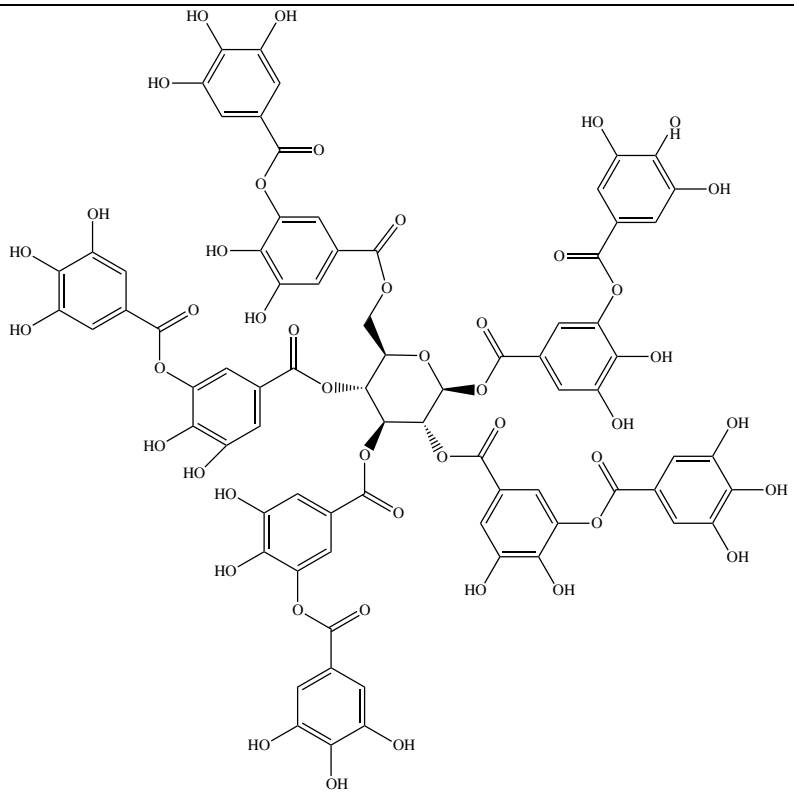
PVCL	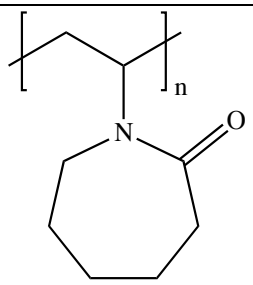

Table 1. Continued

BPEI	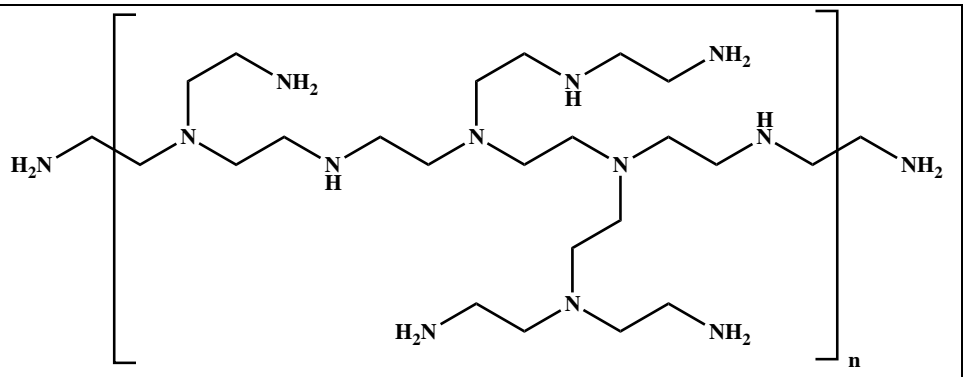
DOX	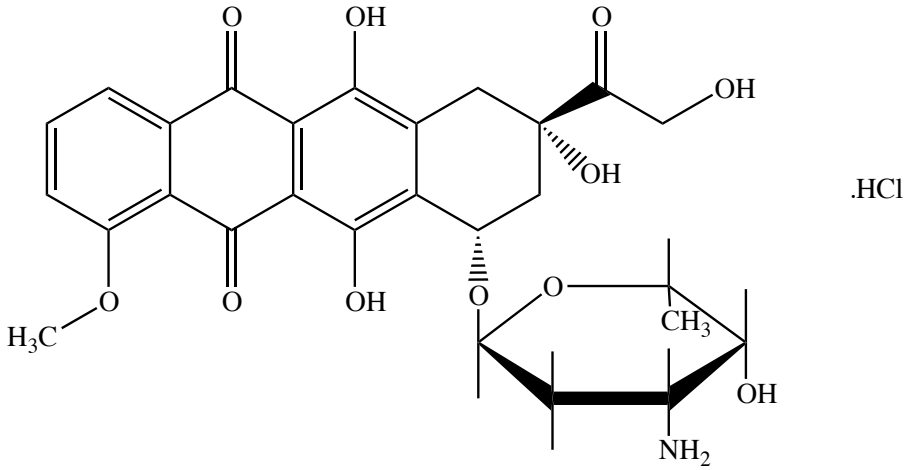 .HCl
PTX	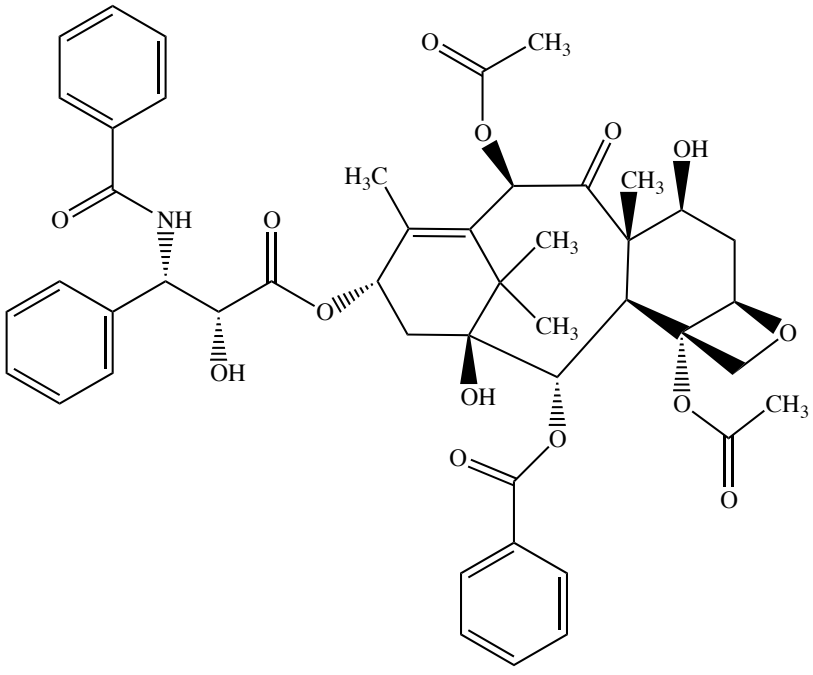

2.2 Instrumentation

Nuclear Magnetic Resonance (NMR): ^{1}H-NMR measurements were performed at room temperature using Brucker Spectrospin Avance DPX-400 Ultra shield instrument operating at 400 MHz. For measurements, 3 mg sample was dissolved in 0.6 mL deuterated chloroform ($CDCl_3$).

Fourier Transform Infrared Spectroscopy (FTIR): Nicolet iS10 FTIR was utilized to perform qualitative analysis. For sampling, KBr pellet method was used. To prepare the pellets, 5 mg sample was pelletized with 100 mg dry KBr.

pH Meter: Ohaus Starter 3000 bench pH meter was used to adjust pH of solutions.

Dynamic Light Scattering (DLS): Hydrodynamic size measurements of samples in the aqueous solution were performed by using Zetasizer Nano-ZS (Malvern Instruments Ltd., U.K.).

UV-VIS Spectroscopy: Multilayer growth on quartz substrates was followed by using VARIAN Cary 100 Bio-UV/Vis Spectrometer.

Atomic Force Microscopy (AFM): AFM imaging of the films was carried out using an NT-MDT Solver P47 AFM in tapping mode using Si cantilever. Roughness values were obtained from images with 5 x 5 μm scan size.

Transmission Electron Microscope (TEM): FEI Tecnai G2 Spirit Bio Twin CTEM with acceleration voltage of 20-120 kV was used for TEM imaging.

Fluorescence Spectroscopy: DOX release from the surface of multilayers were followed by using HITACHI Fluorescence Spectrometer.

2.3 Synthesis of PLGA-*b*-PEG

Poly (D, L-lactide-*co*-glycolide) (PLGA) and poly (ethylene glycol) (PEG) were coupled as described in Cheng's study with slight modification [84]. In the first step of the synthesis process, 30 mg PLGA (~0.0025 mmol) was dissolved in 90 μL dichloromethane (DCM). After dissolution of the polymer, 1.2 mg NHS (0.0100 mmol) and 2 mg EDC (0.0100 mmol) were added into the solution. The solution was stirred at 25 °C for 4 hours. Then, the product was precipitated and cleaned three times by washing with cold mixture of 0.2 mL methanol and 0.4 mL diethyl ether. Unreacted NHS dissolved in methanol, so it was separated. The sample was dried in vacuum oven at 25 °C for one day.

In the second step of the synthesis, 30 mg of the product (~0.0025 mmol) taken from vacuum oven was dissolved in 0.17 mL chloroform. When the dissolution was completed, 10 mg PEG (~0.0030 mmol) and 2 μL (0.0090 mmol) DIPEA were added to the solution. The solution was stirred at 25 °C for 18 hours. Then, the product was precipitated and washed with a mixture of 0.75 mL diethyl ether and 0.5 mL methanol at 4 °C for overnight. The copolymer was washed with the same solvent for two more times to remove excess PEG, and then dried in vacuum oven at 25 °C for two days. The block copolymer was analyzed by both ^{1}H-NMR and FTIR.

2.4 Preparation of (PLGA-*b*-PEG) Polymersomes

The PLGA-*b*-PEG polymersomes were prepared by double emulsion method. The procedure described by Wang and Zhao [82] was slightly modified. According to their procedure, 4 mg PLGA-*b*-PEG (~0.0002 mmol) was dissolved in 0.2 mL DCM. 40 μl DI water was added to the polymer solution dropwise while the solution was stirred. To homogenize water-in-oil emulsion, the mixture was sonicated for 3 minutes. Then, 0.4 mL of 0.1% (w/v) PVA solution was added to the water-in-oil emulsion under stirring. The mixture was emulsified by sonication

for 30 minutes. The prepared water-in-oil-in-water emulsion was diluted by adding to 2 mL of 0.1% (w/v) PVA solution under stirring. The emulsion was homogenized by sonication for 3 minutes.

The organic solvent, DCM, was evaporated while the emulsion was stirred at 25 °C for 2 hours in an open vial. After evaporation was completed, the nanoparticles were collected by centrifugation at 10 000 g for 10 min. The supernatant was separated, and DI water was added to clean particles. The centrifugation was repeated. Finally, the polymersomes were redispersed in PBS buffer (1.6 mg/mL) [82]. The hydrodynamic size of prepared polymersomes was examined by DLS and TEM. The stability of polymersomes was analyzed by using DLS.

2.5 Loading DOX & PTX to PLGA-*b*-PEG Polymersomes

20 mg/mL PLGA-*b*-PEG in DCM solution was prepared. 40 μL of 2 mg/mL Doxorubicin (DOX) solution, which was prepared in DI water, was added into the polymer solution. To encapsulate hydrophilic drug DOX, the mixture was emulsified by sonication for 20 minutes. While prepared emulsion (water-in-oil) was stirred, 0.4 mL of 0.1% w/v PVA and 40 μL of 1 mg/mL Paclitaxel (PTX) solution, which was prepared in DCM, was added respectively. To load hydrophobic drug PTX, the mixture was sonicated for 30 minutes. The subsequent steps of this experiment were identical with procedure described in the preparation of free polymersomes in Section 2.4. PLGA-*b*-PEG polymersomes were characterized using DLS and TEM.

2.6 Deposition of Multilayers of Tannic Acid and Drug Loaded or Free PLGA-*b*-PEG Polymersome

Silicon wafers, quartz slides, and glass slides were used as substrate for preparation of multilayers. Before multilayers were constructed, the substrates were cleaned with sulfuric acid. The substrates were immersed into sulfuric acid for 85 minutes. Then, the substrates were rinsed with tap water, distilled water, and DI water, respectively. The substrates were dried with inert nitrogen gas. After acid treatment, the substrates were treated with 0.25 M NaOH solution for 10 min, and then rinsed and dried as described above.

Before the deposition of TA and PLGA-*b*-PEG polymersomes, the substrates were coated with a precursor layer. The precursor layer was prepared by immersing the substrates into 0.5 mg/mL BPEI solution for 30 minutes. The substrates, taken from BPEI solution were rinsed two times with DI water for 2 minutes. After preparation of precursor layer, TA and PLGA-*b*-PEG polymersomes were alternatingly deposited onto the substrate at 25 $^{\circ}$C, either at pH 2 or at pH 7.5. The deposition of each layer was done for 5 minutes. Firstly, the substrate was immersed into 0.2 mg/mL TA solution. For deposition at pH 2, TA solution was prepared in 0.01 M sodium dihydrogen phosphate buffer whereas for deposition at pH 7.5, TA solution was prepared in 0.01 M disodium hydrogen phosphate dehydrate. After TA deposition, the substrate was rinsed twice with 0.01 M appropriate buffer solution (pH 2 or pH 7.5) and dried with nitrogen gas. Secondly, either free polymersomes or drug loaded polymersomes were deposited on the substrates coated with tannic acid. The substrate was immersed into 1.6 mg/mL solutions of PLGA-*b*-PEG polymersomes either at pH 2 or at pH 7.5. The rinsing and drying steps were identical with TA coating. The subsequent layers of TA and PLGA-*b*-PEG polymersomes were alternatingly coated in the same way described above.

The LbL growth was followed using UV-Vis spectroscopy. Multilayers were deposited onto quartz substrates. For AFM studies, multilayers were deposited onto

silicon wafers. For release experiments, the multilayers were constructed on glass substrates.

2.7 Deposition of Multilayers of Tannic Acid and Drug Loaded PLGA-*b*-PEG Polymersome with PVCL Barrier Layers

PVCL layers were incorporated into PLGA-*b*-PEG polymersomes/TAfilms in two different architectures. First architecture was alternating deposition of DOX and PTX loaded PLGA-*b*-PEG polymersomes/TA and PVCL/TA pairs. Second architecture was deposition of PVCL/TA multilayers on top of DOX and PTX loaded PLGA-*b*-PEG polymersomes/TA films. The deposition of all layers was done for 5 minutes and at pH 2. For barrier layer deposition, 0.2 mg/mL solution of PVCL was prepared in 0.01 M sodium dihydrogen phosphate buffer at pH 2. After deposition of PVCL layer, the substrate was rinsed twice with 0.01 M, pH 2 buffer solution and dried with nitrogen gas. For release experiments, the multilayers were constructed on glass substrates.

2.8 DOX Release from Multilayers

Release from four different types of multilayers were examined 1) multilayers of TA and the polymersome constructed at pH 2, 2) multilayers of TA and the polymersome constructed at pH 7.5, 3) multilayers of TA and the polymersome stacked with TA and PVCL layers constructed at pH 2, 4) alternating multilayers of TA, the polymersome and PVCL constructed at pH 2. For all types of the films containing 15 layers of the polymersome were constituted on both sides of glass slides (2x1.25 cm). DOX release was performed at pH 4, pH 6 and pH 7.5 at 37 $^{\circ}$C. DOX release was followed by immersing 2 films (total 120 layers) into 20 mL of PBS buffer at pH 7.5, pH 6 or pH 4 at 37 $^{\circ}$C. At certain time interval (every 12 hours), DOX fluorescence intensity in each release solution was followed using fluorescence spectrometer. For fluorescence emission of DOX, the solution was

excited at 490 nm, with 5 nm excitation and 10 nm emission slit widths. The emission intensity at 588 nm was followed as a function of time to monitor the release of DOX from the multilayers.

DOX release from PLGA-*b*-PEG polymersomes/TA multilayers at different pH conditions was shown in Fig. 25 and Fig 26, in section 3.7. Figure 25A and Figure 25B were composed by normalizing the fluorescence intensity data to the highest fluorescence intensity obtained from pH 7.5 multilayers at pH 4 and pH 2 multilayers at pH 4, respectively. Figure 26A, Figure 26B and Figure 26C are composed by normalizing the fluorescence intensity data to the highest fluorescence intensity obtained from pH 7.5 multilayers at pH 7.5 and pH 2 multilayers at pH 6 and pH 2 multilayers at pH 4, respectively.

Effect of barrier layers on release kinetics of DOX from the surface was shown in Fig. 27, in Section 3.7.1. Figure 27A, Figure 27B and Figure 27C were composed by normalizing the fluorescence intensity data to the highest fluorescence intensity obtained from $[polymersome/TA/PVCL/TA]_{15}$ multilayers at pH 7.5, $[polymersome/TA]_{15}$ multilayers at pH 6 and $[polymersome/TA]_{15}$ multilayers at pH 4, respectively.

2.9 PTX Release from PLGA-*b*-PEG Polymersomes

HCT-116 epithelial colorectal carcinoma cells were cultivated in high-glucose Dulbecco's Modified Eagle's Medium (Biowest, France) supplemented with 4 mM L-glutamine, 10% Fetal Bovine Serum (Gibco, USA), 100 U/mL penicillin, and 100 μg/mL streptomycin (Sigma-Aldrich, USA). After thawing the stocks, they were cultivated in T25 flasks and the medium was renewed every two or three days. All cell culture flasks were maintained in a humidified atmosphere at 37°C in 95% air and 5% CO_2 using a cell culture incubator.

To determine the anti-cancer effect of Paclitaxel-loaded PLGA-*b*-PEG polymersomes, we seeded 10,000 HCT-116 cells in each well of a 96-well TC-treated tissue culture plate. 1.6 mg/mL of Paclitaxel-loaded polymersomes solution was filter sterilized with a 0.2 μm PES filter. 24 hours after seeding cells, the cells were treated with different concentrations of Paclitaxel-loaded polymeromes (1.6 mg/mL) and compared to the non-treated controls. 24 hours after the treatment, cells were rinsed with PBS and the standard growth medium was replaced with the medium supplemented with 0.5 mg/mL of 3-(4,5-dimethylthiazolyl-2)-2,5-diphenyltetrazolium bromide (MTT) molecule. Cell viability was determined with the MTT protocol. After incubation of the plate for 4 hours in a cell culture incubator, 500 μL of detergent reagent (0.01 N HCl with 100 mg/mL SDS in deionized water) was added in each well to dissolve the formed formazan crystals, and the plate was kept in the cell culture incubator for overnight duration. Three different samples were taken from each well and UV-Vis reading of OD_{570nm} was obtained with a microplate reader and analyzed for comparisons. The treatment groups contained 8 replicates. Results were statistically analyzed by one-way Analysis of Variance (ANOVA) and if ANOVA was significant ($P < 0.05$), treatment values were compared with the control values with Holm-Sidak's multiple-comparisons test. Levels of significance were as follows: (*) $P < 0.05$, (**) $P < 0.01$, (***) $P < 0.001$.

CHAPTER 3

RESULT AND DISCUSSION

3.1 Synthesis of PLGA-*b*-PEG

PLGA-*b*-PEG can be synthesized in two different ways. The first one is ring-opening polymerization of lactide and glycolide monomers in the presence of polyethylene glycol. Indeed, PEG with hydroxyl terminal group is used as an initiator for the ring opening polymerization of lactide and glycolide in the presence of stannous octoate transesterification catalyst [85]. The other method is coupling PEG and PLGA via functional end groups. In this study, second method, the coupling reaction was carried out to synthesize PLGA-*b*-PEG block copolymer [84]. The end-to-end attachment between PLGA and PEG was achieved by using carboxylic acid terminated PLGA and amine-terminated PEG (Fig. 6).

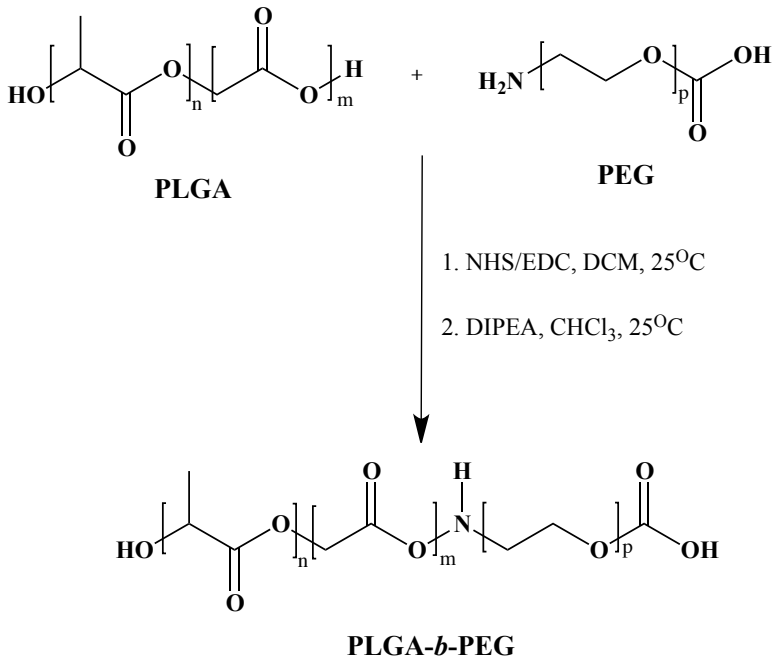

Figure 6. Synthesis of PLGA-*b*-PEG. The coupling reaction of PLGA and PEG.

At first step of the coupling reaction, carboxylic acid terminal group of PLGA is activated by NHS and EDC. As shown in Fig. 7-A, carboxylic acid terminal attacks to carboimide, EDC, and an active intermediate is formed. Then, displacement reaction occurs by nucleophilic attack of NHS to active intermediate. The product of first step is NHS functionalized PLGA (PLGA-NHS). Second step is coupling of PLGA-NHS with amine-terminated PEG. In this step, nucleophilic amine terminal group of PEG attacks to carbonyl group of PLGA-NHS, adjacent to NHS unit, in the presence of non-nucleophilic organic base, DIPEA. Non-nucleophilic organic base provides deprotonation of amine group instead of nucleophilic base substitution. In this way, deprotonated amine easily attacks to carbonyl adjacent to NHS unit (Fig. 7-B).

The coupling reaction involves carboxylic acid activation with EDC/NHS, followed by the reaction between PLGA-NHS and amine terminated PEG to form an amide bond. Therefore, at the end of the reaction, carboxylic acid terminated PLGA and amine-terminated PEG are coupled through an amide bond.

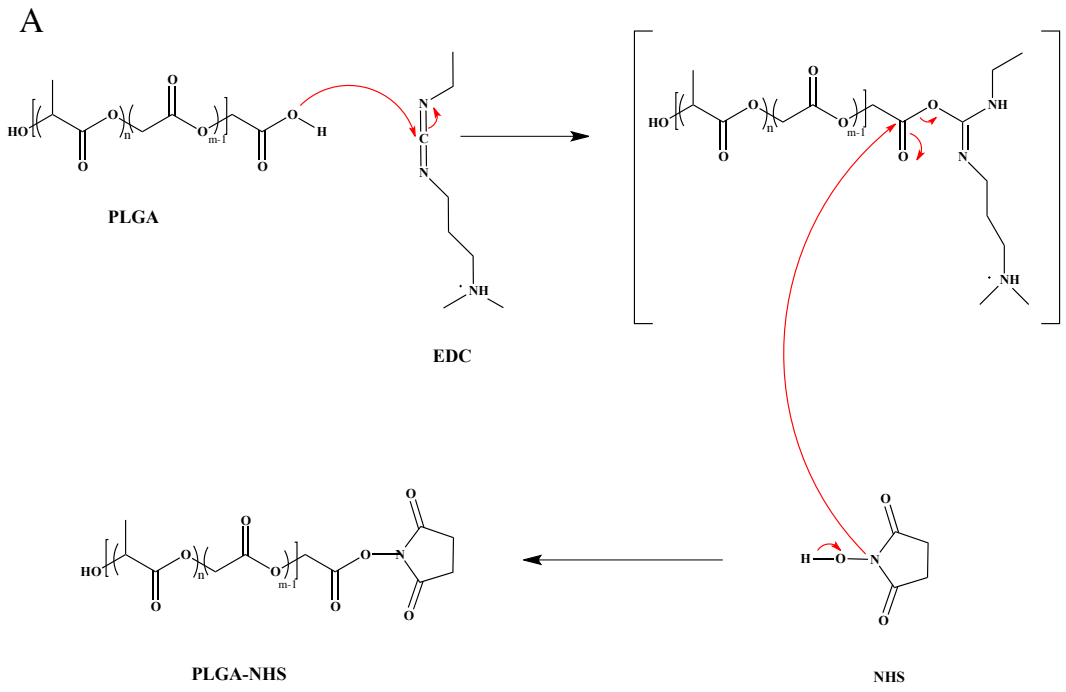

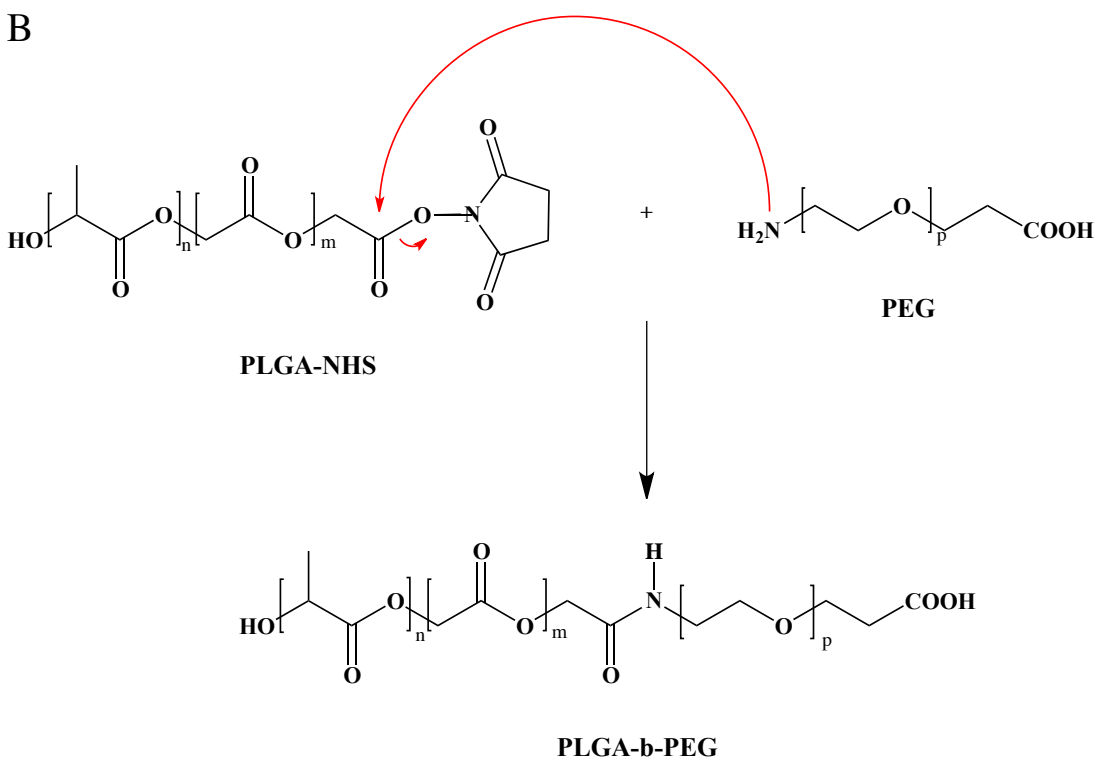

Figure 7. Reaction mechanism of PLGA activation (A) and coupling reaction of PLGA-NHS and PEG-NH_2 (B).

Fig. 8 shows ^{1}H-NMR spectrum of PLGA-*b*-PEG. In this spectrum, methyl protons and methine proton of lactide are detected at 1.55 ppm and 5.25 ppm, respectively. Methylene protons of glycolide are detected at 4.85 ppm. Strong singlet peak at 3.6 ppm is associated with the ethylene protons of PEG.

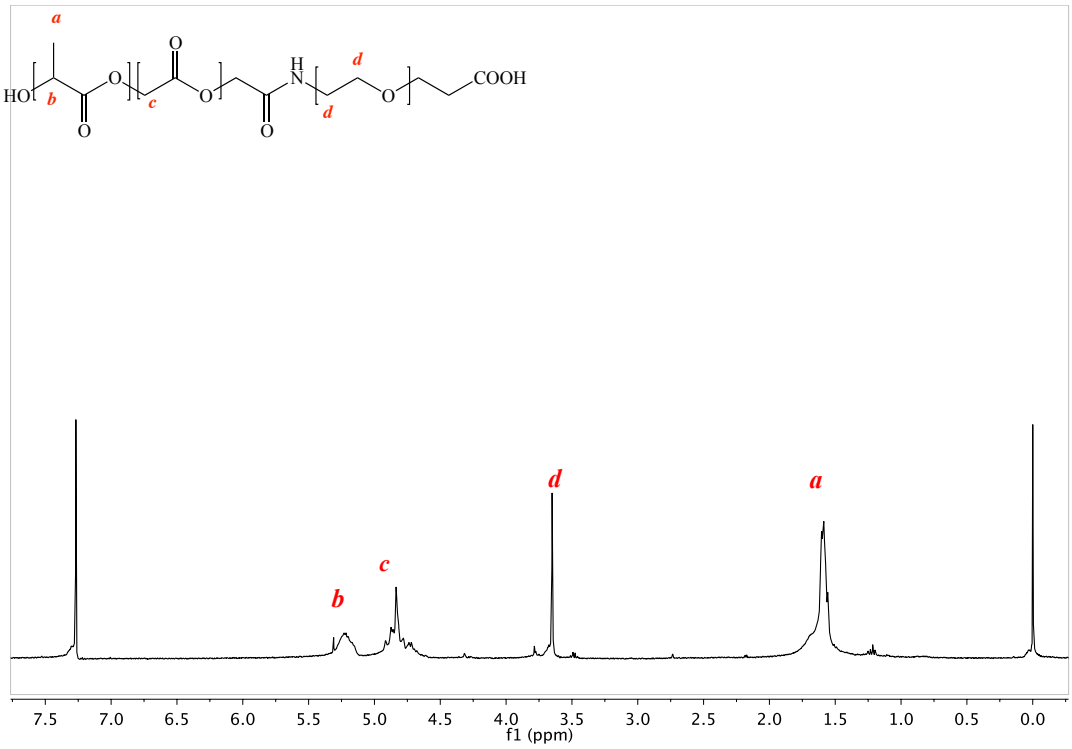

Figure 8. ^{1}H-NMR spectrum of PLGA-*b*-PEG.

PLGA-*b*-PEG was also characterized by FTIR (Fig. 9). For comparison, FTIR spectra of NH_2-PEG-COOH and HO-PLGA-COOH are also presented. According to the spectra shown in Fig. 9, PLGA-*b*-PEG has all vibrational bands characteristic of NH_2-PEG-COOH and HO-PLGA-COOH. PLGA-*b*-PEG spectrum includes 4 additional vibrational bands. The broad peak at 3500 cm^{-1} correlates with the absorption band of terminal hydroxyl groups of PLGA-*b*-PEG (O-H stretching). The peaks around 2900 cm^{-1} are correlated with the C-H bonds in PEG and PLGA chains (C-H stretching). The absorption band of carbonyl group of PLGA is placed at 1800 cm^{-1} (C=O bond stretching). Furthermore, the peak at 1635 cm^{-1} is associated with newly formed amide group (N-H bond vibrations) [82,86].

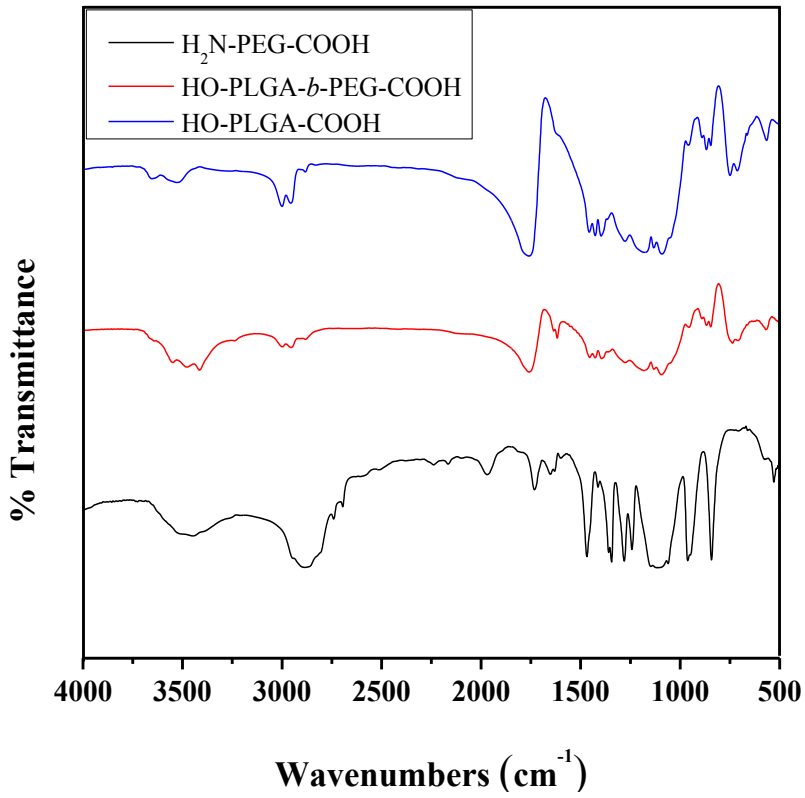

Figure 9. FTIR spectra of H_2N-PEG-COOH, HO-PLGA-COOH and PLGA-*b*-PEG.

3.2 Formation of PLGA-*b*-PEG Polymersome Structure

PLGA-*b*-PEG is an amphiliphilic block copolymer composed of hydrophilic PEG and hydrophobic PLGA blocks. In a selective solvent system, self-assembly of PLGA-*b*-PEG can be induced resulting in formation of nanoaggregates. For example, in aqueous medium, hydrophobic PLGA blocks aggregate whereas hydrophilic PEG blocks are dissolved and extend to water environment, leading to formation of nanosized micelles with core-shell structure. PLGA-*b*-PEG nanoaggregates are generally prepared using three different routes: i) dialysis, ii) double-emulsion and iii) nanoprecipitation methods [84,82,87]. Depending on the preparation method, PLGA-*b*-PEG nanoaggregates can have either hydrophobic or hydrophilic cores, allowing encapsulation of both hydrophobic and hydrophilic drugs in the micellar structures.

In this study, PLGA-*b*-PEG nanoaggregates were formed by double emulsion method [82]. In this method, block copolymer is firstly dissolved in organic solvent, and then small amount of water is added into the polymer solution. After sonication, first homogenous emulsion (water-in-oil) forms, including PLGA-*b*-PEG micelles with hydrophilic PEG-core and hydrophobic PLGA-corona (Fig. 10-B). Further addition of water into the emulsion followed by homogenization via sonication resulted in a second emulsion system (water-in-oil-in-water) (Fig. 10-C). During the formation of the second emulsion, some of the hydrophilic PEG blocks in the core headed towards to corona, so that a hollow sphere-like structure formed, so called "polymersome". The polymersomes were collected via centrifugation and then redispersed in PBS solution. The polymersomes were collected via centrifugation and then redispersed in PBS solution. The reason for dispersing polymersomes in PBS solution was that PBS provided more stable polymersomes in aqueous medium due to its high salt content. The ion molecules present in PBS interact with polar groups of the polymersomes and provide well dispersed nanoaggregates. Indeed, when polymersomes were dissolved in DI water, polymersomes showed significant variation in hydrodynamic size.

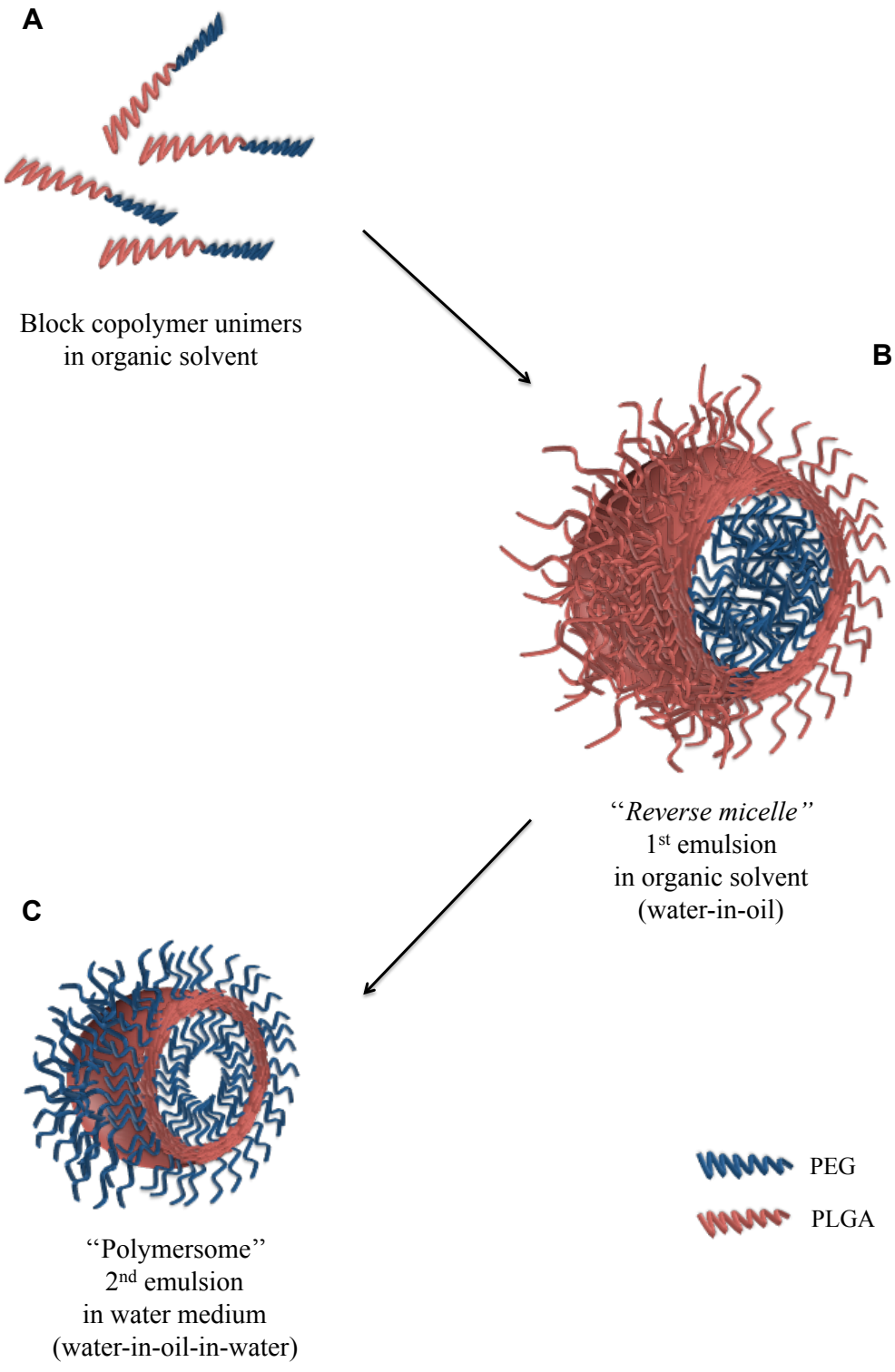

Figure 10. Formation of PLGA-*b*-PEG polymersome by double emulsion method. Completely dissolved unimer chains in organic solvent (A); 1st emulsion process-reverse micelle formation (B); 2nd emulsion process-polymersome formation (C).

The formation of polymersomes was followed by measuring the hydrodynamic size of PLGA-*b*-PEG using dynamic light scattering technique. Fig. 11 shows the size distributions of PLGA-*b*-PEG by number during the double emulsion procedure. PLGA-*b*-PEG chains have 59.4±5.71 nm hydrodynamic size in DCM (Fig. 11-A). When the 1st (water-in-oil) emulsion was prepared by addition of small amount of water, the hydrodynamic size of PLGA-*b*-PEG rised to 2980±406.4 nm (Fig. 11-B). By increasing water content of solution, 2nd (water-in-oil-in-water) emulsion was prepared and polymersomes were formed with 181±18.35 nm (Fig. 11-C). After stabilization of PLGA-*b*-PEG polymersomes in PBS at pH 7.5, the average hydrodynamic size was found as 168.6±6.31 nm (Fig. 11-D).

In the literature, the diameter of PLGA-*b*-PEG nanostructures ranges from 100 nm to 500 nm depending on the preparation method and of the length of PLGA and PEG blocks [40,88].

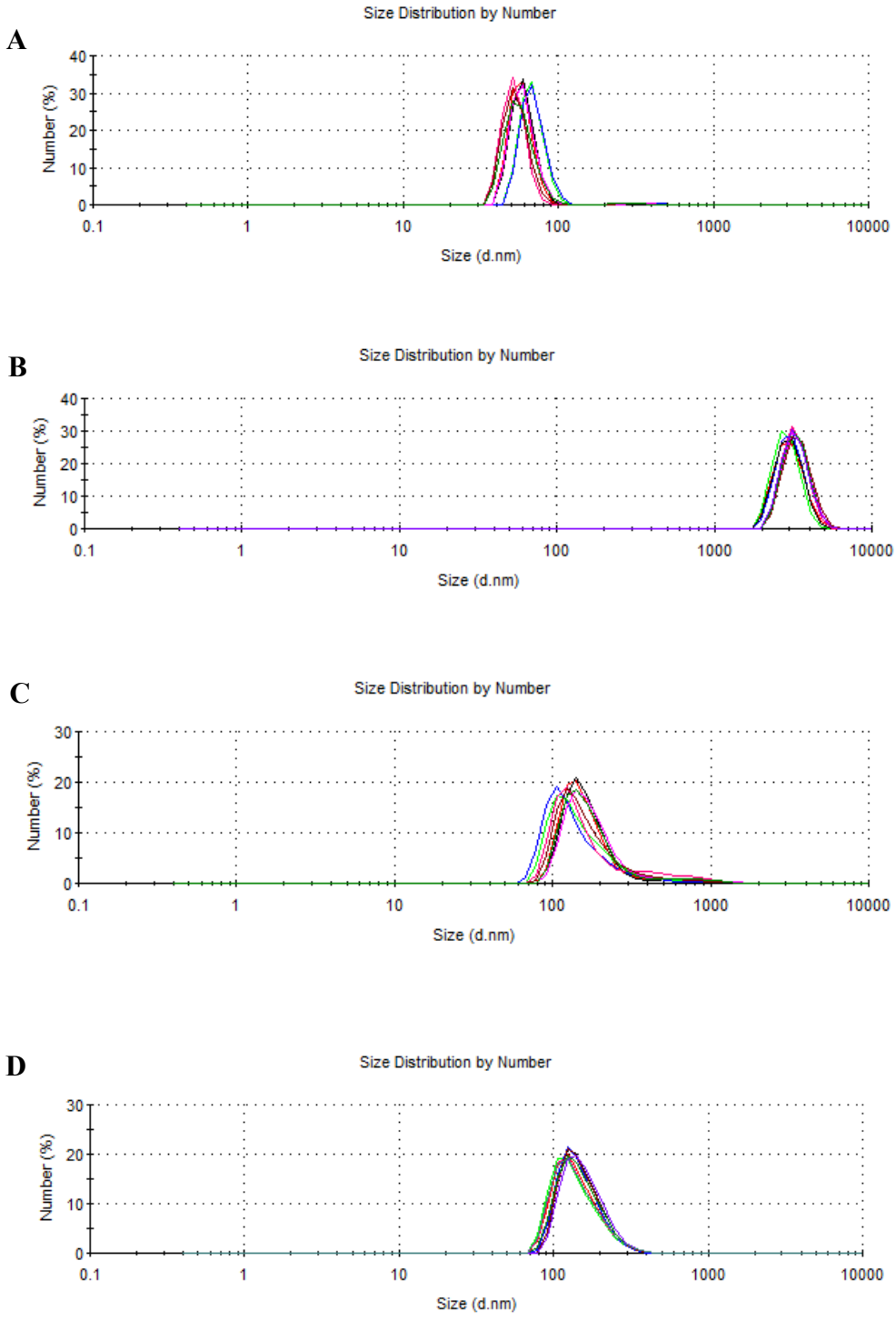

Figure 11. Number average hydrodynamic size distribution of PLGA-*b*-PEG in DCM (A); nanoaggregates after 1st (water-in-oil) emulsion (B); polymersomes after 2nd (water-in-oil-in-water) emulsion (C)
and polymersomes in PBS buffer at pH 7.5 (D).

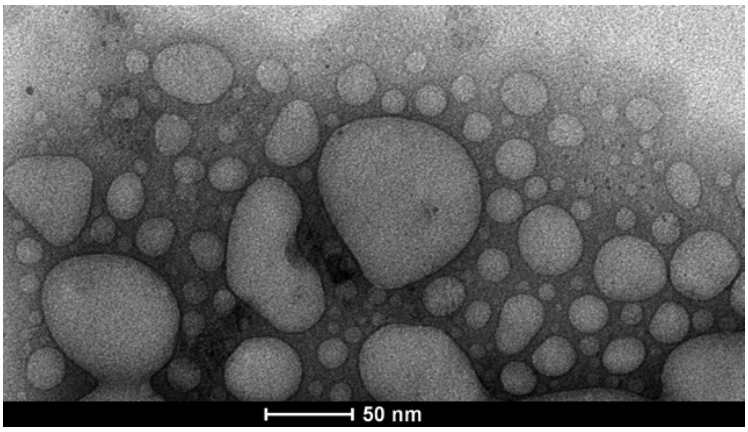

Figure 12. TEM images of PLGA-*b*-PEG polymersomes.

3.3 Aqueous Solution Stability of PLGA-*b*-PEG Polymersomes

PLGA blocks of PLGA-*b*-PEG exhibit hydrolytic degradation via de-esterification mechanism. Water molecules penetrate into PLGA shell and attack to carbonyl groups of glycolic and lactic acid repeating units. Nucleophilic attraction of water causes cleavage of ester linkages with formation of carboxylic acid and hydroxyl ends. At the first stage of de-esterification, PLGA undergo chain scission. Then, the rest of the ester bonds in PLGA are cleaved with time, and water soluble monomers and oligomers are released into the solution [45,89].

As mentioned in Section 1.5 and will be discussed in the next sections in detail, PLGA-*b*-PEG polymersomes were used as building blocks in preparation of ultra-thin multilayer films via LbL self-assembly technique. To confirm the stability of polymersomes, hydrodynamic size of PLGA-*b*-PEG was followed as a function of time at both pH 7.5 and pH 2 at 25 $^{\circ}$C. Note that multilayers were constructed at pH 7.5 and pH 2 at 25 $^{\circ}$C. For this reason, long-term stability of PLGA-*b*-PEG polymersomes was followed at neutral and acidic conditions at room temperature.

Fig. 13 shows the evolution of hydrodynamic size of PLGA-*b*-PEG up to 12 hours. Considering the fact that film preparation process does not take longer than 12 hours and polymersomes retained their integrity as indicated by hydrodynamic size measurements, PLGA-*b*-PEG polymersomes were found to be suitable to be used as building blocks in LbL assembly. The hydrolytic stability of PLGA-*b*-PEG polymersomes was also confirmed by TEM imaging. No significant change in the morphology of the polymersomes was observed in short term. However, hydrolytic degradation of polymersomes in PBS in long term was confirmed by TEM imaging as shown in Fig. 14.

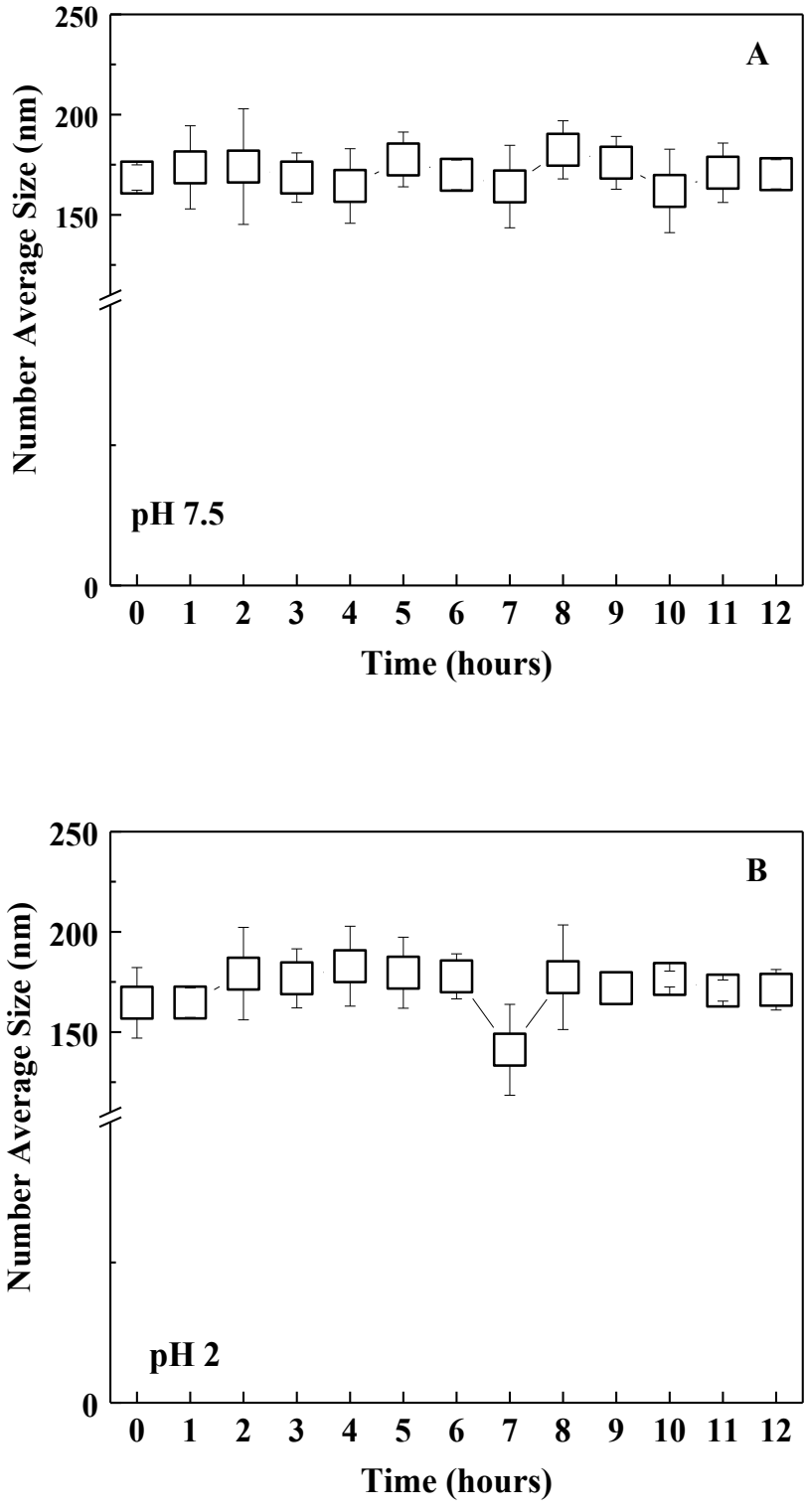

Figure 13. Evolution of hydrodynamic size of PLGA-*b*-PEG polymersomes as a function of time at 25 °C in PBS solution at pH 7.5 (A) and pH 2 (B).

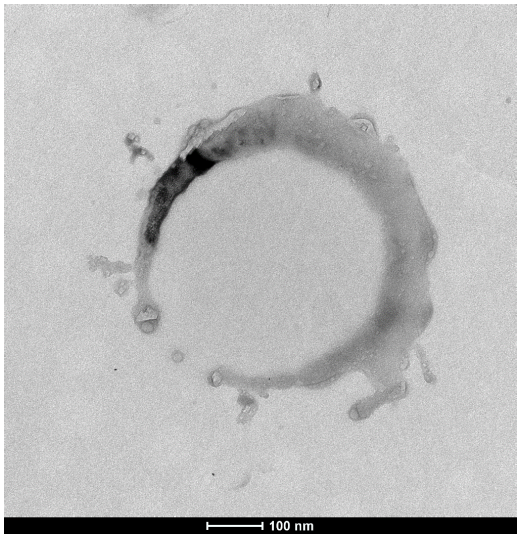

Figure 14. TEM image of a hydrolytically degraded PLGA-*b*-PEG polymersomes in PBS solution after 24 hours.

3.4 LbL Self-Assembly of PLGA-*b*-PEG Polymersomes and Tannic Acid (TA)

PLGA-*b*-PEG polymersomes were layer-by-layer deposited onto BPEI coated silicon wafer/quartz slides at 25 °C at either pH 7.5 or pH 2 using TA, a natural polyphenol with 25 hydrogen donating hydroxyl groups. The BPEI precursor layer provides better adhesion of layers on the substrate. The positively charged BPEI coated substrate was immersed into TA or PLGA-*b*-PEG polymersome solution in an alternating fashion. After each layer deposition, the substrate was rinsed with sodium phosphate buffer solution in order to eliminate loosely bound TA molecules or PLGA-*b*-PEG polymersomes. Scheme 3 illustrates the LbL film formation process. The driving force for LbL film deposition of TA and PLGA-*b*-PEG polymersomes was hydrogen bonding interactions among hydrogen accepting ether oxygens of PEO shell and hydrogen donating protonated hydroxyl groups of TA. Scheme 4 illustrates hydrogen bonding interactions among PLGA-*b*-PEG polymersomes and TA and multilayer films of PLGA-*b*-PEG polymersomes/TA.

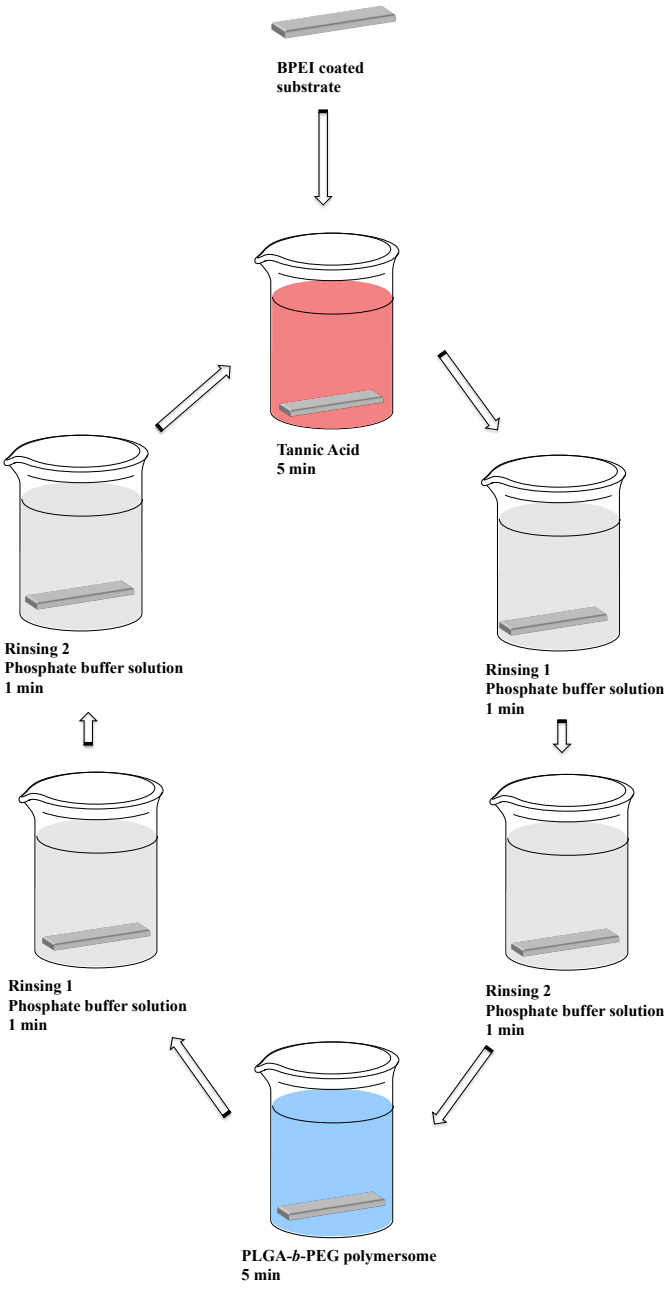

Scheme 3. Schematic representation of LbL thin film production of PLGA-*b*-PEG polymersomes and TA.

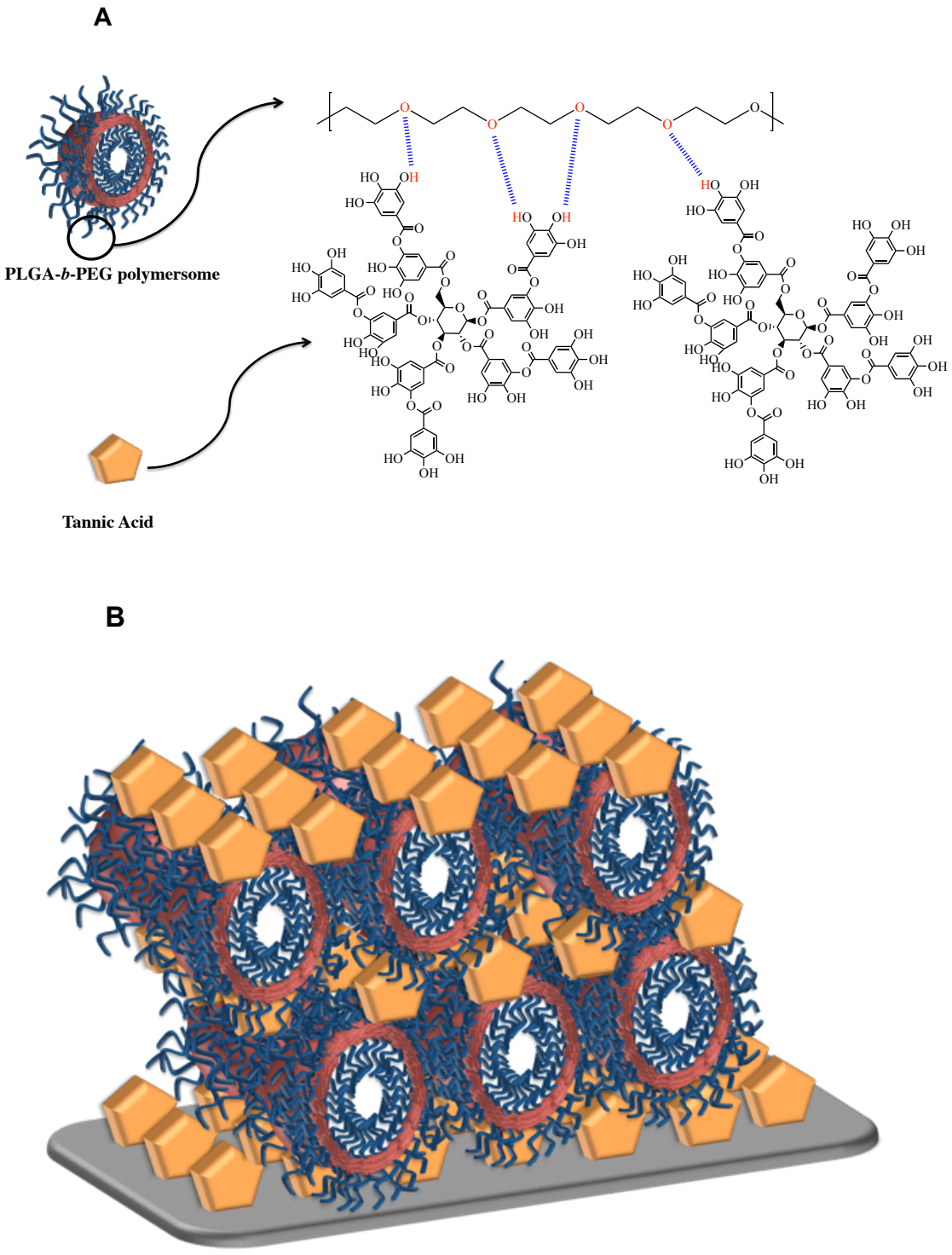

Scheme 4. Schematic representation of hydrogen bonding interactions among PLGA-*b*-PEG polymersomes and TA at acidic pH (Panel A). Schematic representation of multilayers of PLGA-*b*-PEG polymersomes and TA (Panel B).

LbL growth of PLGA-*b*-PEG polymersomes and TA was followed using UV-Visible Spectroscopy. The increase in absorbance was correlated with the deposition of either PLGA-*b*-PEG polymersome or TA layers. Fig. 15 shows UV-Visible spectra of PLGA-*b*-PEG polymersomes/TA films at pH 7.5 and pH 2 at layer number 18. The intensity of the overall spectrum increased upon deposition of every PLGA-*b*-PEG polymersome layer, whereas little decrease in intensity was recorded after deposition of every TA layer at both deposition pH values. Both TA and PLGA-*b*-PEG polymersomes exhibit absorption peaks centered at 220 nm (Appendix, Fig.A.1.). Thus, intensity of the peak at 220 nm was plotted as a function of layer number to monitor the multilayer growth profile. As seen in Fig. 16, PLGA-*b*-PEG polymersomes/TA films demonstrated a zig-zag growth profile. The decrease in the intensity upon deposition of TA layers can be correlated with the partial removal of PLGA-*b*-PEG polymersomes from the surface during TA deposition. This is probably due to large size of PLGA-*b*-PEG polymersomes which might have resulted in an instability at the surface eventually followed by desorption [81,83,90].

Importantly, it is worth to emphasize that although PLGA-*b*-PEG polymersomes desorbed from the surface during TA deposition, TA layer should have been deposited at the surface so that LbL films could have grown successfully.

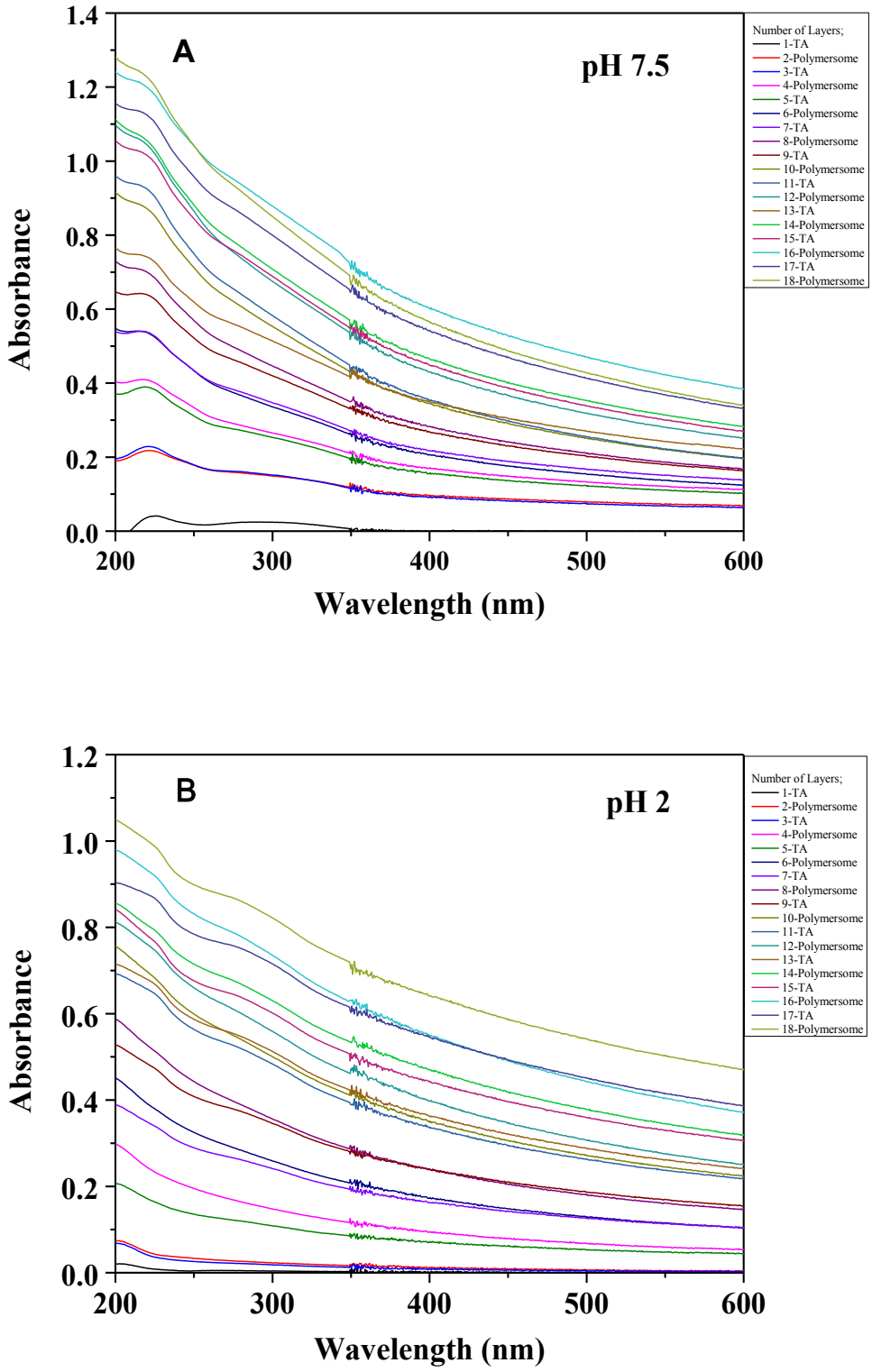

Figure 15. UV-Visible spectra of PLGA-*b*-PEG polymersomes/TA films at pH 7.5 (A) and at pH 2 (B).

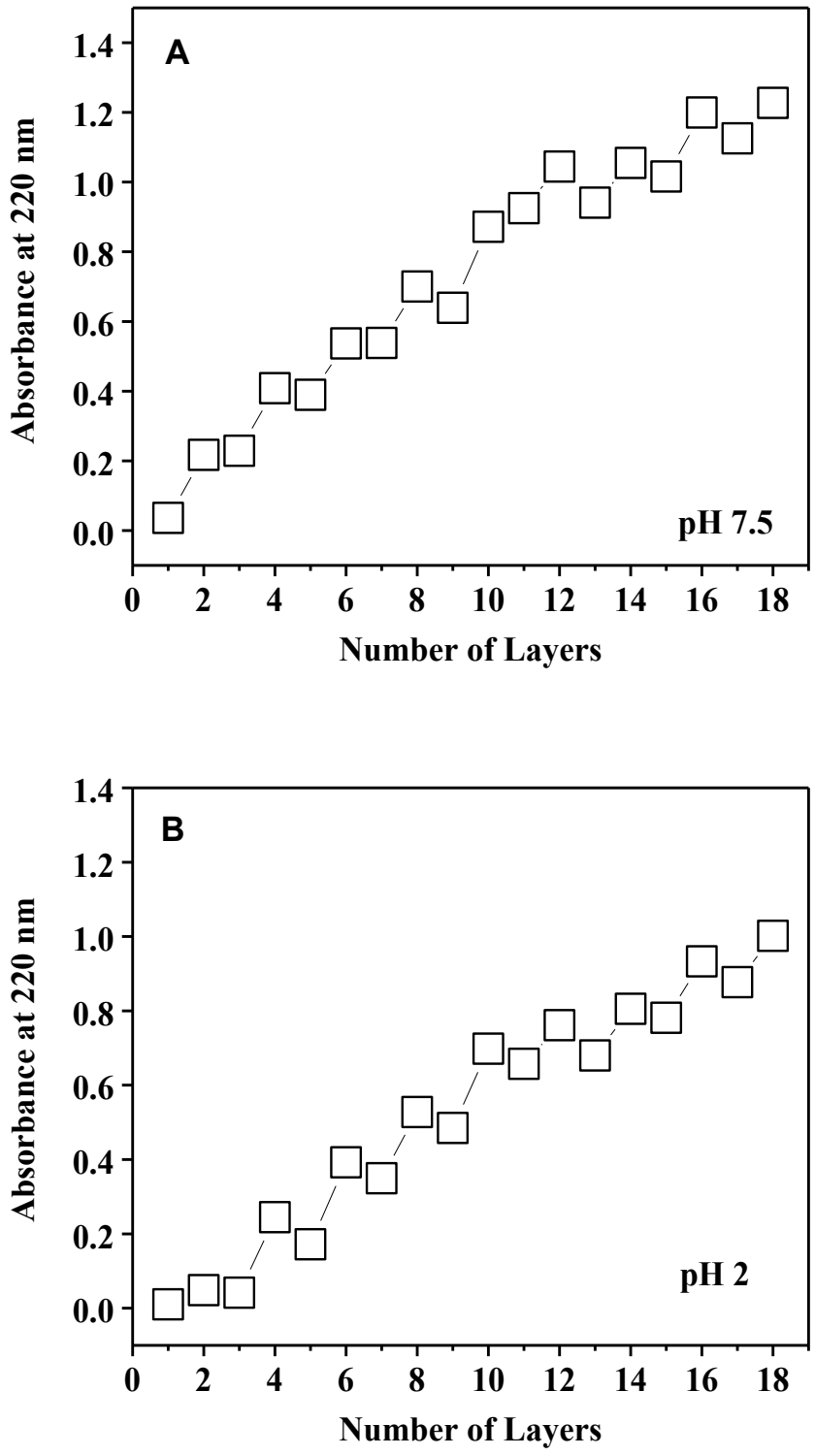

Figure 16. Evolution of absorbance at 220 nm as a function of layer number at pH 7.5 (A) and at pH 2 (B) at 25 °C.

Tannic acid is highly protonated at pH 2, but it is partially ionized at pH 7.5. Therefore, it is expected that there are more number of H-bonding in pH 2 films. This gives rise to form denser films as well as to load more amount of material into the films. In order to analyze and compare films of pH 2 and pH 7.5, AFM and UV-Vis spectroscopy analyses were carried out.

LbL growth of PLGA-*b*-PEG polymersomes and TA was sucessfully followed by UV-Visible Spectroscopy. However, this technique does not provide information about film thickness. Ellipsometry could have been used for measuring the thickness of few layers at the surface. However, the surface of the film became colored (whitish) as the layer number increased and ellipsometry could not provide reliable measurements anymore due to scattering of the light from the colored surface. Therefore, AFM was used to measure the thickness as well as roughness of 6-; 12- and 18-layer films, prepared at pH 7.5 and pH 2. As seen in Fig. 17, both the thickness and roughness increased with increasing layer number at both pH values. However, thickness and roughness values recorded at pH 7.5 were significantly higher than that recorded for films with the same number of layers prepared at pH 2. This difference was correlated with the formation of more intense films at pH 2. TA has a pK_a of 8.5 [91], thus it is highly protonated at pH 2 resulting in formation of greater number of binding points among the layers and more intense films. In contrast, TA is partially ionized at pH 7.5, thus PLGA-*b*-PEG polymersome/TA films have lower number of binding points among the layers resulting in a loose film structure. Fig. 18 shows AFM images of 6-; 12- and 18-layer films prepared at pH 7.5 (Panel A) and pH 2 (Panel B) and clearly demonstrates the difference in roughness specifically for 6- and 12-layer films.

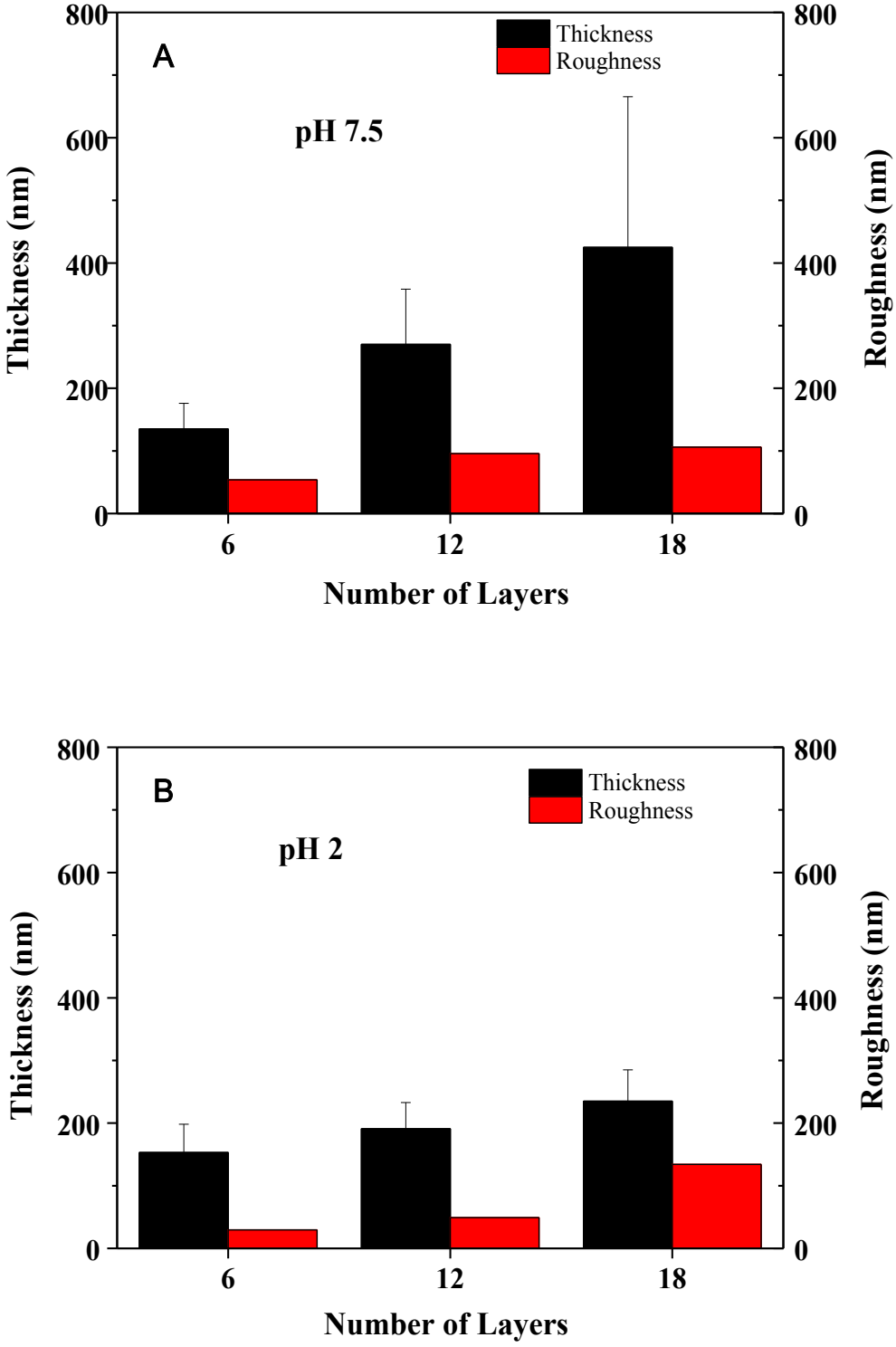

Figure 17. Thickness and roughness of 6-, 12- and 18- layer PLGA-*b*-PEG polymersome/TA films at pH 7.5 (A) and at pH 2 (B).

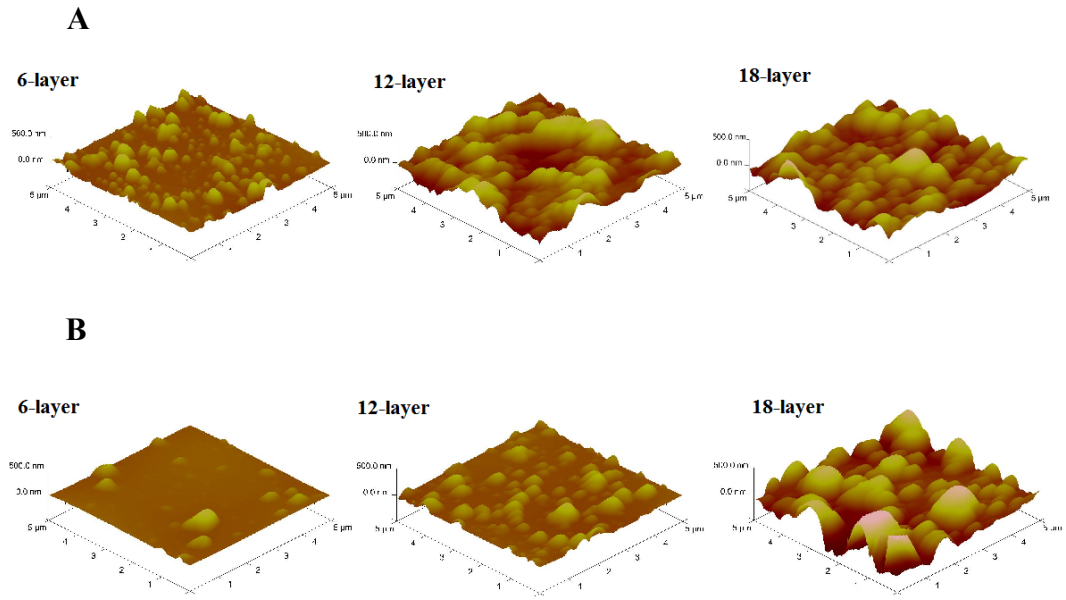

Figure 18. AFM topography images of 6-; 12-; 18-layer PLGA-*b*-PEG polymersome/TA films produced at pH 7.5 (A) and at pH 2 (B).

3.5 Drug Loading into PLGA-*b*-PEG Polymersomes

As mentioned earlier, PLGA-*b*-PEG has both hydrophilic and hydrophobic regions. Therefore, PLGA-*b*-PEG can be ideal carrier for dual drug release from the surface. In this part of the study, two model anti-cancer drugs with different solubilities are water, i.e. Doxorubicin hydrochloride (DOX) and Paclitaxel (PTX) were chosen to load into PLGA-*b*-PEG polymersomes. The solubilities of DOX and PTX in water have been reported as less than 35 mg/mL and 0.1 μg/mL respectively [92,93].Thus, DOX was expected to load in the hydrophilic inner core, whereas PTX was expected to load into hydrophobic PLGA region. Both drugs were incorporated into PLGA-*b*-PEG polymersomes during the micellization. Scheme 5 illustrates DOX and PTX loaded PLGA-*b*-PEG polymersomes.DOX was encapsulated into the inner hydrophilic core during formation of the first emulsion (water-in-oil step). On the other hand, PTX was loaded into PLGA shell during formation of the second emulsion (water-in-oil-in-water step). As mentioned in

Section 3.2, the number average particle size was 168.6±6.31 nm for bare polymersomes (Fig. 19-A). The hydrodynamic size was 198±6 nm for DOX and PTX loaded polymersomes. Fig. 119-B shows the size distribution by number of PLGA-*b*-PEG polymersomes before and after drug loading at pH 7.5. Fig. 19-C shows the TEM images of DOX and PTX loaded polymersomes at pH 7.5. Similar to Fig. 14, Fig. 19-D shows TEM image of a hydrolytically degraded DOX and PTX loaded polymersome after 24 hours in PBS solution at pH 7.5.

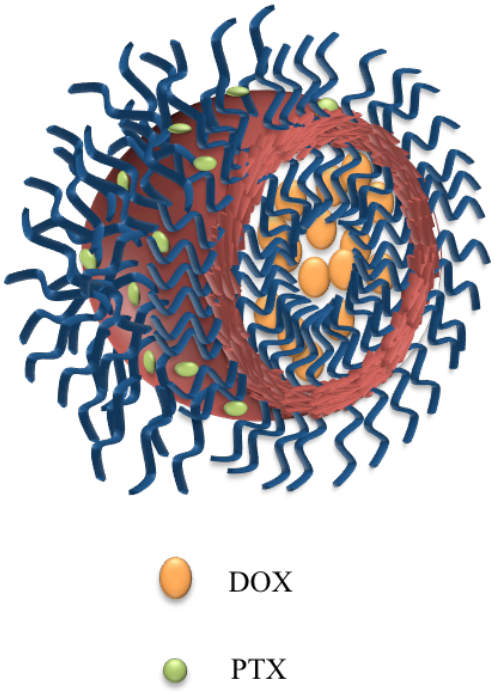

Scheme 5. Schematic representation of DOX and PTX loaded PLGA-*b*-PEG polymersomes.

A

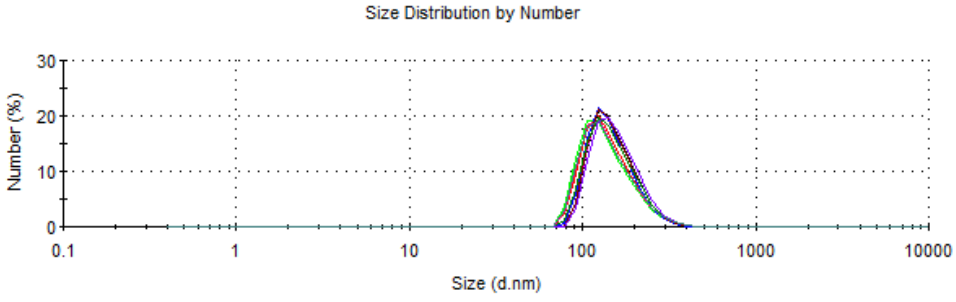

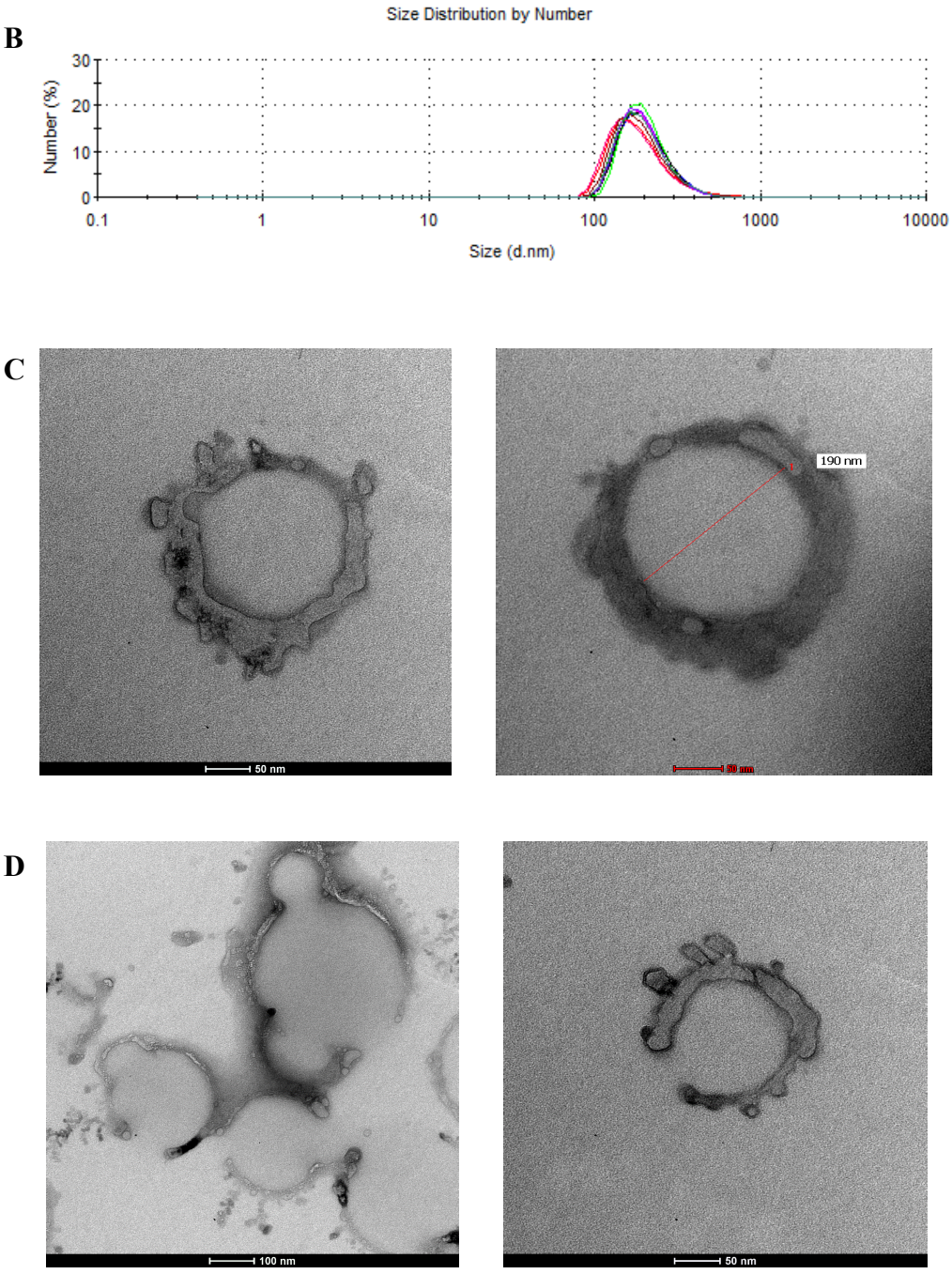

Figure 19. Size distribution by number of bare PLGA-*b*-PEG polymersomes (Panel A); DOX and PTX loaded PLGA-*b*-PEG polymersomes (Panel B) and TEM images of DOX and PTX loaded PLGA-*b*-PEG polymersomes (Panel C) and hydrolytically degraded DOX and PTX loaded PLGA-*b*-PEG polymersomes after 24 hours in PBS solution at pH 7.5 (Panel D).

Since multilayers would be constructed at pH 2, pH-stability of DOX and PTX loaded PLGA-*b*-PEG polymersomes was also examined at acidic conditions. The pH of the solution containing DOX and PTX loaded PLGA-*b*-PEG polymersomes was gradually decreased down to pH 2, followed by hydrodynamic size measurements. The average hydrodynamic size of DOX and PTX loaded PLGA-*b*-PEG polymersomes was recorded as 187±6 nm at pH 2. Fig. 20 shows the size distribution by number of DOX and PTX loaded PLGA-*b*-PEG polymersomes at pH 2.

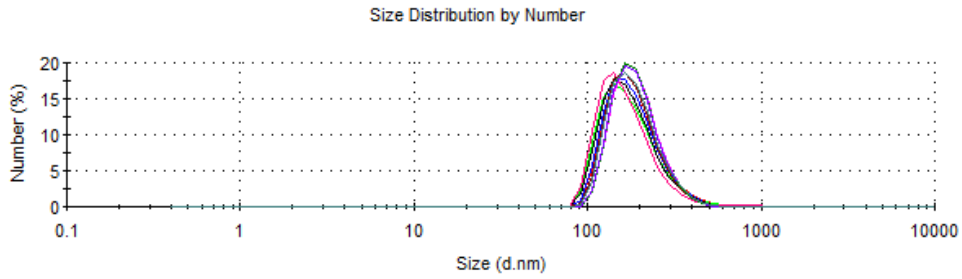

Figure 20. Number average hydrodynamic size distribution of PLGA-*b*-PEG polymersomes in pH 2 PBS buffer.

3.6 LbL Deposition of DOX and PTX Loaded PLGA-*b*-PEG Polymersomes and Tannic Acid

DOX and PTX loaded PLGA-*b*-PEG polymersomes were LbL deposited with TA at the surface at pH 7.5 or pH 2 using the same procedure described in Section 3.4. Multilayer growth was followed using UV-Vis. Spectroscopy and the absorbance values obtained after every layer were contrasted with that of multilayers, constructed using bare PLGA-*b*-PEG polymersomes. Fig. 21 shows the gradual increase in absorbance values with increasing layer number for LbL deposition of DOX and PTX loaded PLGA-*b*-PEG polymersomes and TA at pH 7.5 (Fig. 21-A)

and pH 2 (Fig. 21-B). Fig. 22 contrasts the absorbance at 220 nm for 18-layer films of DOX and PTX loaded PLGA-*b*-PEG polymersomes/TA and 18-layer films of bare PLGA-*b*-PEG polymersomes/TA at pH 7.5 (Fig. 22-A) and at pH 2 (Fig. 22-B). The lower absorbance values recorded for DOX and PTX loaded PLGA-*b*-PEG polymersomes/TA films at both pH values are a result of deposition of lower amount of material at the surface. This can be rationalized by the association of DOX and PEG outer shells. DOX has hydrogen donating hydroxyl groups. In addition, it has an amino group which is protonated at pH 7.5 and pH 2 (pK_a of DOX ~8.3) [94]. The interaction among ether oxygens of outer PEG shell of PLGA-*b*-PEG polymersomes and hydroxyl groups or protonated amino groups of DOX decreases the extent of association among TA and PEG shell of PLGA-*b*-PEG polymersomes during LbL deposition, resulting in lower amount of material at the surface. The difference in the absorbance of DOX and PTX loaded PLGA-*b*-PEG polymersomes/TA films and bare PLGA-*b*-PEG polymersomes/TA films was remarkable specifically at pH 7.5. The difference was lower at pH 2, probably due to greater extent of association among PEG and TA at acidic conditions when TA carries higher number of protonated hydroxyl groups than that at pH 7.5.

Fig. 23 constrasts the thickness values of DOX and PTX loaded PLGA-*b*-PEG polymersomes/TA and bare PLGA-*b*-PEG polymersomes/TA at pH 7.5 and pH 2 obtained via AFM cross-sectional analysis. Thickness values obtained via AFM also showed that multilayers of DOX and PTX loaded PLGA-*b*-PEG polymersomes and TA were thinner than multilayers of bare PLGA-*b*-PEG polymersomes and TA.

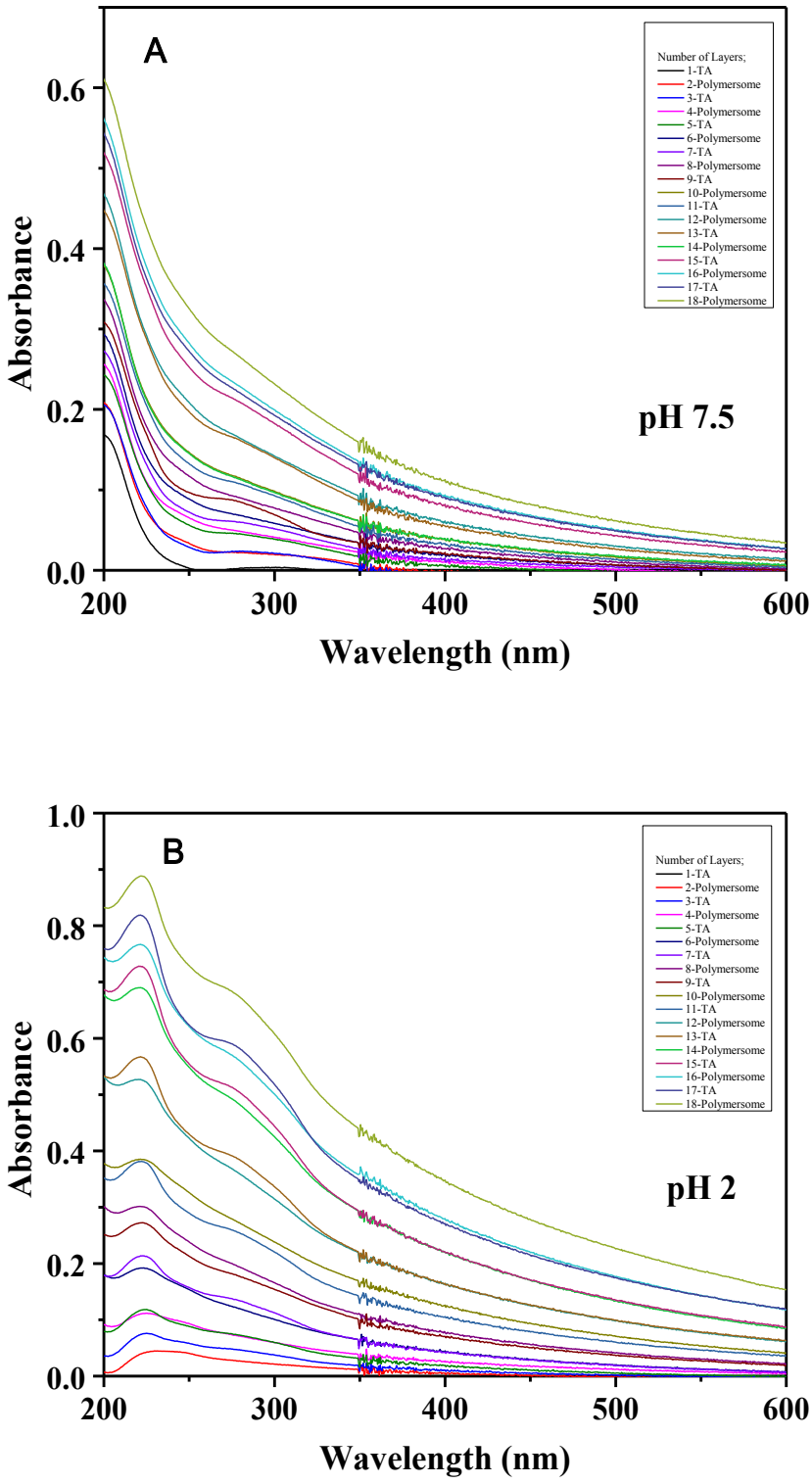

Figure 21. UV-Visible spectrum of DOX and PTX loaded PLGA-*b*-PEG polymersomes/TA after every layer deposition at pH 7.5 (A) and at pH 2 (B).

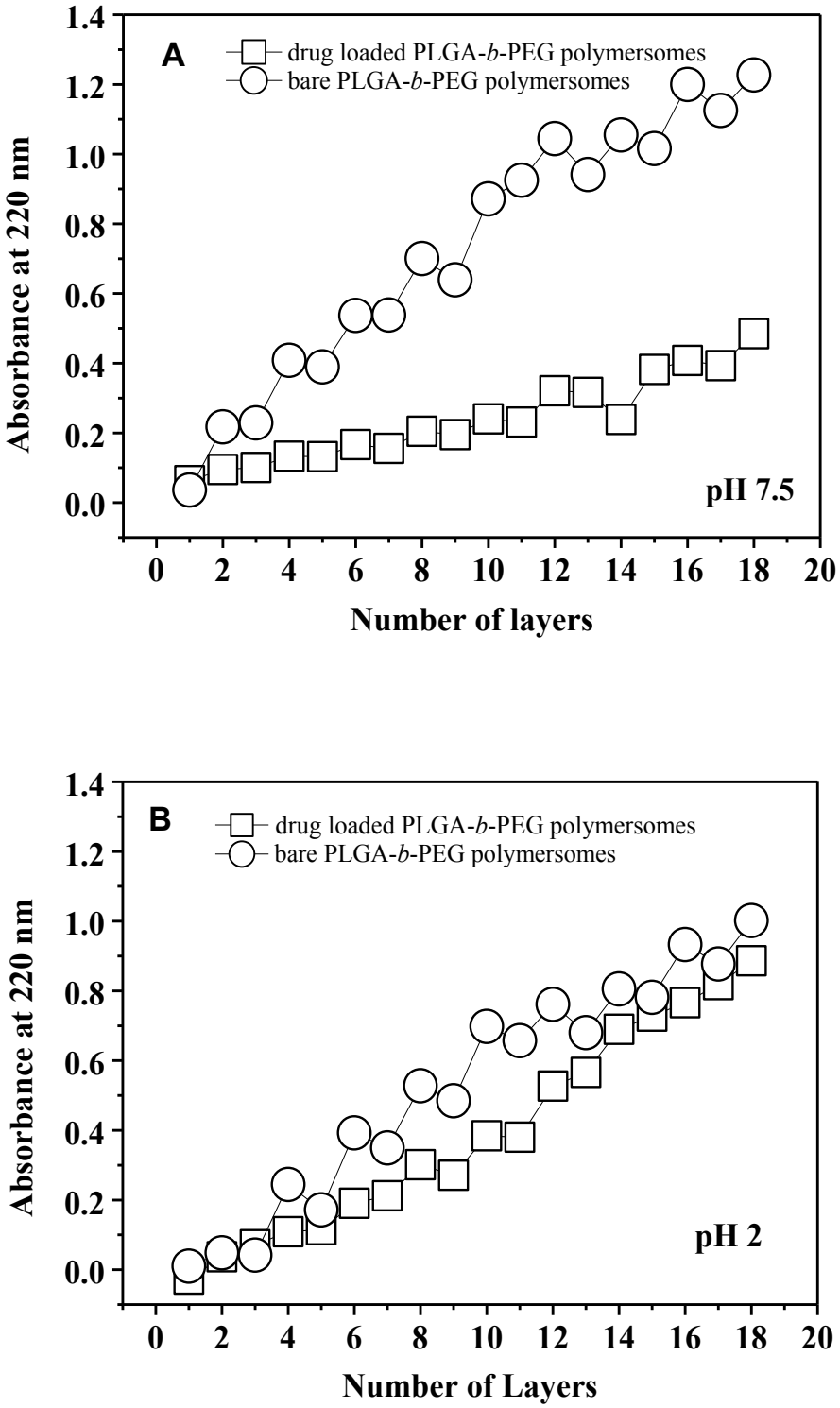

Figure 22. Absorbance at 220 nm for LbL films of DOX and PTX loaded PLGA-*b*-PEG polymersomes/TA and bare PLGA-*b*-PEG polymersomes/TA at pH 7.5 (A) and at pH 2 (B).

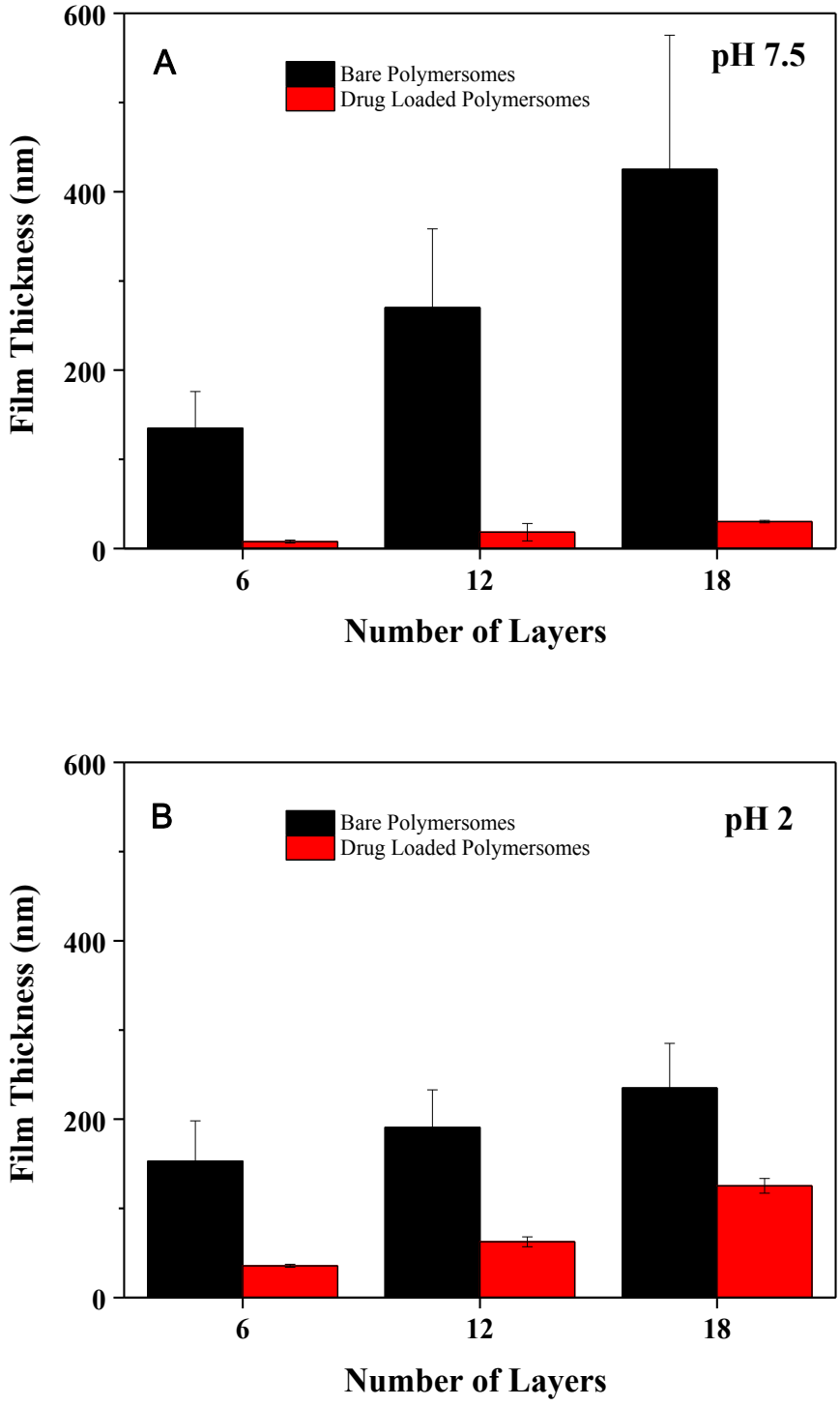

Figure 23. Thickness values of 6, 12 and 18-layer DOX and PTX loaded PLGA-*b*-PEG polymersomes/TA and 6, 12 and 18-layer bare PLGA-*b*-PEG polymersomes/TA at pH 7.5 (A) and at pH 2 (B) via AFM cross-sectional analysis.

Importantly, it was found that the number of bare PLGA-*b*-PEG polymersomes and TA layers that could be deposited at the surface was limited. Similarly, the number of DOX and PTX loaded PLGA-*b*-PEG polymersomes and TA layers that could be deposited at the surface was also limited. The maximum number of layers for bare PLGA-*b*-PEG polymersomes/TA films was found as 18 and 30 at pH 7.5 and pH 2, respectively. However, the amount of deposition per cycle reached the maximum layer number to 24 and 30 at pH 7.5 and pH 2, respectively for DOX and PTX loaded PLGA-*b*-PEG polymersomes/TA films. The reason for limitation in the total number of layers that could be deposited at the surface can be correlated with: i) the high size of PLGA-*b*-PEG polymersomes which results in a loose film structure and facilitates the desorption of specifically outermost layers and ii) relatively weaker H bonding interactions among ether oxygens and hydroxyl groups than that for example between carbonyl and hydroxyl groups.

The reason for lower number of maximum layers at pH 7.5 is due to enhanced ionization of TA, leading to lower extent of association among PEG and TA weaker binding between the layers. Fig. 24 shows the absorbance at 220 nm at every 3-layers of bare PLGA-*b*-PEG polymersomes/TA or DOX and PTX loaded PLGA-*b*-PEG polymersomes/TA films at pH 7.5 (A) and pH 2 (B).

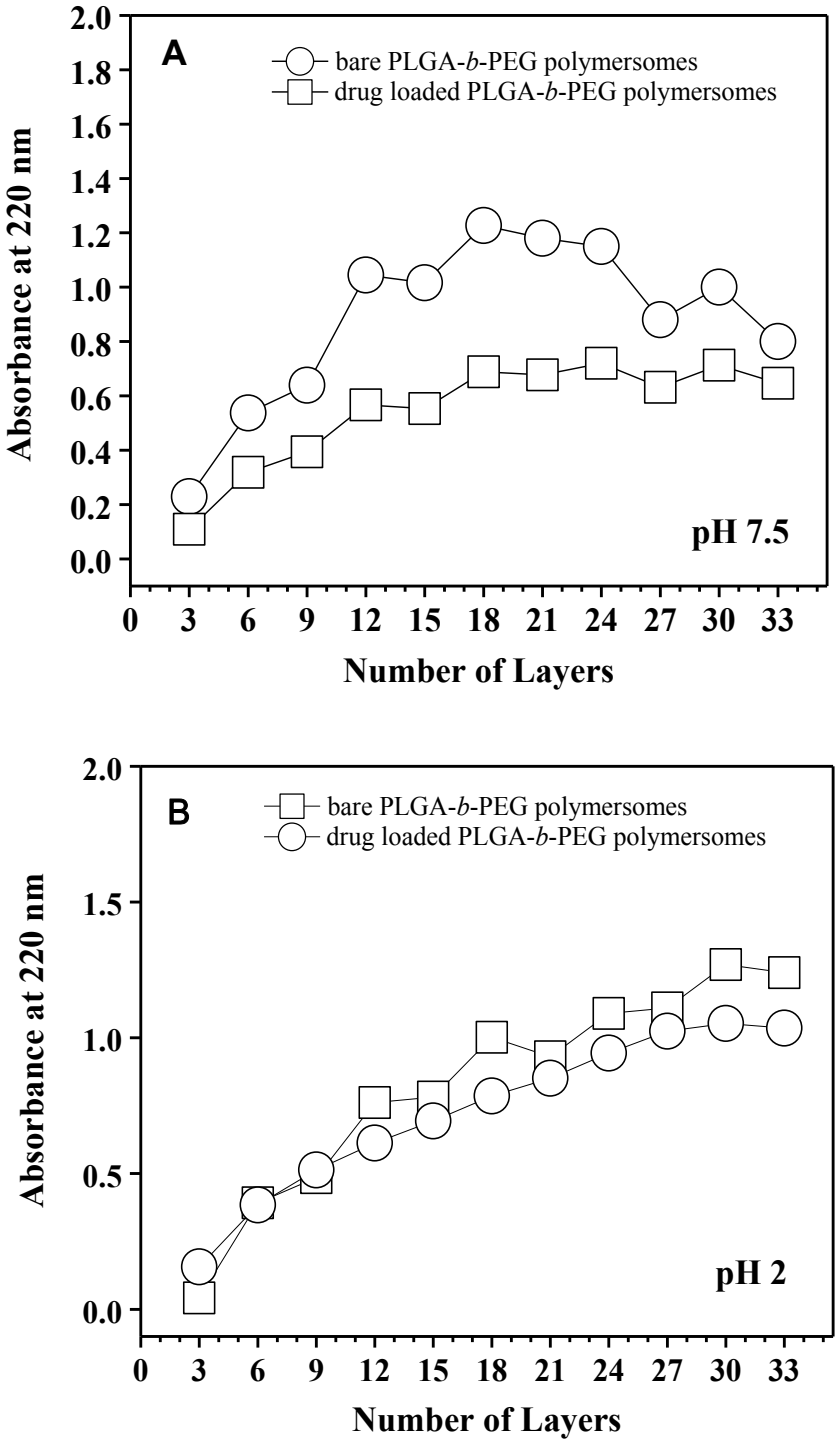

Figure 24. Absorbance at 220 nm at every 3-layers of bare PLGA-*b*-PEG polymersomes/TA or DOX and PTX loaded PLGA-*b*-PEG polymersomes/TA films at pH 7.5 (A) and at pH 2 (B).

3.7 Doxorubicin Release from DOX and PTX Loaded PLGA-*b*-PEG Polymersomes/TA Films

DOX release was followed from 2 different types of multilayers: i) DOX and PTX loaded PLGA-*b*-PEG polymersomes/TA films, constructed at pH 7.5 and ii) DOX and PTX loaded PLGA-*b*-PEG polymersomes/TA films, constructed at pH 2.

To mimick biological conditions, DOX release from the multilayers was followed against PBS solution. It is known that microenvironment of tumor tissues is relatively acidic compared to normal tissues [95,96]. Therefore, release from the multilayers was followed at pH 7.5, pH 6 and pH 4 using fluorescence spectroscopy. Emission spectrum of DOX presents 2 peaks centered at 555 nm and 588 nm when excited at 490 nm (Appendix, Fig. A.2). At lower concentrations, DOX shows strong at peak at 588 nm so the change in the intensity of the peak at 588 nm was followed as a function of time for release experiments (Appendix, Fig.A.2).

As seen in Fig. 25, for both types of the films (constructed either at pH 7.5 or pH 2) majority of DOX released from the multilayers with the same number of layers in the first 24 hours at all pH values. The amount of DOX released from the surface at pH 4 was slightly higher than that released at pH 7.5 or pH 6 for both types of the film. Note that the difference in the amount of DOX released from the surface at pH 7.5 and pH 6 was not significant. The film structure was disrupted at pH 7.5 condition because of weak hydrogen bonding among PEG and TA. The picture shows the partial peeling of both films from the surface at pH 7.5 (Scheme 6). Therefore, the results of pH 7.5 condition were same with pH 6. The higher amount of DOX released from the surface at pH 4 can be correlated with the faster degradation of PLGA at acidic environment. The degradation of PLGA shell could have facilitated the release of DOX from the inner PEG-core. The multilayer deposition pH affected the amount of DOX released from the surface only at pH 4 when PLGA hydrolytic degradation was faster (Fig. 26).

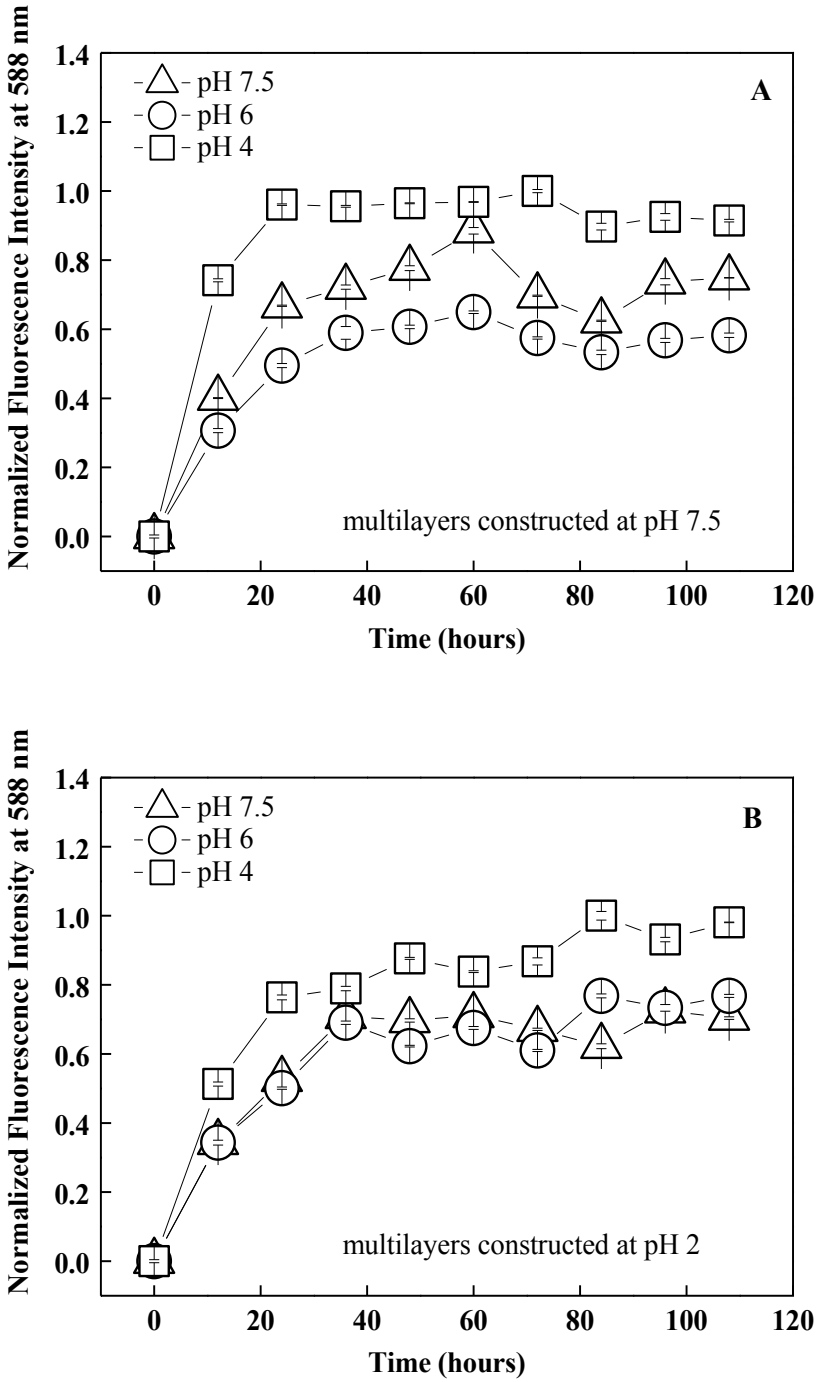

Figure 25. DOX released from DOX and PTX loaded PLGA-*b*-PEG polymersomes/TA films, constructed at pH 7.5 (A) and DOX and PTX loaded PLGA-*b*-PEG polymersomes/TA films, constructed at pH 2 (B). Panel A and Panel B are composed by normalizing the fluorescence intensity data to the highest fluorescence intensity obtained from pH 7.5 multilayers at pH 4 and pH 2 multilayers at pH 4, respectively.

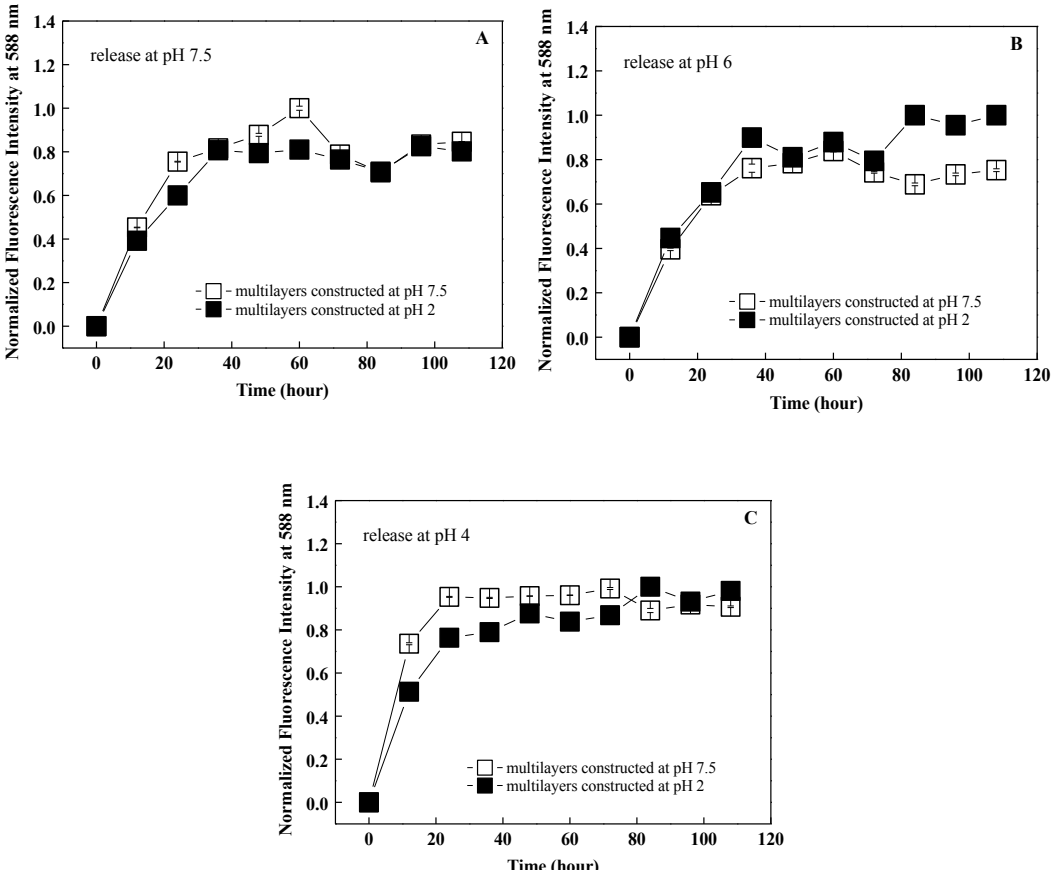

Figure 26. Comparison of the fluorescence intensity of DOX released from DOX and PTX loaded PLGA-*b*-PEG polymersomes/TA films, constructed at pH 7.5 and DOX and PTX loaded PLGA-*b*-PEG polymersomes/TA films, constructed at pH 2 at pH 7.5(A); at pH 6 (B) and at pH 4 (C). Panel A, Panel B and Panel C are composed by normalizing the fluorescence intensity data to the highest fluorescence intensity obtained from pH 7.5 multilayers at pH 7.5 and pH 2 multilayers at pH 6 and pH 2 multilayers at pH 4, respectively.

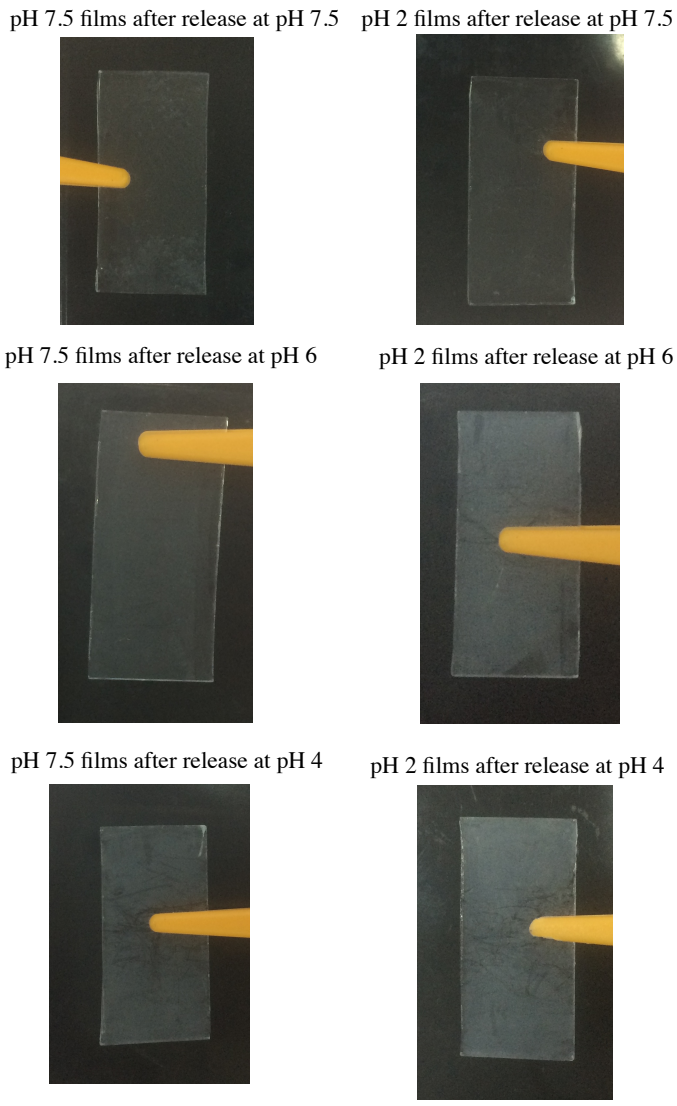

Scheme 6. Photos of the multilayers after release at pH 7.5, at pH 6 and at pH 4.

3.7.1 Effect of Barrier Layers on Release Kinetics of Doxorubicin from The Surface

In this part of the study, film architecture was modified to tune the release kinetics of DOX from the surface. Hydrogen bonding PVCL/TA pair was incorporated into the multilayers in 2 different ways: i) PVCL/TA was incorporated into DOX and PTX loaded PLGA-*b*-PEG polymersomes/TA films in an alternating fashion, i.e. the repeating order of layers was: TA/DOX and PTX loaded PLGA-*b*-PEG

polymersomes/TA/PVCL, ii) PVCL/TA multilayers were deposited on top of DOX and PTX loaded PLGA-*b*-PEG polymersomes/TA films. All multilayers were prepared only at pH 2. Scheme 7 shows the schematic representation of 2 different types of films with barrier layers.

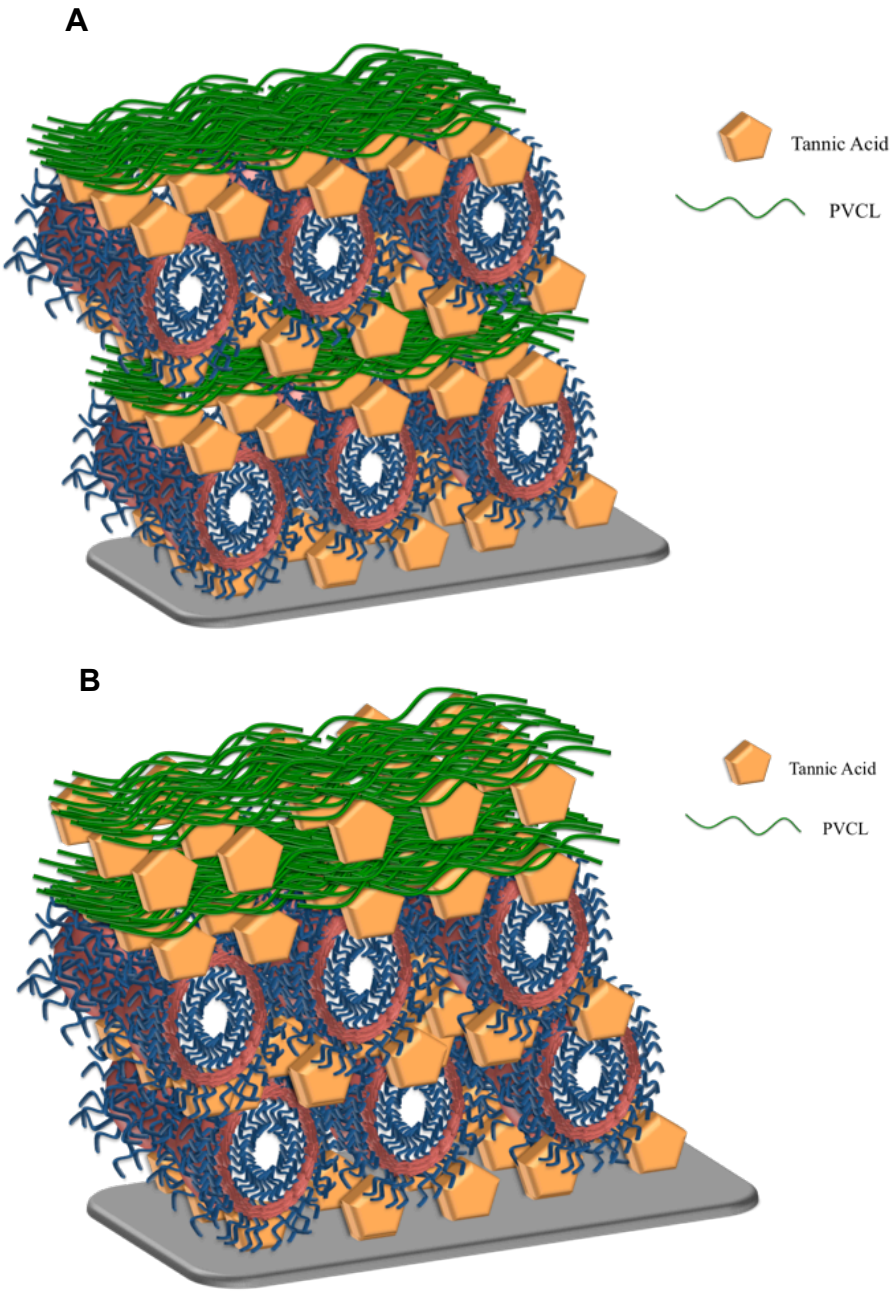

Scheme 7. Schematic representation of multilayers with different film architecture; TA/DOX and PTX loaded PLGA-*b*-PEG polymersomes/TA/PVCL multilayers (Panel A) and PVCL/TA multilayers are deposited on top of DOX and PTX loaded PLGA-*b*-PEG polymersomes/TA films (Panel B).

DOX release was examined from the multilayers with barrier layers with two different architectures at pH 7.5, pH 6.5 and pH 4. The release data of multilayers with no barrier layers is plotted for comparison at all pH values. All multilayers with different architectures included the same number of polymersome layers. As shown in Fig. 27, barrier layers had no significant effect on the release kinetics of DOX from the surface at pH 7.5. This is probably due to instability of the multilayers in PBS solution at pH 7.5. Our control experiments showed that PVCL/TA multilayers were also not stable in PBS solution at pH 7.5.

In contrast to release results at pH 7.5, polymersome/TA multilayers with PVCL/TA stack type barrier layers on the top clearly demonstrated the effect of barrier layers on the release kinetics of DOX at pH 6 and pH 4. Alternating type barrier layers resulted in different kinetics of DOX release from the surface at pH 7.5, pH 6 and pH 4. This difference in the behavior of the films can be rationalized by the instability of both polymersome/TA and PVCL/TA layers in PBS solution at pH 7.5 in long term. However, with decrease in pH, the stability of films increases and alternating layers barriers become effective. Thus, alternating layers slows down DOX release at pH 4. Scheme 8 shows the photos of the multilayers after release at pH 7.5, pH 6 and pH 4 and clearly demonstrates partial removal of the films at pH 7.5.

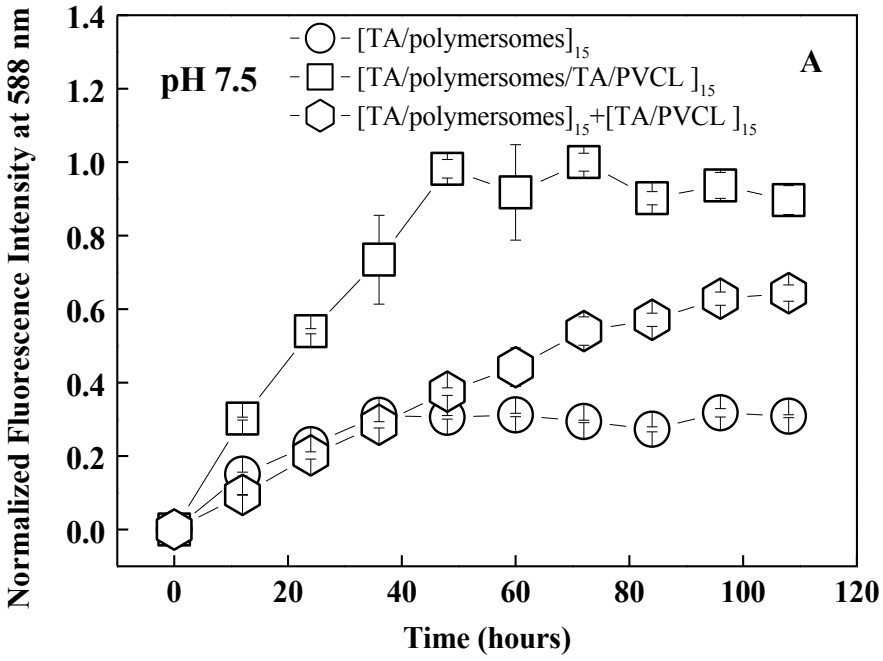
pH 7.5
A
[TA/polymersomes]15
[TA/polymersomes/TA/PVCL]15
[TA/polymersomes]15+[TA/PVCL]15
Normalized Fluorescence Intensity at 588 nm
Time (hours)
0.0
0.2
0.4
0.6
0.8
1.0
1.2
1.4
0
20
40
60
80
100
120

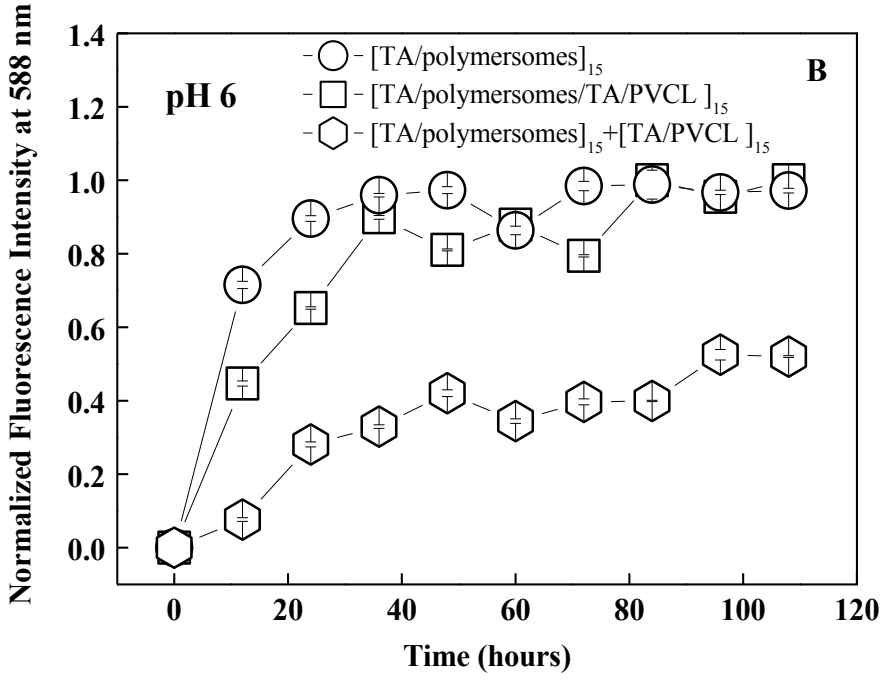
pH 6
B
[TA/polymersomes]15
[TA/polymersomes/TA/PVCL]15
[TA/polymersomes]15+[TA/PVCL]15
Normalized Fluorescence Intensity at 588 nm
Time (hours)
0.0
0.2
0.4
0.6
0.8
1.0
1.2
1.4
0
20
40
60
80
100
120

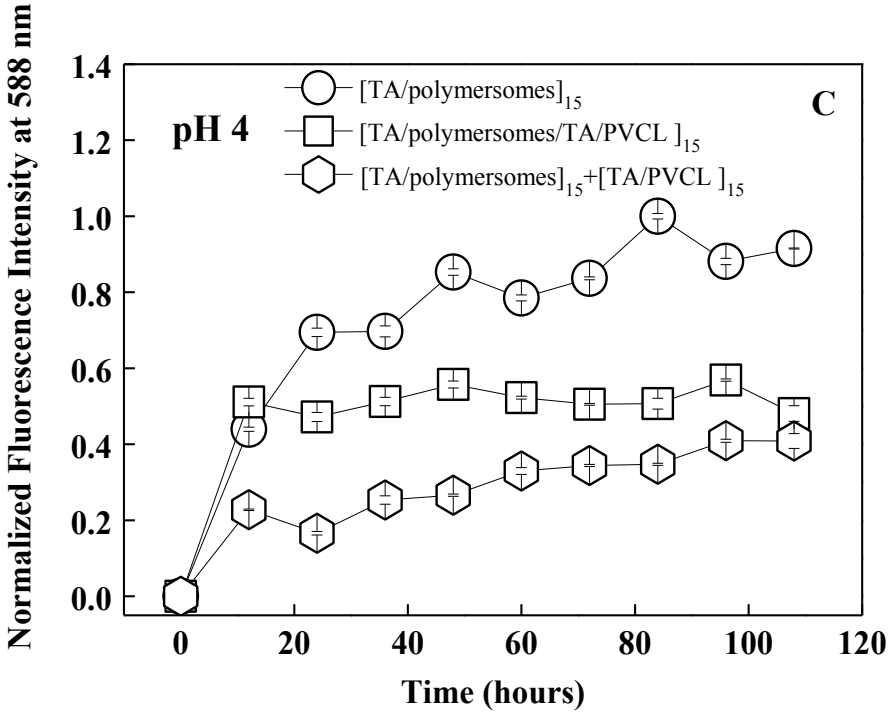

Figure 27. DOX release from multilayers with different architectures $[polymersome/TA]_{15}$ or $[polymersome/TA/PVCL/TA]_{15}$ or $[polymersome/TA]_{15}$+$[PVCL/TA]_{15}$ at pH 7.5 (A); at pH 6 (B) and at pH 4 (C). All films included same number of polymersome layers. Panel A, Panel B and Panel C are composed by normalizing the fluorescence intensity data to the highest fluorescence intensity obtained from $[polymersome/TA/PVCL/TA]_{15}$ multilayers at pH 7.5, $[polymersome/TA]_{15}$ multilayers at pH 6 and $[polymersome/TA]_{15}$ multilayers at pH 4, respectively.

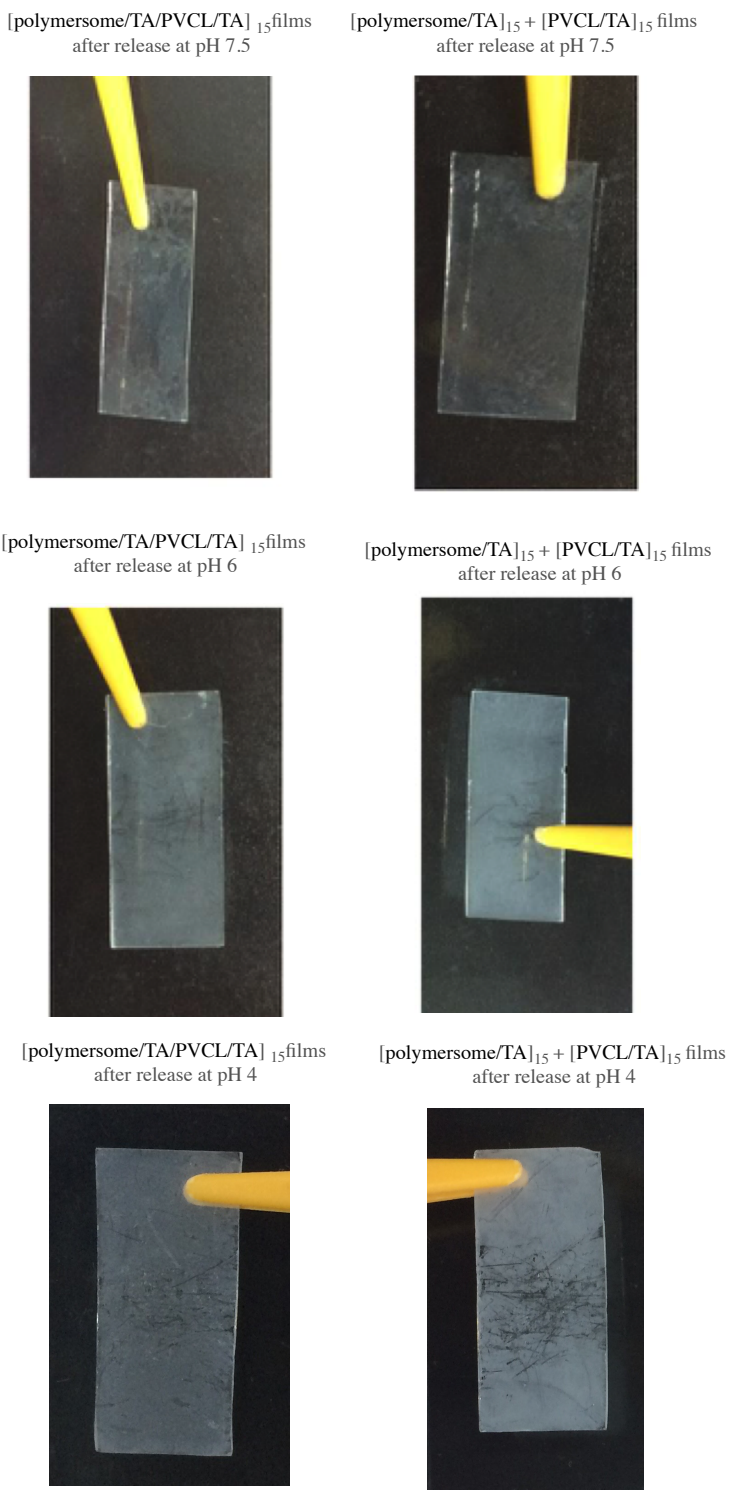

Scheme 8. Photos of the multilayers with barriers after release at pH 7.5, at pH 6 and at pH 4.

3.8 PTX Release from DOX and PTX Loaded PLGA-*b*-PEG Polymersomes/TA Films

Release of PTX could not be monitored spectroscopically because the amount released from the surface was lower than the detection limit of UV-Vis Spectroscopy. PTX release from the surface may be followed by two ways: i) a fluorescent tag can be attached to PTX so that Fluorescent Spectroscopy which has better detection limit than UV-Vis Spectroscopy can be used to monitor the release of PTX from the surface; ii) multilayers can be constructed onto silica nanoparticles so that PTX concentration in the solution would be greater and may be detected using UV-Vis Spectroscopy.

Since PTX release from the surface could not be detected, the capability of the polymersomes to release PTX was examined in an indirect way, by measuring the activity of HCT-116 cells which are colon cancer cells. The activity of cells was determined by MTT method. Fig. 28 demonstrates control group, which is only HCT-116 cells, and the other columns represent the anti-cancer effect of PTX loaded PLGA-*b*-PEG polymersomes. The statistical analysis of the results are carried out wth Analysis of Varience (ANOVA) and Holm-Sidak's test. Significance values are given as the comparisons of column data with the Control column data (* $P<0.05$, ** $P<0.005$, *** $P<0.0005$, **** $P<0.0001$). According to the results, the anti-cancer effect of 1/1000 diluted PTX loaded polymersome solutions was not significant. However, for 1/100 and 1/10 diluted PTX solutions, the anti-cancer effects were significant because PTX loaded polymersomes solutions decreased HCT-116 cell activity. This result confirmed PTX encapsulation into polymersomes and release of PTX from polymersomes.

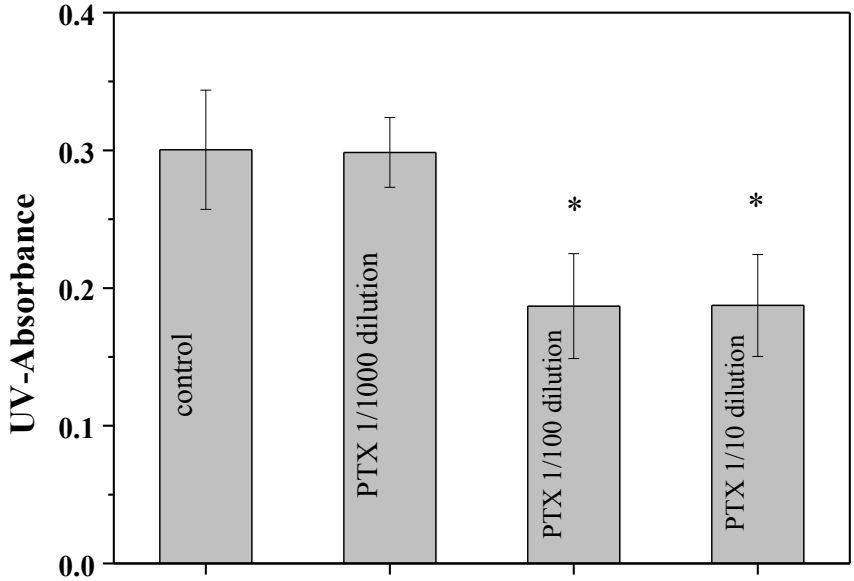

Figure 28. UV-Absorbance of HCT-116 cells. The anti-cancer effect of the drug released from the solution on HCT1-116 cells.

CHAPTER 4

CONCLUSION

PLGA-*b*-PEG was synthesized through coupling carboxylic acid terminated PLGA and amine-terminated PEG via end-groups. PLGA-*b*-PEG polymersomes were prepared by double emulsion method. DOX and PTX were encapsulated in the inner hydrophilic and hydrophobic PLGA region, respectively. Bare PLGA-*b*-PEG polymersomes and DOX/PTX incorporated PLGA-*b*-PEG polymersomes were LbL deposited at the surface using TA via hydrogen bonding interactions among ether oxygens of PEG corona and hydroxyl groups of TA. Lower amount of material was deposited at the surface when DOX and PTX were encapsulated by PLGA-*b*-PEG polymersomes when compared to the amount of material deposited at the surface upon LbL deposition of bare polymersomes. The difference in the amount of material deposited at the surface can be explained by the interaction of ether oxygens of PEG and hydroxyl or amino groups of DOX resulting in a decrease in the number of ether oxygens for multilayer assembly. In addition, the number of layers that could be deposited at the surface was found to be limited to 18 at pH 7.5 and 30 at pH 2 and 24 at pH 7.5 and 30 at pH 2 for LbL deposition of bare PLGA-*b*-PEG polymersomes/TA and DOX/PTX incorporated PLGA-*b*-PEG polymersomes/TA, respectively.

Release of drug molecules from the surface was examined at pH 7.5, pH 6 and pH 4 from DOX/PTX incorporated PLGA-*b*-PEG polymersomes/TA films which were constructed at either pH 7.5 or pH 2. It was found that multilayers were stable at pH 6 and pH 4 regardless of the film deposition pH and DOX was released from the surface with an initial burst release in the first 12 hours, followed by release with small increments. Finally, the effect of barrier layers and film architecture on the release of DOX was examined. PVCL and TA which are known to associate

strongly via hydrogen bonding were used as barrier layers within the multilayers to control the kinetics of release from the surface. PVCL/TA barrier layers which were constructed on top of DOX/PTX incorporated PLGA-*b*-PEG polymersome/TA films slowed down the release of DOX at pH 6 and pH 4, while no effect was recorded at pH 7.5 due to instability of the multilayers in PBS solution at pH 7.5. A film architecture composed of alternating bilayers of DOX/PTX incorporated PLGA-*b*-PEG polymersome/TA and PVCL/TA could not slow down the release of DOX from the surface at pH 7.5 and pH 6 but it was effective at pH 4.

Release of PTX from surface could not be monitored by spectroscopic methods or by activity of cells because the amount released from the surface was low to detect. Therefore, release of PTX from the polymersome solution was evaluated. The results showed that PTX released from the solution is effective on HCT-116 cells.

Multilayers of PLGA-*b*-PEG polymersomes are promising for biomedical applications due to high loading capacity and dual drug release properties via hydrolytic degradation.

CHAPTER 5

OUTLOOK

Results obtained in this study showed that although multilayers of PLGA-b-PEG polymersomes and TA could be successfully constructed at the surface, such films have the disadvantage of instability, i.e. LbL films could not be grown at the surface beyond a certain number of layers. This results in a limitation in the amount of drug loaded at the surface.

This problem can be overcome by preparing multilayers on 3D substrates such as silica nanoparticles so that the amount of drug released from the surface could be increased by higher number of substrates. In this way, monitoring PTX release is also expected to be no longer a problem due to possibly greater amount of PTX release from the surface which is expected to be higher than the detection limit of the instruments such as HPLC or UV-Vis Spectroscopy.

The work presented in this thesis will also be continued by investigating the potential of PLGA-b-PEG polymersomes for encapsulating iron oxide magnetic nanoparticles in the hydrophilic inner core. In this way, such polymersomes will be of use for both dual drug release and imaging purposes.

REFERENCES

[1] M.F. Maitz, Applications of synthetic polymers in clinical medicine, Biosurface and Biotribology. 1 (2015) 161–176.

[2] A.S. Kulshrestha, A. Mahapatro, Polymers for Biomedical Applications, in: ACS Symp. Ser., Americal Chemical Society, Washington, DC, 2008: pp. 1–7.

[3] J.R. Joshi, R.P. Patel, Role of biodegradable polymers in drug delivery, Int. J. Curr. Pharm. Res. 4 (2012) 74–81.

[4] B.D. Ulery, L.S. Nair, C.T. Laurencin, Biomedical Applications of Biodegradable Polymers, J Polym Sci B Polym Phys. 49 (2011) 832–864.

[5] R.P. Brannigan, A.P. Dove, Synthesis, properties and biomedical applications of hydrolytically degradable materials based on aliphatic polyesters and polycarbonates, Biomater. Sci. 5 (2016).

[6] J. Tsung, D.J. Burgess, Biodegradable Polymers in Drug Delivery Systems, in: S. Juergen, R.A. Siegel, M.J. Rathbone (Eds.), Fundam. Appl. Control. Release Drug Deliv., Springer, 2012: pp. 75–105.

[7] S.G. Kumbar, C.T. Laurencin, M. Deng, Natural and Synthetic Biomedical Polymers, in: Nat. Synth. Biomed. Polym., Elsevier, 2014: pp. 259–285.

[8] J.B. Eilert, P. Binder, P.W. McKinney, J.M. Beal, J. Conn, Polyglycolic acid synthetic absorbable sutures, Am. J. Surg. 121 (1971) 561–565.

[9] J.P. Jain, W.Y. Ayen, A.J. Domb, N. Kumar, Biodegradable Polymers in Drug Delivery, in: Biodegrad. Polym. Clin. Use Clin. Dev., First, John Wiley & Sons, Inc, 2011: pp. 3–58.

[10] A. Kumari, S.K. Yadav, S.C. Yadav, Biodegradable polymeric nanoparticles based drug delivery systems, Colloids Surfaces B Biointerfaces. 75 (2010) 1–18.

[11] F. Maytal, Z. Meital, Drug delivery from gelatin-based systems, Expert Opin. Drug Deliv. 12 (2015) 1547–1563.

[12] M.M. Welz, C.M. Ofner, Examination of self-crosslinked gelatin as a hydrogel for controlled release, J. Pharm. Sci. 81 (1992) 85–90.

[13] A.O. Mahmoud Abbas, Chitosan for biomedical applications, University of Iowa, 2010.

[14] F. Li, J. Li, X. Wen, S. Zhou, X. Tong, P. Su, H. Li, D. Shi, Anti-tumor activity of paclitaxel-loaded chitosan nanoparticles: An in vitro study, Mater. Sci. Eng. C. 29 (2009) 2392–2397.

[15] J.J. Wang, Z.W. Zeng, R.Z. Xiao, T. Xie, G.L. Zhou, X.R. Zhan, S.L. Wang, Recent advances of chitosan nanoparticles as drug carriers., Int. J. Nanomedicine. 6 (2011) 765–774.

[16] A. Domb, N. Kumar, A. Ezra, Biodegradable Polymers in Clinical Use and Clinical Development, John Wiley & Sons, Inc., New Jersey, 2011.

[17] K. Leja, G. Lewandowicz, Polymer biodegradation and biodegradable polymers - A review, Polish J. Environ. Stud. 19 (2010) 255–266.

[18] A. Göpferich, Mechanisms of polymer degradation and erosion, Biomoterials. 17 (1996) 103–114.

[19] C. Park, E.Y. Kim, Y.T. Yoo, S.S. Im, Effect of Hydrophilicity on the Biodegradability of Polyesteramides, J. Appl. Polym. Sci. 90 (2003) 2708–2714.

[20] L.S. Nair, C.T. Laurencin, Biodegradable polymers as biomaterials, Prog. Polym. Sci. 32 (2007) 762–798.

[21] S. Li, Hydrolytic Degradation Characteristics of Aliphatic Polyesters Derived from Lactic and Glycolic Acids, J. Biomed. Mater. Res. 48 (1998) 342–353.

[22] Y. Fu, W.J. Kao, Drug release kinetics and transport mechanisms of non-degradable and degradable polymeric delivery systems., Expert Opin. Drug Deliv. 7 (2010) 429–44.

[23] J. Siepmann, A. Göpferich, Mathematical modeling of bioerodible, polymeric drug delivery systems, Adv. Drug Deliv. Rev. 48 (2001) 229–247.

[24] R. Dinarvand, N. Sepehri, S. Manoochehri, H. Rouhani, F. Atyabi,

Polylactide-co-glycolide nanoparticles for controlled delivery of anticancer agents., Int. J. Nanomedicine. 6 (2011) 877–895.

[25] G. Gaucher, M.H. Dufresne, V.P. Sant, N. Kang, D. Maysinger, J.C. Leroux, Block copolymer micelles: Preparation, characterization and application in drug delivery, J. Control. Release. 109 (2005) 169–188.

[26] K. Letchford, H. Burt, A review of the formation and classification of amphiphilic block copolymer nanoparticulate structures: micelles, nanospheres, nanocapsules and polymersomes, Eur. J. Pharm. Biopharm. 65 (2007) 259–269.

[27] N.M. Dand, P.B. Patel, A.P. Ayre, J.K. Vilasrau, A. Ayre, L.H. Hiranandani, Polymeric micelles as a drug carrier for tumor targeting, Chronicles Young Sci. 4 (2013) 94–101.

[28] J. Pachioni-Vasconcelos, A. Moreni Lopes, A. Conceição Apolinário, J. Karina Valenzuela-Oses, J. Souza Ribeiro Costa, L. de Oliveira Nascimento, A. Pessoa Jr, L. Ramos Souza Barbosa, C. de Oliveira Rangel-Yagui, Nanostructures for protein drug delivery, Biomater. Sci. 4 (2016) 205–218.

[29] M. Jones, J. Leroux, Polymeric micellesea new generation of colloidal drug carriers., Eur. J. Pharm. Biopharm. 48 (1999) 101–111.

[30] H.K. Cho, I.W. Cheong, J.M. Lee, J.H. Kim, Polymeric nanoparticles, micelles and polymersomes from amphiphilic block copolymer, Korean J. Chem. Eng. 27 (2010) 731–740.

[31] G. Kwon, M. Naito, M. Yokoyama, T. Okano, Y. Sakurai, K. Kataoka, Block copolymer micelles for drug delivery: loading and release of doxorubicin, J. Control. Release. 48 (1997) 195–201.

[32] G.S. Kwon, M. Naito, M. Yokoyama, T. Okano, Y. Sakurai, K. Kataoka, Physical Entrapment of Adriamycin in AB block Copolymer Micelles, Pharm. Res. 12 (1995) 192–195.

[33] T.J. Martin, K. Prochá, P. Munk, S.E. Webber, Communications to the Editor pH-Dependent Micellization of Poly(2-vinylpyridine)-block-poly(ethylene oxide), Macromolecules. 29 (1996) 6071–6073.

[34] Y. Li, G. Hui Gao, I. Chan Kwon, D. Sung Lee, pH-Sensitive Polymeric

Nanoparticles as Carriers for Cancer Therapy and Imaging, in: Z. Gu (Ed.), Bioinspired Biomim. Polym. Syst. Drug Gene Deliv., First, Wiley-VCH Verlag GmbH & Co. KGaA, 2014: pp. 203–222.

[35] J. Cui, M.P. Van Koeverden, M. Müllner, K. Kempe, F. Caruso, Emerging methods for the fabrication of polymer capsules, Adv. Colloid Interface Sci. 207 (2014) 14–31.

[36] J.S. Lee, J. Feijen, Polymersomes for drug delivery: Design, formation and characterization, J. Control. Release. 161 (2012) 473–483.

[37] W. Li, T. Luo, Y. Yang, X. Tan, L. Liu, Formation of Controllable Hydrophilic/Hydrophobic Drug Delivery Systems by Electrospinning of Vesicles, Langmuir. 31 (2015) 5141–5146.

[38] W. Chen, F. Meng, R. Cheng, Z. Zhong, pH-Sensitive degradable polymersomes for triggered release of anticancer drugs: A comparative study with micelles, J. Control. Release. 142 (2010) 40–46.

[39] J. Du, R.K. O 'reilly, Advances and challenges in smart and functional polymer vesicles, Soft Matter. 5 (2009) 3544–3561.

[40] E. Locatelli, M.C. Franchini, Biodegradable PLGA-b-PEG polymeric nanoparticles: Synthesis, properties, and nanomedical applications as drug delivery system, J. Nanoparticle Res. 14 (2012) 1–17.

[41] R. Gref, Y. Minamitake, M.T. Peracchia, V. Trubetskoy, V. Torchilin, R. Langer, Biodegradable Long-Circulating Polymeric Nanospheres, Source Sci. 263 (1994) 1600–1603.

[42] F. Danhier, E. Ansorena, J.M. Silva, R. Coco, A. Le Breton, V. Préat, PLGA-based nanoparticles: An overview of biomedical applications, J. Control. Release. 161 (2012) 505–522.

[43] D.H. Lewis, Controlled Release of Bioactive Agents from Lactide/Glycolide Polymers, in: M. Chasin, R. Langer (Eds.), Biodegrad. Polym. as Drug Deliv. Syst., Marcel Dekker, New York, 1990: pp. 1–42.

[44] J. Tsung, D.J. Burgess, J. Tsung, Biodegradable Polymers in Drug Delivery Systems, in: M.J. Rathbone, J. Siepmann, R.A. Siegel (Eds.), Fundam. Appl. Control. Release Drug Deliv., Springer, 2011: pp. 107–123.

[45] H.K. Makadia, S.J. Siegel, Poly Lactic-co-Glycolic Acid (PLGA) as Biodegradable Controlled Drug Delivery Carrier., Polymers (Basel). 3 (2011) 1377–1397.

[46] T.G. Park, Degradation of poly(lactic-co-glycolic acid) microspheres: effect of copolymer composition, Biomaterials. 16 (1995) 1123–1130.

[47] R.K. Iler, Multilayers of Colloidal Particles, J. Colloid Interface Sci. 21 (1966) 569–594.

[48] G. Decher, J.D. Hong, J. Schmitt, Buildup of ultrathin multilayer films by a self-assembly process: III. Consecutively alternating adsorption of anionic and cationic polyelectrolytes on charged surfaces, Thin Solid Films. 210 (1992) 831–835.

[49] B.M. Wohl, J.F.J. Engbersen, Responsive layer-by-layer materials for drug delivery, J. Control. Release. 158 (2012) 2–14.

[50] D. Volodkin, A. Skirtach, H. Möhwald, LbL Films as Reservoirs for Bioactive Molecules, Adv. Polym. Sci. 240 (2011) 135–161.

[51] P.T. Hammond, Building biomedical materials layer-by-layer, Mater. Today. 15 (2012) 196–206.

[52] M.M. De Villiers, D.P. Otto, S.J. Strydom, Y.M. Lvov, Introduction to nanocoatings produced by layer-by-layer (LbL) self-assembly, Adv. Drug Deliv. Rev. 63 (2011) 701–715.

[53] N. Estillore, W. Knoll, R. Advincula, Functional Layer-by-Layer Polyelectrolytes: Assembly Strategies, Characterization, and Selected Applications, in: A. Ciferri, A. Perico (Eds.), Ion. Interact. Nat. Synth. Macromol., First, John Wiley & Sons, Inc., 2012: pp. 643–682.

[54] F. Caruso, R.A. Caruso, H. Möhwald, Nanoengineering of Inorganic and Hybrid Hollow Spheres by Colloidal Templating, Science (80-.). 282 (1998) 1111–1114.

[55] S. Pavlukhina, S. Sukhishvili, Polymer assemblies for controlled delivery of bioactive molecules from surfaces, Adv. Drug Deliv. Rev. 63 (2011) 822–836.

[56] B.-S. Kim, W. Park, P.T. Hammond, Hydrogen-Bonding Layer-by-Layer-Assembled Biodegradable Polymeric Micelles as Drug Delivery Vehicles from Surfaces, ACS Nano. 2 (2008) 386–392.

[57] N.A. Kotov, Layer-by-layer self-assembly: the contribution of hidrophobic interactions, NanoStructured Mater. 12 (1999) 789–796.

[58] M. Sato, Sano Masahito, van der Waals Layer-by-Layer Construction of a Carbon Nanotube 2D Network, Langmuir. 21 (2005) 11490–11494.

[59] G.K. Such, J.F. Quinn, A. Quinn, E. Tjipto, F. Carıso, Assembly of Ultrathin Polymer Multilayer Films by Click Chemistry, J. AM. CHEM. SOC. 128 (2006) 9318–9319.

[60] J. Chen, L. Huang, L. Ying, G. Luo, X. Zhao, W. Cao, Self-Assembly Ultrathin Films Based on Diazoresins, Langmuir. 15 (1999) 7208–7212.

[61] Y. Shimazaki, M. Mitsuishi, S. Ito, M. Yamamoto, Preparation and Characterization of the Layer-by-Layer Deposited Ultrathin Film Based on the Charge-Transfer Interaction in Organic Solvents, Langmuir . 14 (1998) 2768–2773.

[62] H.-G. Hong, T.E. Mallouk, Electrochemical Measurements of Electron Transfer Rates through Zirconium 1,2-Ethanediylbis(phosphonate) Multilayer Films on Gold Electrodes, Langmuir. 7 (1991) 2362–2369.

[63] M.A. Rahim, H. Ejima, K.L. Cho, K. Kempe, M. Mü, J.P. Best, F. Caruso, Coordination-Driven Multistep Assembly of Metal−Polyphenol Films and Capsules, Chem. Mater. 26 (2014) 1645–1653.

[64] J.D. Hong, K. Lowack, J. Schmitt, G. Decher, Layer-by-layer deposited multilayer assemblies of polyelectrolytes and proteins: from ultrathin films to protein arrays, Trends Colloid Interface Sci. VII. 102 (1993) 98–102.

[65] X. Zhang, H. Chen, H. Zhang, Layer-by-layer assembly: from conventional to unconventional methods, Chem. Commun. (2006) 1395–1405.

[66] W.B. Stockton, M.F. Rubner, Molecular-Level Processing of Conjugated Polymers. 4. Layer-by-Layer Manipulation of Polyaniline via Hydrogen-Bonding Interactions, Macromolecules. 30 (1997) 2717–2725.

[67] N. Ma, H. Zhang, B. Song, Z. Wang, X. Zhang, Polymer Micelles as Building Blocks for Layer-by-Layer Assembly: An Approach for Incorporation and Controlled Release of Water-Insoluble Dyes, Chem. Mater. 17 (2005) 5065–5069.

[68] B. Kim, S.W. Park, P.T. Hammond, Hydrogen-Bonding Layer-by-Layer-Assembled Biodegradable Polymeric Micelles as Drug Delivery Vehicles from Syrfaces, ACS Nano. 2 (2008) 386–392.

[69] Y. Guan, Y. Zhang, Dynamically bonded layer-by-layer films: Dynamic properties and applications, J. Appl. Polym. Sci. 131 (2014) 26–29.

[70] D. Choi, J. Hong, Layer-by-layer assembly of multilayer films for controlled drug release, Arch. Pharm. Res. 37 (2014) 79–87.

[71] P.M. Nguyen, N.S. Zacharia, E. Verploegen, P.T. Hammond, Extended Release Antibacterial Layer-by-Layer Films Incorporating Linear-Dendritic Block Copolymer Micelles, Chem. Mater,. 19 (2007) 5524–5530.

[72] A.J. Chung, M.F. Rubner, Methods of Loading and Releasing Low Molecular Weight Cationic Molecules in Weak Polyelectrolyte Multilayer Films, Langmuir. 18 (2002) 1176–1183.

[73] S.A. Sukhishvili, S. Granick, Layered, Erasable Polymer Multilayers Formed by Hydrogen-Bonded Sequential Self-Assembly, Macromolecules. 35 (2002) 301–310.

[74] I. Erel, H.E. Karahan, C. Tuncer, V. Butun, A.L. Demirel, Hydrogen-bonded multilayers of micelles of a dually responsive dicationic block copolymer, Soft Matter. 8 (2012) 827–836.

[75] S.N. Matsumi, K. Jain, R. Vedarajan, M. Watanabe, M. Ishikiriyama, N. Matsumi, Tunable LCST behavior of poly(N-isopropylacrylamide/ionic liquid) copolymers Kamiya, Polym. Chem. 6 (2015) 6763–6896.

[76] J.F. Quinn, F. Caruso, Facile Tailoring of Film Morphology and Release Properties Using Layer-by-Layer Assembly of Thermoresponsive Materials, Langmuir. 20 (2004) 20–22.

[77] Z. Zhu, N. Gao, H. Wang, S.A. Sukhishvili, Temperature-triggered on-demand drug release enabled by hydrogen-bonded multilayers of block

copolymer micelles, J. Control. Release. 171 (2013) 73–80.

[78] K. Ren, J. Ji, J. Shen, Tunable DNA Release from Cross-Linked Ultrathin DNA/PLL Multilayered Films, Bioconjugate Chem. 17 (2006) 77–83.

[79] E. Vá Zquez, D.M. Dewitt, P.T. Hammond, D.M. Lynn, Construction of Hydrolytically-Degradable Thin Films via Layer-by-Layer Deposition of Degradable Polyelectrolytes, J. Am. Chem. Soc. 124 (2002) 13992–13993.

[80] K.C. Wood, J.Q. Boedicker, D.M. Lynn, P.T. Hammond, Tunable Drug Release from Hydrolytically Degradable Layer-by-Layer Thin Films, Langmuir. 21 (2005) 1603–1609.

[81] T.G. Kim, H. Lee, Y. Jang, T.G. Park, Controlled Release of Paclitaxel from Heparinized Metal Stent Fabricated by Layer-by-Layer Assembly of Polylysine and Hyaluronic Acid-g-Poly(lactic-co-glycolic acid) Micelles Encapsulating Paclitaxel, Biomacromolecules. 10 (2009) 1532–1539.

[82] H. Wang, Y. Zhao, Y. Wu, Y. Hu, K. Nan, G. Nie, H. Chen, Enhanced anti-tumor efficacy by co-delivery of doxorubicin and paclitaxel with amphiphilic methoxy PEG-PLGA copolymer nanoparticles, Biomaterials. 32 (2011) 8281–8290.

[83] M. Coustet, J. Irigoyen, T.A. Garcia, R.A. Murray, G. Romero, M. Susana Cortizo, W. Knoll, O. Azzaroni, S.E. Moya, Layer-by-layer assembly of polymersomes and polyelectrolytes on planar surfaces and microsized colloidal particles, J. Colloid Interface Sci. 421 (2014) 132–140.

[84] J. Cheng, B.A. Teply, I. Sherifi, J. Sung, G. Luther, F.X. Gu, E. Levy-Nissenbaum, A.F. Radovic-Moreno, R. Langer, O.C. Farokhzad, Formulation of Functionalized PLGA-PEG Nanoparticles for In Vivo Targeted Drug Delivery, Biomaterials. 28 (2007) 869–876.

[85] H.S. Yoo, T.G. Park, Biodegradable polymeric micelles composed of doxorubicin conjugated PLGA–PEG block copolymer, J. Control. Release. 70 (2001) 63–70.

[86] T. Phuong Tuyen Dao, T. Hoai Nguyen, V. Vinh To, T. Ha Ho, T. Anh Nguyen, M. Chien Dang, A new formulation of curcumin using poly (lactic-co-glycolic acid)—polyethylene glycol diblock copolymer as carrier material, Adv. Nat. Sci. Nanosci. Nanotechnol. 5 (2014).

[87] Z. Song, R. Feng, M. Sun, C. Guo, Y. Gao, L. Li, G. Zhai, Curcumin-loaded PLGA-PEG-PLGA triblock copolymeric micelles: Preparation, pharmacokinetics and distribution in vivo, J. Colloid Interface Sci. 354 (2011) 116–123.

[88] K. Avgoustakis, A. Beletsi, Z. Panagi, P. Klepetsanis, A.. Karydas, D.. Ithakissios, PLGA–mPEG nanoparticles of cisplatin: in vitro nanoparticle degradation, in vitro drug release and in vivo drug residence in blood properties, J. Control. Release. 79 (2002) 123–135.

[89] D.J. Hines, D.L. Kaplan, Poly(lactic-co-glycolic) acid-controlled-release systems: experimental and modeling insights., Crit. Rev. Ther. Drug Carrier Syst. 30 (2013) 257–76.

[90] D. V Volodkin, P. Schaaf, H. Mohwald, J.-C. Voegel, V. Ball, Effective embedding of liposomes into polyelectrolyte multilayered films: the relative importance of lipid-polyelectrolyte and interpolyelectrolyte interactions, Soft Matter. 5 (2009) 1394–1405.

[91] I. Erel-Unal, S.A. Sukhishvili, Hydrogen-Bonded Multilayers of a Neutral Polymer and a Polyphenol, Macromol. 2008,. 41 (2008) 3962–3970.

[92] X. Li, D.J. Hirsh, D. Cabral-Lilly, A. Zirkel, S.M. Gruner, A.S. Janoff, W.R. Perkins, Doxorubicin physical state in solution and inside liposomes loaded via a pH gradient, Biochim. Biophys. Acta - Biomembr. 1415 (1998) 23–40.

[93] T. Konno, J. Watanabe, K. Ishihara, Enhanced solubility of paclitaxel using water‐soluble and biocompatible 2‐methacryloyloxyethyl phosphorylcholine polymers, J. Biomed. Mater. Res. Part A. 65A (2003) 209–214.

[94] Z. Fülöp, R. Gref, T. Loftsson, A permeation method for detection of self-aggregation of doxorubicin in aqueous environment, 2013.

[95] V. Estrella, T. Chen, M. Lloyd, J. Wojtkowiak, H.H. Cornnell, A. Ibrahim-Hashim, K. Bailey, Y. Balagurunathan, J.M. Rothberg, B.F. Sloane, J. Johnson, R.A. Gatenby, R.J. Gillies, Acidity Generated by the Tumor Microenvironment Drives Local Invasion, Am. Assoc. Cancer Res. 73 (2013) 2013.

[96] J.W. Wojtkowiak, D. Verduzco, K.J. Schramm, R.J. Gillies, Drug resistance and cellular adaptation to tumor acidic pH microenvironment, Mol Pharm. 8

(2011) 2032–2038.

APPENDIX

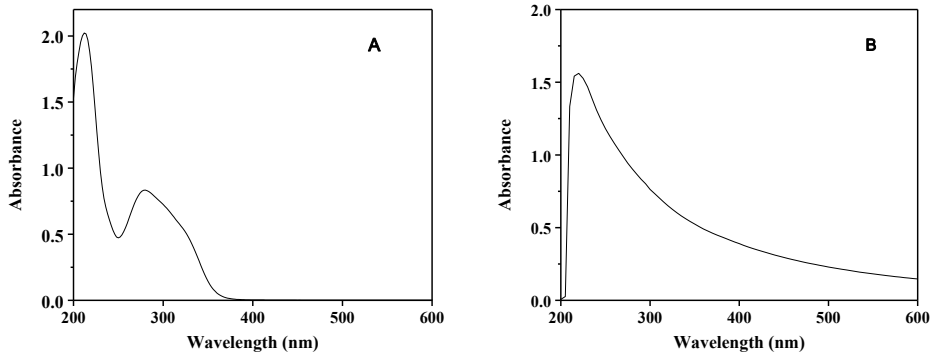

Figure A.1. UV-Vis absorption spectra of Tannic acid solution (A) and PLGA-*b*-PEG polymersomes solution (B).

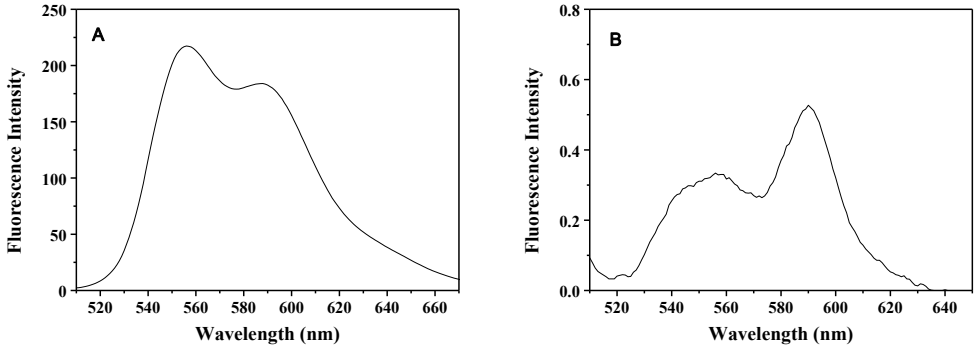

Figure A.2. Fluorescence spectra of DOX solutions at concentration of $1x10^{-2}$ mg/mL (A) and $5x10^{-5}$ mg/mL (B).

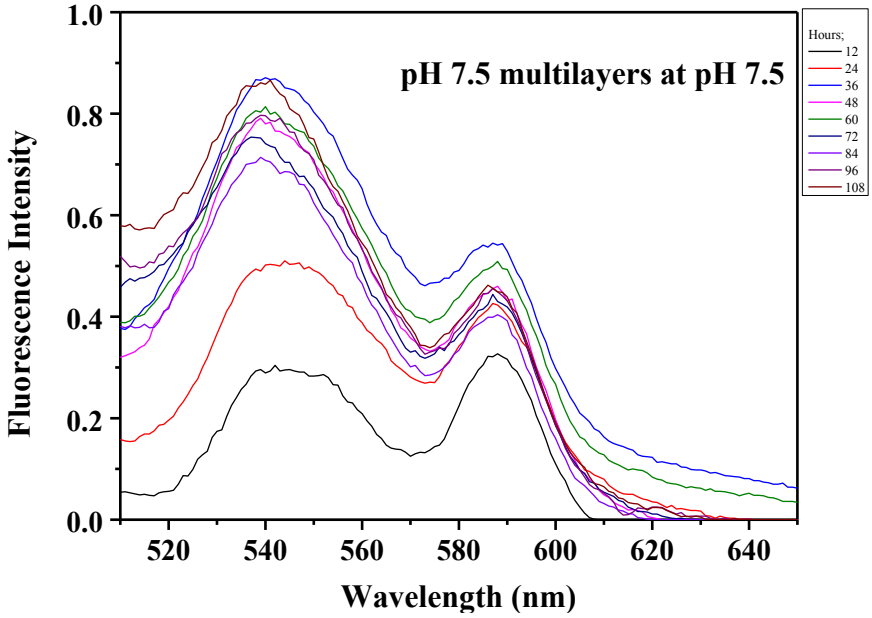

Figure A. 3. Fluorescence spectra of DOX released at pH 7.5 from multilayers of tannic acid and DOX and PTX loaded PLGA-*b*-PEG polymersomes prepared at pH 7.5.

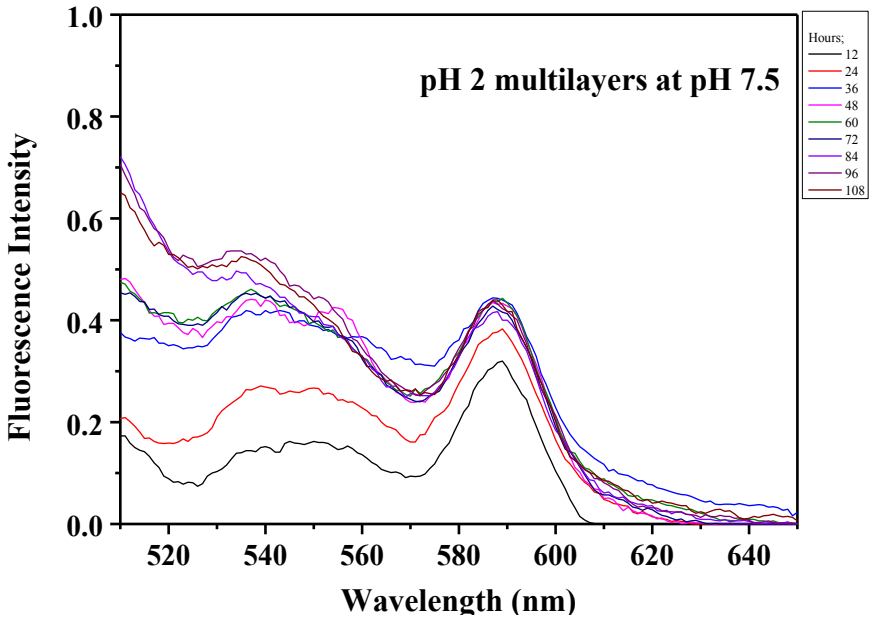

Figure A. 4. Fluorescence spectra of DOX released at pH 7.5 from multilayers of tannic acid and DOX and PTX loaded PLGA-*b*-PEG polymersomes prepared at pH 2.

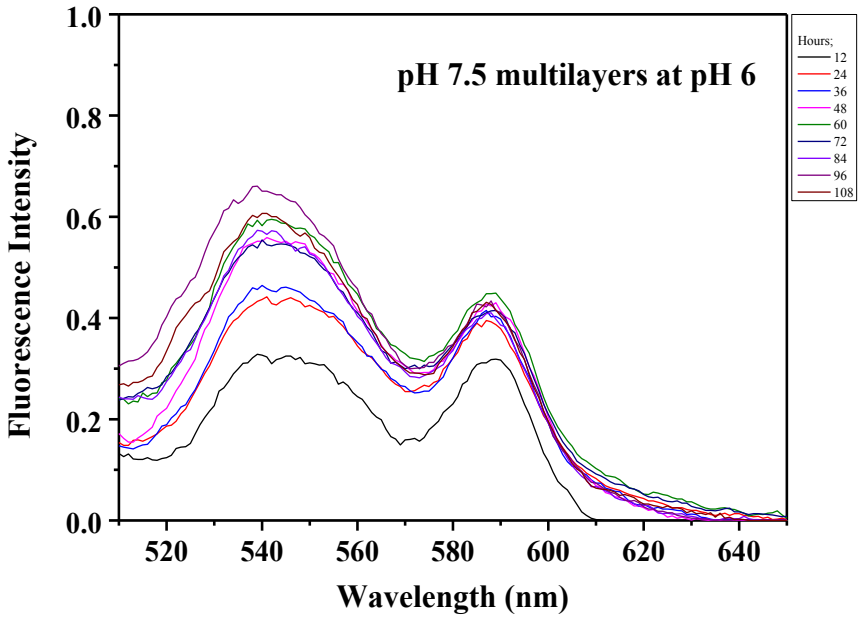

Figure A. 5. Fluorescence spectra of DOX released at pH 6 from multilayers of tannic acid and DOX and PTX loaded PLGA-*b*-PEG polymersomes prepared at pH 7.5.

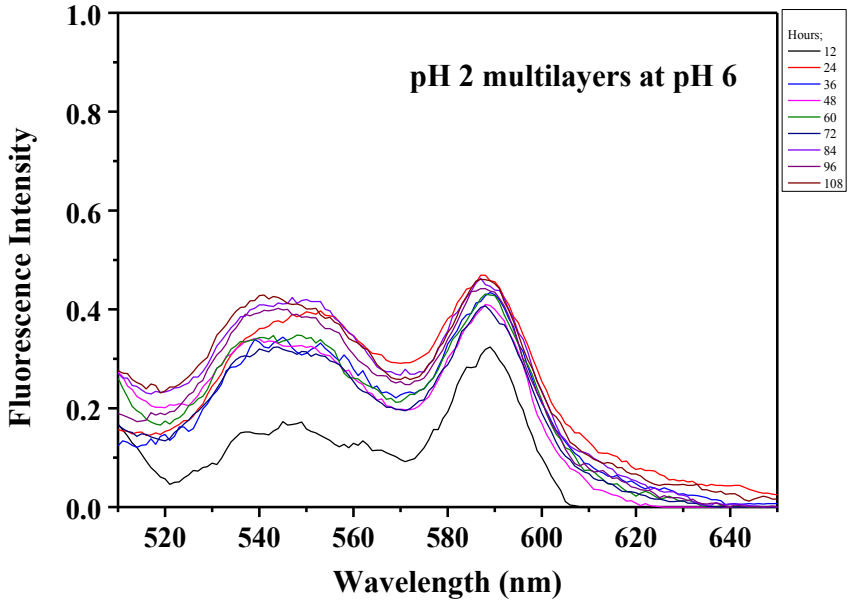

Figure A. 6. Fluorescence spectra of DOX released at pH 6 from multilayers of tannic acid and DOX and PTX loaded PLGA-*b*-PEG polymersomes prepared at pH 2.

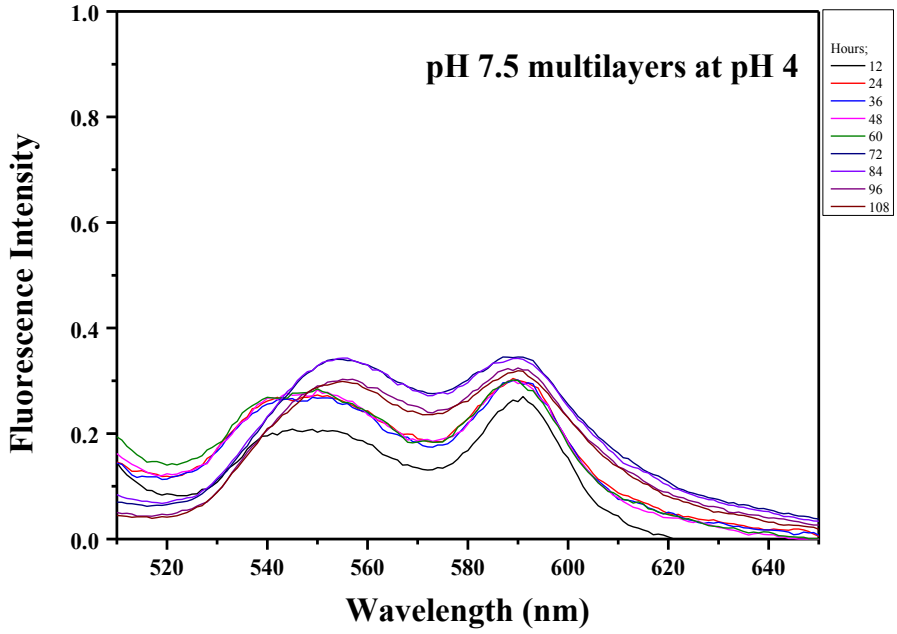

Figure A. 7. Fluorescence spectra of DOX released at pH 4 from multilayers of tannic acid and DOX and PTX loaded PLGA-*b*-PEG polymersomes prepared at pH 7.5.

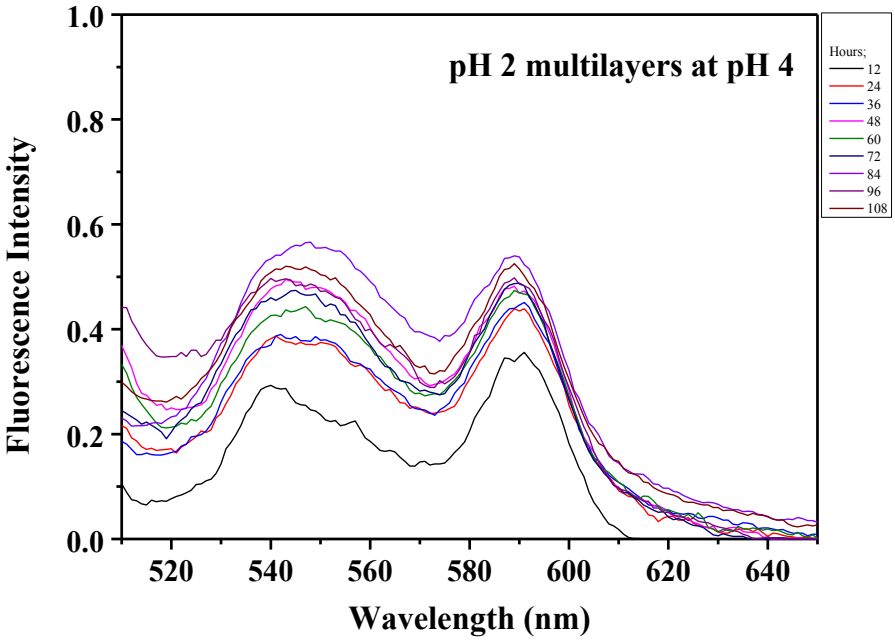

Figure A. 8. Fluorescence spectra of DOX released at pH 4 from multilayers of tannic acid and DOX and PTX loaded PLGA-*b*-PEG polymersomes prepared at pH 7.5.

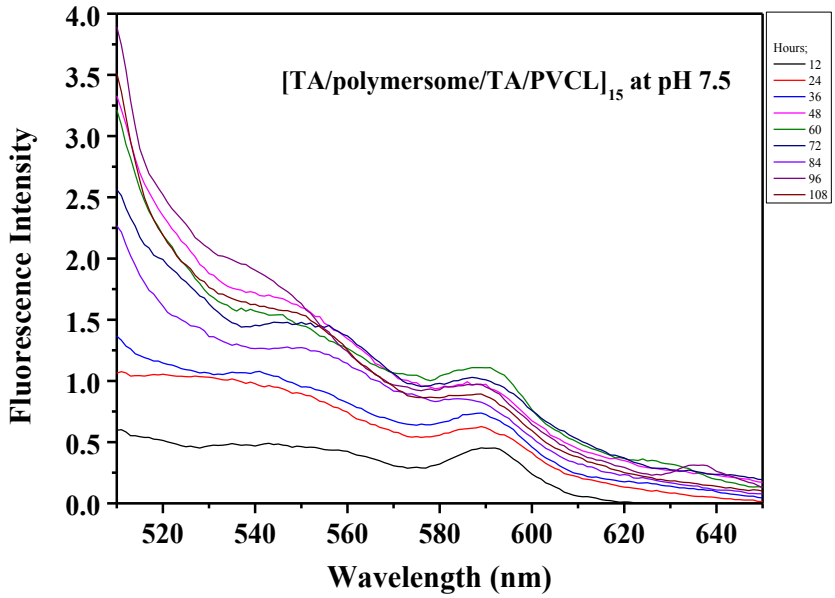

Figure A. 9. Fluorescence spectra of DOX released at pH 7.5 from multilayers of TA/ DOX and PTX loaded PLGA-*b*-PEG polymersomes/TA/PVCL prepared at pH 2.

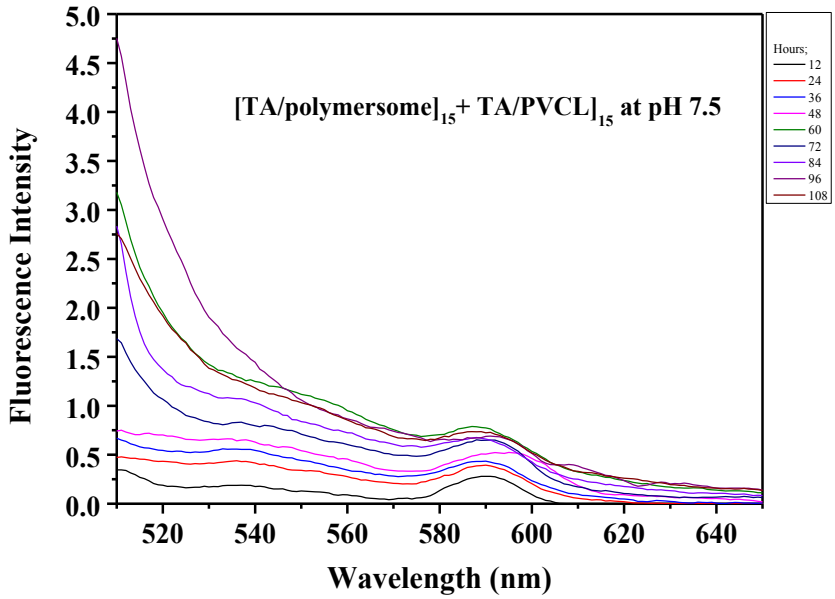

Figure A. 10. Fluorescence spectra of DOX released at pH 7.5 from multilayers of TA/ DOX and PTX loaded PLGA-*b*-PEG polymersomes+TA/PVCL prepared at pH 2.

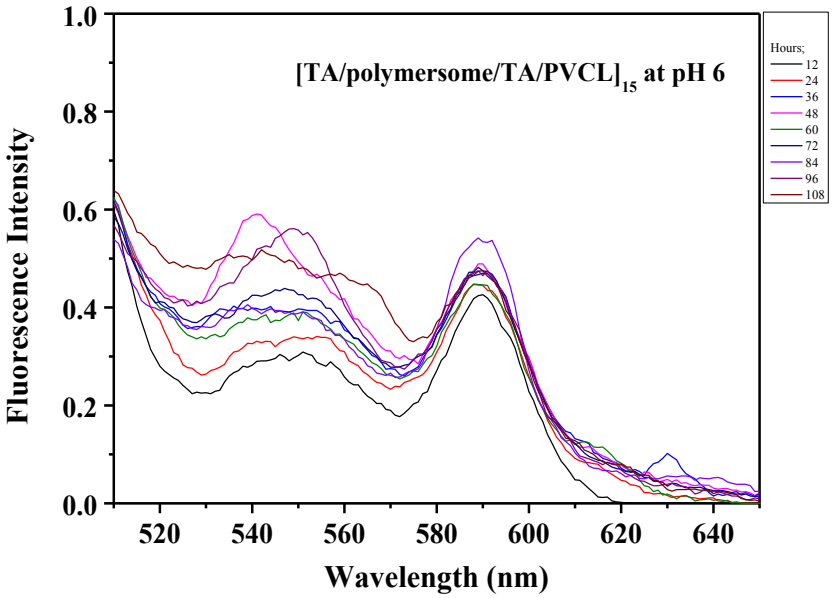

Figure A. 11. Fluorescence spectra of DOX released at pH 6 from multilayers of TA/ DOX and PTX loaded PLGA-*b*-PEG polymersomes/TA/PVCL prepared at pH 2.

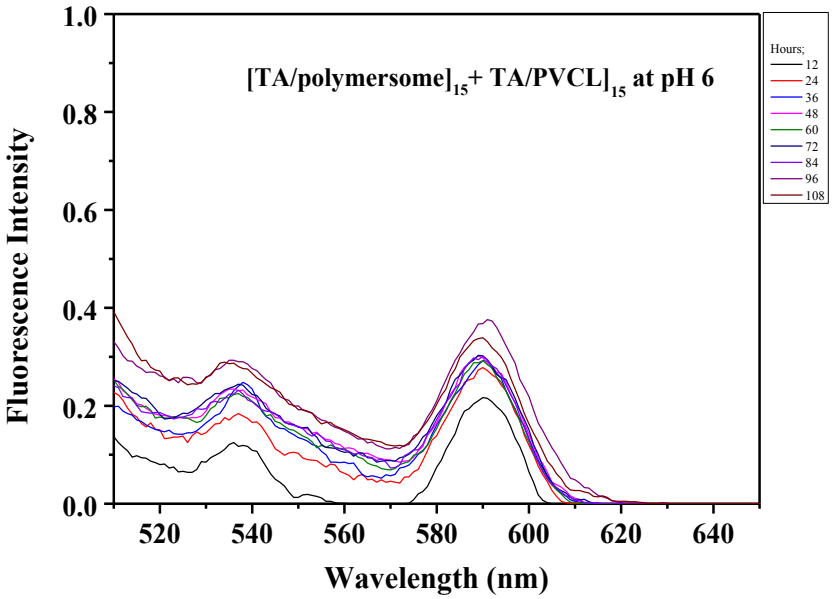

Figure A. 12. Fluorescence spectra of DOX released at pH 6 from multilayers of TA/ DOX and PTX loaded PLGA-*b*-PEG polymersomes+TA/PVCL prepared at pH 2.

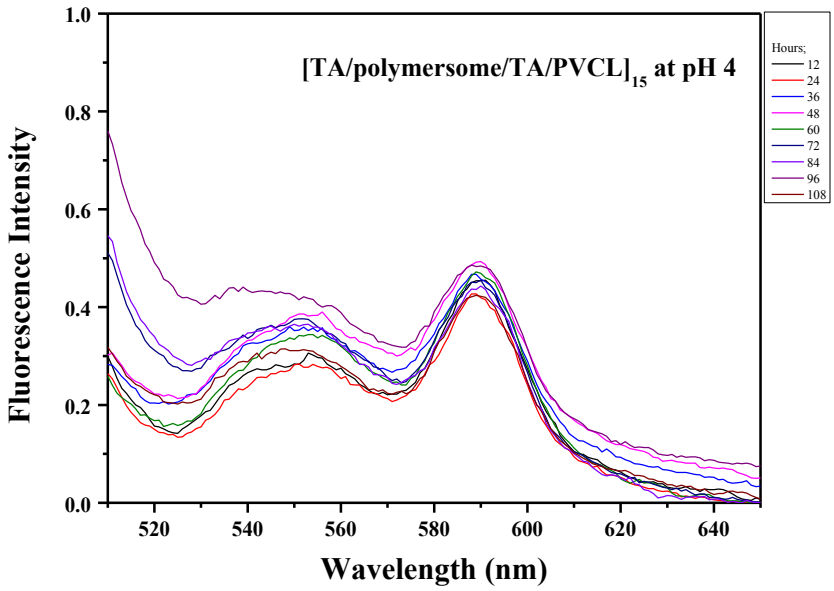

Figure A. 13. Fluorescence spectra of DOX released at pH 4 from multilayers of TA/ DOX and PTX loaded PLGA-*b*-PEG polymersomes/TA/PVCL prepared at pH 2.

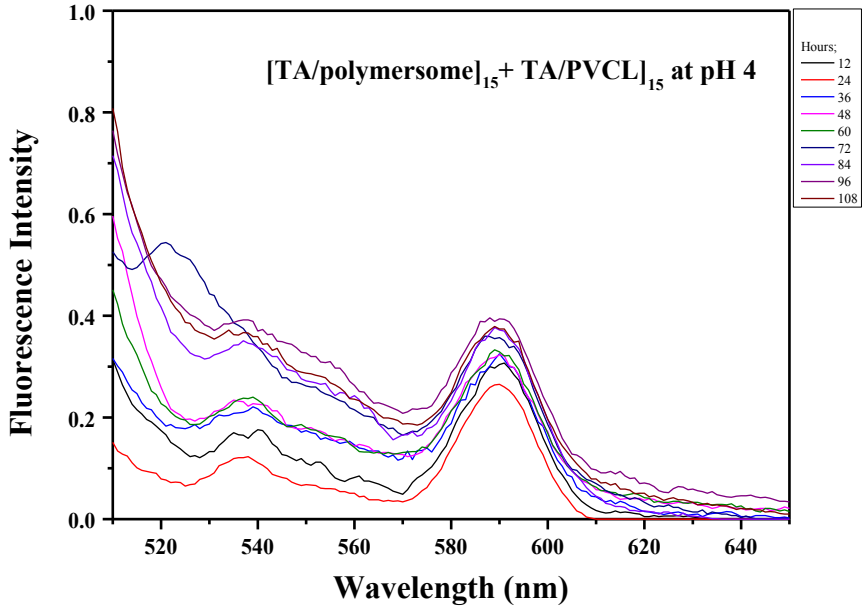

Figure A. 14. Fluorescence spectra of DOX released at pH 4 from multilayers of TA/ DOX and PTX loaded PLGA-*b*-PEG polymersomes+TA/PVCL prepared at pH 2.